Control Strategies for Adaptive DSTATCOM with an Accommodating Power Management System in AC Microgrid

Epsita Das

Doctor of Philosophy (Engineering)

Department of Electrical Engineering

Faculty Council of Engineering & Technology

Jadavpur University

Kolkata, India

2024

Control Strategies for Adaptive DSTATCOM with an Accommodating Power Management System in AC Microgrid

Supervisors

Prof. Sujit Kumar Biswas

Professor,

Electrical Engineering,

Jadavpur University, Kolkata,

West Bengal, India, Pin 700032

Prof. Ambarnath Banerji

Professor,

Electrical Engineering

Narula Institute of Technology, Kolkata,

West Bengal, India, Pin 700109

Prof. Sudipta Debnath

Professor,

Electrical Engineering,

Jadavpur University, Kolkata,

West Bengal, India, Pin 700032

List of Publications:

1. **E. Das**, A. Banerji, and S. K. Biswas, "A robust microgrid using an inverter with CCS-MPC control and resilient operation," *Int. J. Power Electron. Drive Syst.*, vol. 14, no. 4, p. 2217, 2023, doi: 10.11591/ijpeds.v14.i4.pp2217-2229.

2. **E. Das**, A. Banerji and S. K. Biswas, "Cloud Assisted IOT operated Small Residential Microgrid with Collusive Model Approach for Energy Trading", accepted for publication in Jordon Journal of Electrical Engineering

List of Patents   Nil

List of Presentations in National/International/Conferences/Workshops :

[1] E. Das, S. Roy, S. R. Chowdhury, A. Banerji, and S.K. Biswas, "Cloud-based P2P Energy Transfer in a Residential Photovoltaic System Community," in *Energy Systems, Drives, Power Electronics, Measurement and Sensors (ESDPEMS -2023)*, Kolkata: Department of Electrical Engineering, Narula Institute of Technology, 2023, pp. 4–7.

[2] E. Das, K. Biswas, S. K. Biswas, A. Banerji, and R. Chakrabarti, "Economic Analysis for the Players Participating in a

Hybrid Solar Virtual Power Plant," *Proc. IEEE VLSI DCS 2022 3rd IEEE Conf. VLSI Device, Circuit Syst.*, vol. 2022, no. February, pp. 98–103, 2022, doi: 10.1109/VLSIDCS53788.2022.9811469.

[3] E. Das, S. Basak, S. Sarkar, B. Ganguly, A. Banerji, and S. K. Biswas, "Fuzzy PID Controlled DSTATCOM for Delivering Quality Power," in *Proceedings of 2nd International Conference on VLSI Device, Circuit and System, VLSI DCS 2020*, 2020. doi: 10.1109/VLSIDCS47293.2020.9179920.

[4] E. Das, A. Bhattacharjee, S. Roy, B. Ganguly, A. Banerji, and S. K. Biswas, "A Supervised Hybrid Algorithm based DSTATCOM to Cater to Dynamic Load Changes," in *UEMGREEN 2019 - 1st International Conference on Ubiquitous Energy Management for Green Environment*, 2019. doi:10.1109/UEMGREEN46813.2019.9221544.

[5] E. Das, A. Banerji, and S. K. Biswas, "State of art control techniques for

DSTATCOM," *2017 IEEE Calcutta Conf. CALCON 2017 - Proc.*, vol. 2018-January, pp. 268–273, 2017, doi: 10.1109/CALCON.2017.8280737.

FACULTY OF ENGINEERING & TECHNOLOGY
JADAVPUR UNIVERSITY

PROFORMA – 1

"Statement of Originality"

I **Epsita Das** registered on **20.02.2017** do hereby declare that this thesis entitled "**Control Strategies for Adaptive DSTATCOM with an Accommodating Power Management System in AC Microgrid**" contains literature survey and original research work done by the undersigned candidate as part of Doctoral studies.

All information in this thesis have been obtained and presented in accordance with existing academic rules and ethical conduct. I declare that, as required by these rules and conduct, I have fully cited and referred all materials and results that are not original to this work.
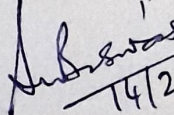
I also declare that I have checked this thesis as per the "Policy on Anti Plagiarism, Jadavpur University, 2019", and the level of similarity as checked by iThenticate software is ___03___ %.

Signature of Candidate: *Epsita Das*

Date : 14/02/24

Certified by Supervisor(s):
(Signature with date, seal)

1._____

Prof. Sujit K. Biswas with date & seal

> Dr. Sujit K. Biswas
> Former Professor & Head
> Department of Electrical Engineering
> Jadavpur University, Kolkata-700032

2._____ 14/02/2024

Prof Ambarnath Banerji with date & seal

> Dr. Ambarnath Banerji
> Professor,
> Department of Electrical Engineering,
> Narula Institute of Technology.

3.___ S. Debnath ___

Prof Sudipta Debnath with date & seal

> Professor
> Electrical Engineering Department
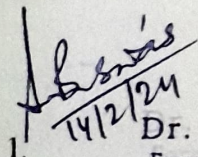> JADAVPUR UNIVERSITY
> Kolkata - 700 032

FACULTY OF ENGINEERING & TECHNOLOGY
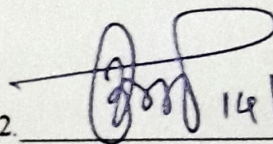## JADAVPUR UNIVERSITY

PROFORMA - 2

CERTIFICATE FROM THE SUPERVISOR/S

This is to certify that the thesis entitled "**Control Strategies for Adaptive DSTATCOM with an Accommodating Power Management System in AC Microgrid**" submitted by Smt **Epsita Das**, who got her name registered on **20.02.2017** for the award of **Ph. D. (Engineering)** degree of Jadavpur University is absolutely based upon her own work under the supervision of **Prof. Sujit K. Biswas, Professor, Electrical Engineering Department, Jadavpur University, Prof. Ambarnath Banerji, Professor, Electrical Engineering Department, Narula Institute of Technology, Kolkata** and **Prof. Sudipta Nath, Professor, Electrical Engineering Department, Jadavpur University** and that neither her thesis nor any part of the thesis has been submitted for any degree/diploma or any other academic award anywhere before.
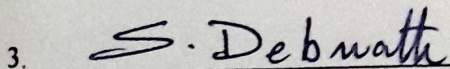
1. _____ Dr. Sujit K. Biswas
   14/12/24 Former Professor & Head
Prof. Sujit K. Biswas with date & office
seal   Jadavpur University, Kolkata-700032

2. _____ 14/02/2024 Dr. Ambarnath Banerji
Prof. Ambarnath Banerj with date & office   Professor,
seal   Department of Electrical Engi
   Narula Institute of Technolo

3. ___S. Debnath____
Prof. Sudipta Debnath with date & office
seal
_____

Professor
Electrical Engineering Department
JADAVPUR UNIVERSITY
Kolkata - 700 032

Abstract

The aim of this thesis can be divided in two factors. They are as follows:

1. To investigate plug-and-play operation for DSTATCOM for reactive power management and voltage regulation.

2. To investigate a strategic method for reducing energy consumption cost of the small residential energy producers in MG

Proportional-integral-derivative (PID) controllers need rigorous installation tuning processes, which require sufficient time and human expertise. This thesis investigates a plug-and-play operation of DSTATCOM for voltage regulation. Artificial neural network (ANN) is used in this thesis for system identification to avoid human intervention. Two adaptive techniques were introduced in this thesis to achieve this aim.

    i)   an adaptive neuro-fuzzy inference system (ANFIS)

    ii)   continuous control set (CCS) model predictive control (MPC)

Both methods yield good results for voltage regulation when used in plug and play mode.

The penetration of the distributed energy resources (DER) in the power market initiates changes in the price dynamics. Demand Side Management (DSM) is the measure to optimize energy consumption, providing incentives for less energy consumption, especially during peak demand. In this thesis DSM is performed using smart electrical gadgets over the internet. This thesis uses low-cost, open-source IoT devices to monitor and control domestic loads of microgrids. Two distinct modes are used to operate the MG

    a) within the MG (peer-to-peer or P2P)

    b) with the utility grid.

Microgrid operator (MO) takes responsibility for energy transfer operation. Hardware simulation of the P2P transfer is experimentally performed with open-source IoT applications from the cloud.

Selling energy by a prosumer when needed by fellow residents in the MG is considered a token of social service towards the community. A social service counter (SSC) is chosen to identify services for each prosumer in the MG. When a seller sells energy within the community, the SSC increases. Few residents from the community are elected as delegates because they support community welfare. This approach distributes the surplus generated energy among community members at price lower than that from the grid. This minimizes the carbon footprint. MO only allows prosumers to participate in energy trading with the grid during the high-demand hours of the day. Delegates are essential in protecting the community's

interest while selling energy outside the community. They try to form a coalition among participants to reduce installed capacity and maximize the cumulative payoff. A comparative study between the proposed coordination game and two competitive game approaches, Cournot and Stackelberg's algorithm in the restricted domain, reveals that the proposed method is well suited for a small residential microgrid. An index called Shapley value is used as a tool that identifies each delegate's contribution during the game. The delegate having higher Shapley value are rewarded with a commensurate part of the cumulative profit of the community. The thesis thus searches for a method to identify the most balanced payoff for individual players for the overall coordination game.

Acknowledgement

I would like to express my deepest gratitude to all those who have supported me throughout my PhD journey and contributed to the successful completion of this thesis. First and foremost, I am indebted to my Supervisors, Prof. (Dr) Sujit Kumar Biswas, former Professor, Dept. of Electrical Engg, Jadavpur University, Kolkata, Prof. (Dr) Ambarnath Banerji, Professor, EE Dept., Narula Institute of Technology, Kolkata and Prof. (Dr.) Sudipta Debnath, Professor, Dept. of Electrical Engg, Jadavpur University, Kolkata, for their unwavering guidance, invaluable insights, and continuous encouragement. Their expertise and mentorship have been instrumental in shaping the direction of my research and the overall quality of this thesis.

I extend my heartfelt thanks to the members of my doctoral committee, Prof. Biswanath Roy, HoD, EE, Jadavpur University, Prof. Suparna Kar Chowdhury, Dept. of EE, Jadavpur University Prof. Subrata Paul, Dept of EE, Jadavpur University, and Prof. Samarjit Sengupta, External Expert, Dept. of Applied Physics, Electrical Engineering Section, University of Calcutta, University College of Science & Technology, 92, A. P. C. Road, Kolkata 700009, for their constructive feedback, scholarly discussions, and the time and effort invested in evaluating my work.

I am grateful to the Department of Electrical Engineering, Jadavpur, for providing the necessary resources and research facilities. The academic environment and the supportive faculty and staff have played a crucial role in my intellectual development. Special thanks go to fellow researchers who have shared their knowledge and experiences, fostering a collaborative and stimulating research environment. I am grateful to my colleagues and Meghnad Saha Institute of Technology management for supporting me.

I sincerely **appreciate** my **family's** unconditional love, understanding, **and** encouragement. Their unwavering support has been my pillar of **strength** throughout this **challenging** journey.

Last **but** not **least, I want** to **acknowledge** and express my gratitude to all my friends who have **stood** by me during the **highs** and lows of this academic pursuit.

Epsita Das

Epsita Das
14/2/24

Date: 14.2.24.

Jadavpur University

Kolkata-700032

Table of Contents

List of Figures

List of Tables

List of Abbreviations

ANFIS	Adaptive Neuro Fuzzy Inference System
AI	Artificial Intelligence
ANN	Artificial Neural Network
API	Application Program Interface
BEMS	Battery Energy Management
CCS-MPC	Continuous Control Set Model Predictive Control
COP21	Climate Change Conference 21
DERs	Distributed Energy Resources
DR	Demand Response
DS	Dynamic Security
DSM	Demand Side Management
EMS	Energy Management Systems
ESS	Energy Storage System
FACTS	Flexible Ac Transmission System
FCS-MPC	Finite Control Set Model Predictive Control
GA	Genetic Algorithm
IGBT	Insulated Gate Bipolar Transistor
IoT	The Internet Of Things
MG	Microgrid
MHC	Moving Horizon Control

MLIP	**Mixed Linear Integer Programming**
MO	**Microgrid Operator**
MPC	**Model Predictive Control**
MQTT	**Message Queuing Telemetry Transmission**
NARX	**Non-Linear Autoregressive Exogenous**
NLP	**Non-Linear Programming**
P2P	**Peer-To-Peer**
PCC	**Point Of Common Coupling**
PSO	**Particle Swarm Optimization**
PV	**Photovoltaic**
RES	**Renewable Energy Systems**
RHC	**Receding Horizon Control**
SG	**Smart Grid**
SOC	**State Of Charge**
SPWM	**Sine Pulse Width Modulation**
TCP/IP	**Transmission Control Protocol / Internet Protocol**
TOU	**Time Of Use**
VPP	**Virtual Power Plants**
VSI	**Voltage Source Inverter**

Chapter 1

Preface

1.0. Introduction

In the Climate Change Conference (COP21) organized in Paris in 2015, 196 countries signed a treaty on climate change for control the rise in temperature by reducing greenhouse gases. COP27, organized in Sharm el-Sheikh, Egypt, decided to identify the scientific and technological aspects of implementing effective policies to reduce the carbon footprint. The greenhouse gases come out in large amounts when fossil fuels are burnt. Therefore, limiting fossil fuel use can improve the world's environmental scenario. Substitutes for fossil fuel-based energy are renewable energy. These energies are derived from natural sources like the sun, wind etc. and emit almost no greenhouse gases or pollutants into the environment. Society is moving towards electric vehicles (EVs) to reduce pollution and rising temperatures. EV charging can also supply energy to the grid, as mentioned in [1]. With smart meters (SM) and effective energy management systems (EMS), power transfer between two independent local renewable energy-generators become possible. Renewable energy systems (RES) can also be present in power networks as distributed energy resources (DER) to improve environmental conditions. However microgrids (MG) in the form of an energy community would encourage common people to participate in the energy business and contribute to the world energy scenario. Domestic households with solar rooftops could generate and consume electrical energy, reducing the demand on the grid. Storing excess electricity in the battery banks serves the local load in the absence of the sun or main grid during high demand. The microgrid operator (MO) connects traditional grid systems with the MG. MO maintains the EMS so that community residents or consumers can monitor their energy consumption in real-time, observe

market demand, and take responsibility in demand response management, predicting their electricity generation and personal load demand. They can take part in the energy market through MO. Therefore, microgrids are becoming an essential part of the energy sector worldwide.

However, interconnected MGs with the main grid have a number of power quality issues. Flexible AC Transmission System (FACTS) are installed in MGs to improve power quality problems. The sources in the MGs have low inertia compared to conventional synchronous generators. Therefore, reactive power management at the load end is important for the operational stability and reliability of the microgrid. A distribution static synchronous compensator (DSTATCOM) is a shunt compensation device that can be connected to the load end for reactive and active power management.

However, to overcome the drawback of intermittent natural sources and also to make the MGs commercially viable, MGs are evolving in several clustered architectures like community MGs, networked MGs etc. [2] Virtual Power Plants (VPP) are another form of clustered interconnected MGs to address technical and economic issues[3][4][5]. This form of MGs improves the reliability of the power supply. However MGs face power quality issues due to their architecture and components [6]. Moreover, the voltage drop in the MG can be compensated by the reactive power management[7]. So, the reactive power in MGs must be compensated in grid-connected and islanded modes [8][9]. Therefore, energy management systems (EMS) have become essential in MGs to manage available distributed energy resources (DERs), especially photovoltaic (PV) or the wind, which are intermittent and can easily be disturbed by nature. Various control strategies are available in the literature, including security and stability, control and loss management, and economic operation of MGs [10].

With technological advancements, the Smart Grid (SG) is becoming a new option for countries to employ more reliable, sustainable and flexible energy options. In SG, conventional

one-way communication is replaced by real-time two-way communication with adaptive and predictive algorithms and state variable optimization. But this area also has several challenges [11]. Therefore, this thesis researches on the following:

i) to maintain the voltage level of a MG with reactive power management

ii) to propose a method for reducing energy consumption cost of the small residential energy producers in MG

1.1. Research Objective

This thesis searches for methods to improve MGs' performance and reliability as an energy community, making them economically viable. The residents of the communities are small domestic consumers, small industry. Therefore, a real-time dynamic approach for voltage regulation in MG and operational planning depending on power generation and demand forecast is required. This research considers photovoltaic (PV) cells as distributed energy resources (DER). Renewable energy-based power systems, being weak systems, require reactive power generation close to load to unburden the sources. Reactive power management at the load end improves the power factor, reduces the load on the sources, and reduces cost. Though several ways of reactive power management are present in literature, in this thesis, DSTATCOM is adapted for real-time voltage control of the AC bus voltage of the MG. DSATCOM is a flexible AC transmission system (FACTS) device connected in parallel with loads. It has been considered here that the FACTS device is installed at the load end. The main components of DSTATCOM are a voltage source inverter (VSI), a coupling reactor and a capacitor and a battery on the dc side. Therefore, it can exchange both active and reactive power. A resident of MG who can both produce and consume is called prosumer. Prosumer

can produce its own power. A smart solar inverters (SSI) installed at the prosumer end provide active and reactive power in the daytime and only the reactive power at night.

Prosumers with solar roof-tops generate and consume electricity during the day. The battery bank stores excess electrical power generation. This arrangement needs real-time monitoring of the electrical power generation, power prediction on weather conditions, load assessment with time, demand response management etc. The Internet of Things (IoT) connects the regular electrical system with the user, employing internet protocol, smart sensors and interfacing software. Interfacing software connects the user or prosumer with the energy operator (MO), through which one can request for electrical energy buying or selling. During the day, the proposed community support one another with peer-to-peer(P2P) energy transfer. The community sells electrical energy to the grid during peak demand. Therefore, this thesis has considered real-time market pricing on market demand mechanisms.

1.2. Thesis Arrangements

The thesis chapters are arranged as follows:

Chapter 2 introduces the different methods, techniques, algorithms, designs, and facts used to establish this research article. The importance of this chapter lies in the arrangement of the techniques and methods present in the literature for a comprehensive understanding of the research topic.

PID controller is one of the popular control techniques in industry. However, it has some limitations, like trial and error tuning methods. **Chapter 3** explores the difficulty of using simple trial-and-error tuning techniques in the DSTATCOM application.

4

Adaptive methods are present in the literature to overcome these limitations (as discussed in **Chapter 2**). **Chapter 4** narrates an adaptive neuro fuzzy (ANFIS) controller in DSTATCOM for voltage regulation and reactive power management.

MG generally has several micro sources, which may require multiple inverters connected with them. **Chapter 5** applies a continuous control set (CCS) model predictive control (MPC) to the inverter for robust microgrid operation. A single inverter control is presented to illustrate the operation of the inverters within the microgrid. As the microgrid is spread over a small area, the insulated gate bipolar transistor (IGBT)-based VSI with CCS-MPC control is assumed to be connected to the point of common coupling (PCC).

Electric energy production from renewable energy resources in MG reduces the burden on the central grid system. Being energy producers, they can transfer energy to the grid if required. Due to their small size, all these prosumers must form a club to participate in energy trading in the central grid system. This arrangement requires two-way communication between small energy producers and the grid. **Chapter 6** demonstrates a small hardware prototype of a IoT-operated system.

Chapter 7 emphasizes the most economical trading option for the small residential MG.

Finally, **Chapter 8** concludes the whole thesis.

Chapter 2

Literature Review

2.0. Introduction

Microgrids (MGs) are becoming an essential part of the energy sector worldwide with the unfolding of renewable energy resources (RES) and advancement in power electronics and energy storage systems (ESS). MGs can improve power scenarios and reduce carbon footprints, improving power network reliability. However, the sources of MGs are generally natural resources and intermittent; therefore, standalone MGs have limitations. So, the solution is the interconnection of MGs with the primary grid wherever possible. However, interconnected MGs with the main grid have several power quality issues[12]. Frequency and voltage are two essential factors for the stable operation of a microgrid system [13]. Therefore, a power electronic interface like a Flexible AC Transmission System (FACTS) device is employed in MGs to improve real power, reactive power and power quality scenarios[14]. The sources in the MGs have low inertia compared to the conventional synchronous generator. Therefore, reactive power management at the load end is essential for the microgrid's operational stability and reliability. A distribution static synchronous compensator (DSTATCOM) consists of a voltage source inverter (VSI), a coupling reactor and a capacitor installed at the point of common coupling (PCC). This FACTs device is always connected in parallel with the load This device with a dc bus helps maintain MG's dynamic voltage, controlling reactive and active power. It also improves the transient stability margin of the system.

2.1. Voltage Regulation

The main component of DSTATCOM is a VSI. Therefore, by controlling the modulation index of the inverter, its output voltage can be controlled. Voltage is maintained at the critical load bus, controlling active and reactive power transfer. Active power (P) transfer depends on the magnitude of load bus voltage (V) of MG and DSTATCOM voltage (E) where as reactive power (Q) transfer relies on the angles of the phase angles $(\angle\delta_V, \angle\delta_E)$ of the respective voltages. The relation of these four parameters, as shown in Table 2.1, decides the transfer of active and reactive power. The voltages and phase angles are indicated in Fig.2.1.
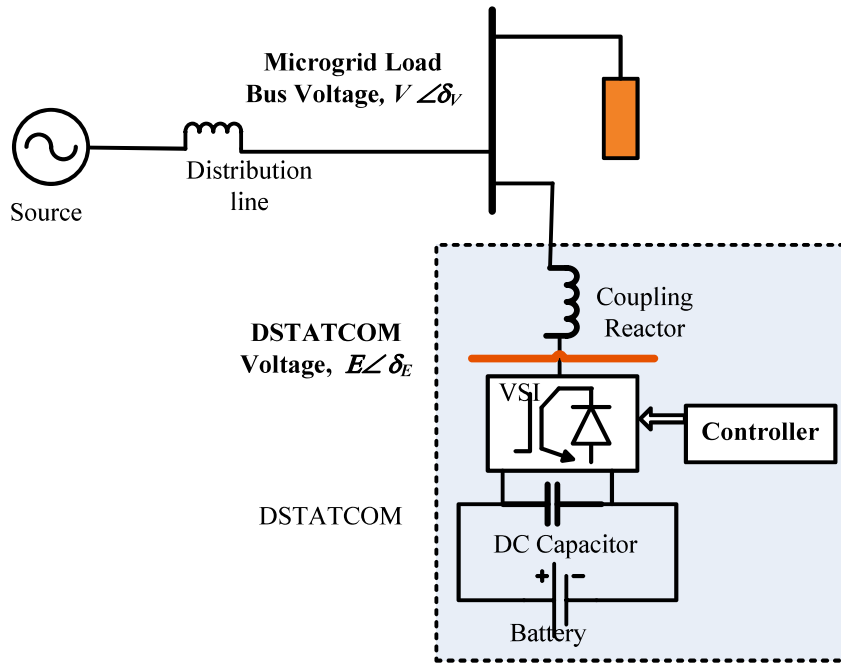
Fig.2.1 DSTATCOM connected at the microgrid load bus

The pulse width modulation (PWM) technique controls the inverter output voltage. An inverter with two-way communication abilities and compatible digital architecture can act as a smart inverter in a smart DSTATCOM. Here, the PWM signal for the generation of gate pulses

is automatically adjusted on the reference signal. The inverter supplies active and reactive power. So, the reference signal for active and reactive components is generated using mathematical transformations which convert the three-phase ac signal into direct (*d*) and quadrature (*q*) components. A set point controller compares the reference signal of the *d* and *q* axis with the system requirement. For any smart device, this controller needs to be intelligent; therefore, it can handle the power flow automatically without minimum intervention from the operator. Therefore the control strategies have significant importance here. Several control methods are available in the literature to incorporate smart features in the inverter. The three-phase signal is converted in the synchronous reference frame (*d*-*q*) following mathematical transform as follows[15]:

$$
\begin{bmatrix} i_d \\ i_q \\ i_0 \end{bmatrix} = \begin{bmatrix} \cos\theta & -\sin\theta & \dfrac{1}{2} \\ \cos(\theta - \dfrac{2\pi}{3}) & -\sin(\theta - \dfrac{2\pi}{3}) & \dfrac{1}{2} \\ \cos(\theta + \dfrac{2\pi}{3}) & \sin(\theta + \dfrac{2\pi}{3}) & \dfrac{1}{2} \end{bmatrix} \begin{bmatrix} i_{La} \\ i_{Lb} \\ i_{Lc} \end{bmatrix} \tag{2.1}
$$

The three-phase supply from the *d*-*q* frame is then obtained using Park's transformation as expressed in (2.3)

Table2.1. Simultaneous Exchange of Active and Reactive Power by DSTATCOM

$\angle\delta v, \angle\delta E$ V and E	$\angle\delta_E$ leads $\angle\delta v$	$\angle\delta_E$ lags $\angle\delta v$
$|E|>|V|$	Supply both P & Q	Supplies Q and Absorbs P
$|E|<|V|$	Supplies P and Absorbs Q	Absorb both P, Q

$$\begin{bmatrix} i_{sar} \\ i_{sbr} \\ i_{scr} \end{bmatrix} = \begin{bmatrix} \cos\theta & \sin\theta & 1 \\ \cos(\theta - \frac{2\pi}{3}) & \sin(\theta - \frac{2\pi}{3}) & 1 \\ \cos(\theta + \frac{2\pi}{3}) & \sin(\theta + \frac{2\pi}{3}) & 1 \end{bmatrix} \begin{bmatrix} i_{dr} \\ i_{qr} \\ i_{0r} \end{bmatrix} \qquad (2.2)$$

Proportional (P) and Integral (I) controllers are very popular as controllers. However, from voltage-frequency control, active-reactive power management communication capabilities are essential for a smart inverter. Parameter estimation, adaptability, and communication-induced optimal operation demand response management need internet connectivity and cloud compatibility. Therefore, simple proportional integral derivative (PID) techniques do not satisfy this purpose, and an internet-enabled robust intelligent digital controller is essential, as shown in Fig.2.2. As the power system is entirely nonlinear thus, if operating condition changes the PI controllers need to be retuned. Therefore at least adaptive tuning methods needs along with PI controllers.
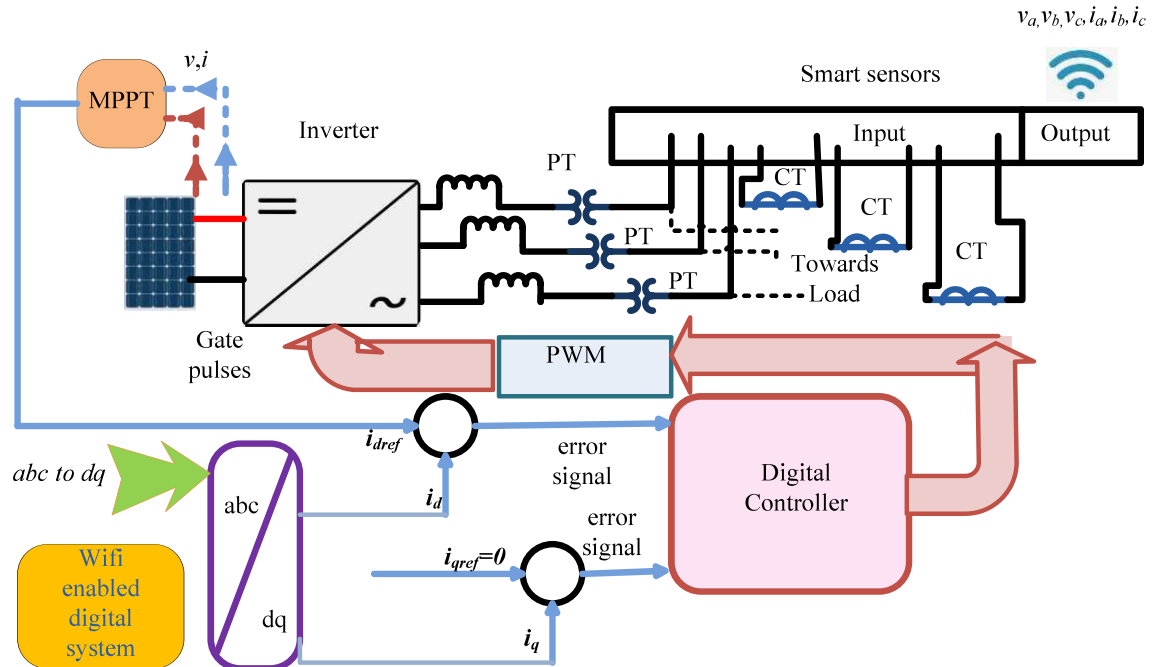
Fig.2.2. Smart inverter connected in microgrid system

9

2.2 Adaptive PI Tuning

Several adaptive PI controller tuning is present in the literature for smart inverter operation in MGs. A fuzzy logic controller is implemented in [16]-[17] to impose self-adjustment of the co-efficient of PI controllers. An offline gain scheduling approach is proposed in [16] to identify the current operating conditions of the system. PSO extracts the best K_p and K_i from defined fitness functions. An adaptive backpropagation algorithm is proposed in the literature[17] for auto-tuning the PI controller. However, the limitation of backpropagation is the slow convergence speed. Therefore, bat echolocation is implemented to overcome the delay. The genetic Algorithm (GA) implemented in [18] optimizes gain constants and tunes the PI controllers to reduce disturbances. An advanced control technique that is applicable to DSTATCOM was proposed in [19] to overcome regular and severe disturbances at an electric ship power system. In [20], following a bus voltage reduction from reference quantity particle swarm optimization (PSO)-based tuned four PI controllers, the regular load condition took necessary steps to energize the capacitors to pull up the bus voltage level. For severe load fluctuations, artificial immune system based control action takes steps until the system returns to its original condition. A model-free technique to control a DSTATCOM is illustrated in [21] based on input and output data tabulation for different operation conditions. Artificial Neural Network (ANN) is used in STATCOM to calculate a wind farm's proportional and integral gain constants [22]. A nonlinear robust fuzzy PI controller is demonstrated in [23] to maintain better performance than fixed PI controllers.

A simple Sugeno-type fuzzy controller is described in [24]where the Grey Wolf Optimization technique is employed to design the scaling factors. A self-adaptive learning bat algorithm fuzzy controller is demonstrated in [25], where the controller works for both

STATCOM and power system stability. In this article, the PI controller of STATCOM is replaced by the fuzzy controller. Therefore, Alternatives to PI control schemes and other control algorithms for DSTATCOM are also much more prevalent among researchers.

2.3 Adaptive and Predictive Control Methods for DSTATCOM

2.3.1. Adaptive Linear Neuron (Adaline)

Adaline is a type of artificial neural network (ANN) used for supervised learning in machine learning. Adaline adapts its weights using gradient descent during the training process. The weights are continuously monitored and adapted to minimize the error between the predicted and the target outputs. Least mean square (LMS).A least mean square- Least Mean Fourth (LMS- LMF) algorithm is proposed in [26] to overcome power quality problems at PCC for zero voltage regulation as well as unity power factor mode. Bhattacharya proposed the Adaline technique to improve power quality as well as to cope with the uncertainty in filter parameters [27].In [28], a control scheme also applied Adaline to eliminate harmonics in load current. In [29], Adaline extracts a balanced positive sequence fundamental frequency component of the load current. The hyperbolic tangent-based function-based LMS algorithm is used to control permanent magnet synchronous generator voltage in an autonomous system [30]. Here, the LMS algorithm changes the learning rate depending on an error between the reference source and the current load current. Kumar et al. applied a fuzzy logic controller at the DC bus for maximum power extraction and for the AC bus, Adaline, to enhance power quality [31]. The Adaline controller tracks reference current in the same direction as the unit voltage template with the least possible error. A finite set model predictive control is designed with the Adaline technique for the determination of switching instants of a VSI [32].

2.3.2.Adaptive Neuro-fuzzy Inference System (ANFIS)

ANFIS is a fuzzy Intefence system (FIS) with learning ability from an artificial neural network (ANN). It overcomes the need for human expertise for the fuzzy system. The faster training, the effective learning algorithm, and the clarity in the software approach give ANFIS significant advantages over the others. A DSTATCOM with ANFIS control technique is proposed in [33] to improve power quality. The method is compared with PI-based and ANN-based control. The percentage voltage sag with the ANFIS method gives a better response than the other two methods. To avoid the tedious tuning process of the PI controller in a wind turbine emulator described in [34]. The application of ANFIS in a wind farm is discussed [35]. Other applications of power oscillation control between two areas, such as controller design for electric vehicles, are also available in the literature. This thesis also uses ANFIS for reactive power management to maintain a voltage profile at the point of common coupling (PCC).

2.3.3. Predictive Control

Predictive control prediction of the control variable's future behaviour is estimated using the plant's model. Predictive control is classified as deadbeat control and model predictive control. Both of the controls are popular among researchers but have limitations.

2.3.3.1. Deadbeat Predictive Control

This control predicts the precise input, which brings the system to a steady state in the lowest possible time steps [36]. The switching signal for the inverter needs reference current

12

extraction. Therefore, the deadbeat controller minimizes error in a single step, i.e., the difference between the measured current, *i(n)*, at a particular sampling instant and the reference current, i_{ref} *(n),* within the next sampling time. Predictions are made using a discrete-time system model. A modulator circuit is required to generate the phase voltage, which diminishes the error. The benefit of the modulator is fixed frequency switching, which reduces harmonics[37]. [38][39][40][41] demonstrate this control strategy upon three-phase inverters.

2.3.3.2. Model Predictive Control

Model predictive control (MPC) has powerful features in controlling inverters. This strategy is classified into two categories: continuous control set (CCS MPC) and finite control set (FCS MPC). FCS-MPC does not require any modulator, yet complex calculations lead to variable switching of the inverter. An increased number of switching states causes harmonic penetration in voltage and current waveform, leading to power loss, audible noise etc. CCS-MPC needs a modulator but results in fixed-frequency switching. MPC's strategy to control the inverter is proposed in [42]. The authors applied an observer to remove the voltage and current sensors. As MPC depends on the model, unmodeled dynamics can affect system performance; therefore, it needs a more considerable amount of calculation, which introduces a time delay between measurement and implementation. A co-ordinated voltage control with the MPC technique is proposed to reduce voltage variation and optimize the reactive power demand in the wind farm [43]. A Finite Control Set (FCS) MPC-driven grid-connected inverter switching is also presented [44][45]. As it depends on the model, unmodeled dynamics can affect system performance, and MPC needs a more considerable amount of calculation, which introduces a time delay between measurement and implementation. An observer-actuated nonlinear MPC is used in [46] for reactive power management. A droop-controller
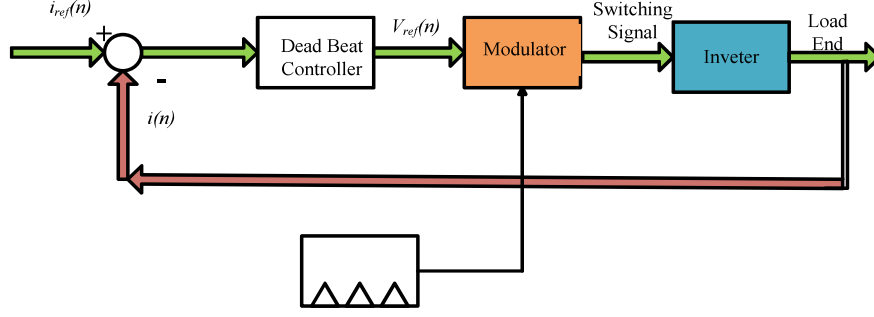
Fig.2.3(a). Dead Beat Predictive Control Schematics
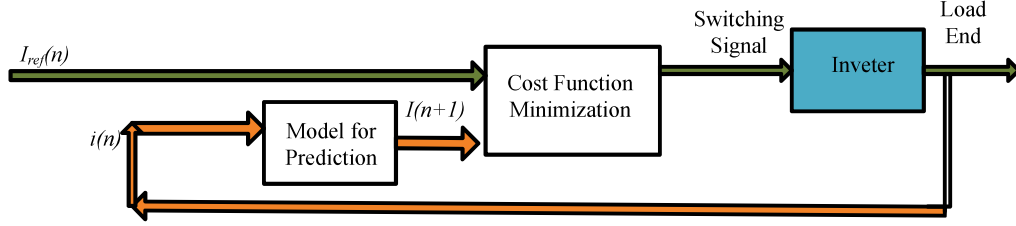
Fig.2.3(b). Model Predictive Control Schematics

assisted with the MPC technique is proposed [47] to reduce voltage variation in the wind farm. A finite control set (FCS) MPC-driven grid-connected inverter switching is presented [48][49], [50]. The general drawback of this method is the variable frequency switching, which leads to harmonic generation and, therefore, needs a complex filter design. CCS MPC can overcome this problem.[51], [52] demonstrates the application of CCS MPC for inverters. A fuzzy logic controller with a Lyapunov stability function is proposed to control STATCOM and improve the transient stability of the power network [53].

2.3.4. Miscellaneous Control Techniques

A nonlinear control approach for STATCOM is proposed in [54] for application in an electric arc furnace. For inputs within range and with appropriate Lyapunov function, the authors established the system to be asymptotically stable and derived a single control parameter with only the criterion of being large positive, which was definitely simpler in technique than double loop PI control where four numbers of controller gains were required.

Feedback linearisation is a technique to transform nonlinear system dynamics into linear one. This technique is proposed in [55][56][57]. Stability and desired transient response are significant in designing a controller for STATCOM operation. Under parametric uncertainties, the authors proposed a zero set concept that calculates the state feedback parameter set for STATCOM and placed closed loop poles at the required complex plane area to get a more robust system response than the system designed by linear matrix inequalities (LMI)[58]. A particular port-controlled Hamiltonian system form and an input-output linearisation tracking control strategy have also been proposed. A least mean mixed norm adaptive control is prescribed for reactive power compensation [59]. Lyapunov theorem is used to determine the stability of a system. A back-stepping control with Lyapunov stability analysis is demonstrated in [60].

2.4. Smart Inverters

The primary component of the FACTS device is voltage source inverter (VSI). Inverter is also an essential component for solar-powered ac microgrids. Therefore, inverters with bi-directional communication abilities, software compatible digital architecture interfaced with microgrid systems with the appropriate control can also address power quality issues in MG. Reactive power management using smart inverters are proposed in [61]–[63]. Voltage and frequency control of an islanded microgrid using a smart inverter is demonstrated in [64]. A smart DSTATCOM in [65] achieves a stability enhancement voltage profile. [66] also indicates the application of smart inverter in the MG system's controllability and stability.

2.5. Energy Management in AC Microgrid

Reactive power management is a part of the energy management of a microgrid system. From the literature study, various objectives of energy management in MGs are observed. It can be broadly classified into two divisions.

i)   to manage the loss of energy without involving direct financial transactions [67].

ii)   to manage demand responses, especially for profit maximization [68].

2.6. System Behaviour Model

Analysis of system behaviour is essential for modelling microgrid sources [69]. Mathematical modelling generally considers random variables of the environment or uses any deterministic data. As per the analysis, Stochastic and deterministic approaches are available in the literature.

2.6.1 Stochastic and Probabilistic Approaches

Renewable energy sources (RES) like photovoltaic (PV) or wind are weather dependent. Energy production is dependent on various random environmental factors. Therefore, the application of stochastic and probability theory in literature is eminent for energy management for power system planning and reliable functioning[70]–[74]. Probabilistic power flow methods demonstrate the impact of uncertainties on the power flow[75], [76].

2.6.2.Determinsistic Approches

Deterministic approaches are also available in the literature to analyze the impact of energy management on MGs. For example, a deterministic approach is described in [77] for the cost minimization of MG. In addition, parameters for the one-year operation of a stand-alone microgrid is calculated [78] using a deterministic model.

2.7. Optimization for Solution

An optimization process is essential for energy management in a microgrid. Therefore, several optimization tools are used in literature to minimize energy losses or maximize energy generation. Linear and nonlinear optimizations are available in the literature for this purpose.

2.7.1. Linear programming (LP)

This method is applicable only if the model is linear. A mixed linear integer programming (MLIP) is proposed in [79] where an optimum generation and load demand minimizes the cost function. The battery's charging and discharging power cycle is obtained in [80]using LP to minimize the overall energy consumption cost, considering several operational aspects in microgrids. In another article, MILP minimizes the total cost of MG considering the technical constraints [81]. A battery-based hybrid microgrid uses MILP [82].

2.7.2. Non-Linear programming (NLP)

A mixed integer nonlinear programming (MINLP) is applied in [83]. A non-convex MINLP is solved using a global optimization technique in [84] and a Q learning algorithm in [85].

2.7.3. Metaheuristic Optimization

Metaheuristic process is the iterative process where computational tools continuously try to identify the best solution for a purpose. Artificial intelligence is a key tool of this technique.[86] applies a fuzzy neural for the prediction of solar energy generation. A hybrid algorithm with wavelet transform and fuzzy logic is applied for solar power generation prediction in [87], whereas load forecasting using artificial neural network (ANN) is proposed in [88]. The particle swarm optimization technique for battery energy storage systems (BESS) is applied in [89][90][91]. The genetic algorithm(GA)uses the theory of natural selection procedure to optimize power generation of distributed energy resources (DES) in [91], whereas in [92] and [93], GA is used for minimization of operational cost.

2.8. Hierarchical Control

EMS focuses principally on three aspects: a) Primary: security and stability of the network b) Secondary: operation and control of microgrid c) Tertiary: operation co-ordination between one or more microgrids and the main grid. Resilience towards fault and flexibility to move back to normal operating conditions is the primary function of EMS, especially for autonomous microgrids where support from the main grid is absent from balancing generation

and load demand. Primary control is the fastest among all three sets of control. Secondary control is responsible for maintaining steady state voltage-frequency variation in a microgrid. An effective energy management system pulls down the losses and is able to flatten the load curve at peak load hours. It maintains power balance in the microgrid, preserving power quality. Tertiary control communicates between the main grid and microgrid for economic operations.

2.8.1 Primary Control

Existing security and stability analysis practices for microgrids can be classified into probabilistic and risk assessment methods. A static security assessment can be classified into offline and online modes. The offline method evaluates possibilities of over or under voltage in the system or condition of overload. In online mode, the security system estimates data from the system and takes corrective action if required. This is the fastest among the three hierarchical controls. Online dynamic security (DS) assessment in microgrids is described in [92][93][94]. Dynamic stability improvement of a hybrid microgrid is addressed in [95]. Literature reviews on security aspects are discussed in [70], [71], [96], [97]. MGs are the cornerstone of smart grids, where communication with equipment through the internet is possible. This increases the risk of a cyber-attack on the grid system. Prevention of MG from cyber-attack is discussed in [98]–[100].

2.8.2. Secondary Control

Secondary control includes control of steady-state voltage frequency and active-reactive power variation. This level regulates the battery energy management (BEMS) system

or energy storage system (ESS) of microgrids to control the system's power flow. It is responsible for the reliable operation of MG. Papers [101][102][103] describe the secondary control action in the MG system.

2.8.3 Tertiary Control

This is primarily responsible for optimal energy management as well as market operation. Among all three control sets, it is the slowest. After achieving stable operation in primary or secondary control, the tertiary layer initiates load balancing among the DERs and controls the generation using a prediction mechanism to reduce operational cost, demand response and demand side management. The articles [104] and [105] demonstrate tertiary control for the optimal operation of MG. Demand-side management aims to optimize energy consumption by educating consumers and providing incentives for less energy consumption, especially during peak demand. Demand Side Management (DSM) and two-way communication are two important basic features of SES. Advanced Metering systems are indispensable for two-way communication, making residential commercial or industrial consumers evolve as active entities or players in the new grid system. Demand response programs can significantly improve the dynamic stability of microgrids [106]–[109].

2.9. Control Architecture

The central control or distributed control generally takes care of hierarchical controls. Master-slave and droop control are very popular among researchers in implementing control algorithms [110]. With a central controller architecture, a reactive power sharing with hhierarchical droop control upon converter parameter is developed in [111].

2.9.1 Centralized Controller

The master-slave control strategy is a typical example of the centralized control architecture. In this method, local load controllers are used to connect to the devices but cannot operate unless they get a command from the master central controllers. A centralized controller with tertiary control for economical operation is described in [111].

2.9.2. Distributed Controller

In this architecture, the local controllers do not always depend upon the master controller. Here, the independence of the local controller is more than a centralized system. Therefore the downtime is much less. Distributed control is demonstrated in [112] and [113].

2.9.3. Decentralized Controller

This control is robust, especially in terms of cyber attacks. This control employs parallel processing in order to avoid failure[114]. Decentralized control is described in [102], [115].

2.10. Demand Side Management (DSM)

Residential microgrids are gaining interest in the modern power sector. Demand-side management effectively saves energy and increases system efficiency with cost reduction. It

manages electrical demand in a power network for a longer duration with demand response (DR) management, energy efficiency and strategic load growth as its elements [116]. DR operates in two basic forms-

1. Incentive-based DR and

2. Price-based DR.

The first method introduces incentives to reorient the consumer's energy consumption patterns. [117], [118] applied incentive-based DR for energy management. Discount in time of use (TOU) is applied in [119], and retail pricing-based DR is proposed in [120]. A parametric time utility model is observed in [121]. [122] discusses a detailed literature review on TOU. Artificial Intelligence (AI) tools and techniques provide convenient solutions for DR.[120],[123] applies machine learning (ML) for scheduling electrical loads.

In this context, Dynamic Programming is applied [124], [125] for demand management at the consumer end. Authors applied MILP to optimise batteries' charging and discharging time and demand response hours in power system networks [126]. Reinforce learning and fuzzy logic is applied for demand response management (DRM) in a residential system[123]. Reinforcement learning with Markov decision process (MDP) uses the state transition function and reward function to model the random decisions in DSM [127]–[129]. But if reward and state transition functions are unclear, Q table reinforcement learning is the choice.[130], [131] uses the Q learning mechanism to obtain the optimal result. The demand response optimization strategy in the literature can also be deterministic or stochastic. The deterministic approach is used in [132], [133], and the stochastic approach is observed in [134], [135].

2.11. Managing Energy with an Economical Aspect

Energy trading is also present in literature in the form of energy management. The inclusion of RES in the power network has compelled conventional energy systems to provide space for green electrical energy [136]. This scenario increases the possibility of peer-to-peer (P2P) energy transfer where a comparatively more minor energy producer with RES can contribute to society's energy demand. However, the uncertainty demands an association energy storage system (ESS) with these sources. ESS acts as a load during charging and as a source during discharging. The lifespan of a battery also depends upon its charging current. Therefore, optimization of the battery energy management system is crucial in this scenario. Now adays, electric vehicles are also part of the grid system. In this context, the cost of ESS with charging equipment and electricity pricing are optimized [137]. Optimization of ESS is also an important aspect for the energy community [138], industrial or commercial consumers [139] and even for onboard ships [140][141]. However, all these procedures need smart electrical gadgets over the Internet [142]. As optimization methods solve for the best possible strategies for a given set of problems within a boundary condition, they finally aid the economic benefit for the given system. Therefore, it also helps P2P energy trading, providing a systemic approach. Meeting the load demand locally is advantageous in reducing transportation costs and opens an online platform to trade electricity directly from seller to buyer via an energy operator . Due to the small size of the electrical energy producers by RES (prosumers), operator works as an aggregator and is responsible for monitoring and controlling energy transfer. Trading methodology and risk management are distinct characteristics of P2P energy trading.

In literature, trading in the local market is between two individuals directly or through a mediator [143]. Multiple sellers and buyers with different cost functions participate in this market structure in auctions for buying or selling electricity [144]. Game theory [145][146], a

strategy for decision-making in a rational environment, is also used in this context. In literature, game theory is also used to balance utilities and consumers in the form of demand response management[147], [148].

However, peer-to-peer (P2P) energy transfer can be possible within the community microgrid (MG) if it follows a common microgrid bus (MB) architecture [149]. P2P differs significantly from the conventional energy business model and has become popular among researchers. In this model, small energy producers can participate in an energy trading platform following specific regulations. The authors discuss three methods to determine the unit price of energy in MG for P2P energy trading [150]: bill sharing among community residents depending upon own consumption, midmarket price between buying and selling energy rate and auction strategy. However, it did not consider the installation and maintenance expenses. Anon *et al*. proposed the Stackelberg game as a model for price determination in [151]. Here, the seller acts as the leader and the buyer as the follower. It ensures *that* this negotiation reduces the energy price by almost 47% more than conventional fixed-price purchasing. However, this paper did not explain the community's demand and supply relation or the market clearing price (MCP). A bilevel-optimized bidding strategy is formulated in [152], where renewable and conventional energy bidding happens simultaneously in the same energy market. A multi-agent system (MAS) is used for P2P energy transfer in the active distribution network (ADN) for electricity price and quantity determination [153]. The author suggested that several agents are working here to ensure an optimized price to prosumers but did not consider the cost for the agent network. A strategic bidding model is proposed using reinforced MAS [154]. A bilateral energy contract was proposed in [155], where the author proposed a bilateral arrangement between the generator and consumer, bypassing the community controller, who is charged for providing ancillary support. However, the method of searching the buyers and sellers, bypassing the operator, is not adequately modelled in the proposed method. The authors

assessed the effect of interaction between a wind power plant and a system operator with a bi-level bilateral contract on price in the day ahead market [156]. In [157], the authors considered the storage unit of a community microgrid as a virtual power bank and modelled the residents' actions for minimizing total energy cost and maximizing individual profits by applying dynamic game.

Microgrids with RES as sources need smart monitoring and control, which can be possible using the Internet of Things (IOT). It makes it possible to control loads from anywhere in the world through a web application that serves efficiently for demand response management (DRM), managing and transferring energy, observation, control, and protection of new age grid systems. A conventional grid uses a low-cost, cloud-based load monitoring approach [158] for electricity theft detection. Energy management for dispatchable and non-dispatchable sources with controllable and non-controllable loads is proposed in [158]. Spano et al. proposed an IOT-based power scheduling for a consumer concerned new age grid system. However, IOT produces extensive data per unit of time, which requires the cloud to store that data efficiently.

However, cyber security issues are crucial if these devices are operated online and constantly interact with internet traffic. Therefore, including security features with the IOT devices is vital to identify possible threats [159], [160]. Blockchain is an important security concept for distributed databases as IOT devices share a web-based cloud. In the blockchain, data are structured into immutable data blocks, providing security[161]. A blockchain model in the Ethereum platform for energy trading is proposed in[162]. In [163], a permission Hyperledger Besu blockchain is employed for efficient and secured P2P trading. As DRM is also an essential criterion for economic welfare and energy optimization, researchers studied different methods of DRM for MGs [164], [107], [165]. To lessen carbon footprints, all possible ways of including DER in the power network can be an apt measure. Therefore, even small households with rooftop solar can be a possible solution for a sustainable future with

storage. However, appropriate contemporary plans are essential to motivate small, non-professional energy producers. Proper legislation is required to balance small energy producers and traditional professional players in the energy market. For an improved society, social consciousness and commitment towards an independent, reduced carbon energy efficient community can be one of the solutions in this aspect. The literature survey specifies that these small energy communities appear as networked microgrids [166] under a community microgrid operator (MO) operation. However, every community has different characteristics, and the operation is successful if it is driven by the community's needs [167].

In [168], a two-stage energy community model is proposed. In this model, the prosumers are connected with the supplier, and the net meter measures the incoming and outgoing energy, and a balancing cost (positive or negative) is determined. They can participate in community trading depending on the balancing value of the net meter. The authors consider a central agency that would schedule the flexible loads' operating time to optimize the electricity cost. However, this approach reduces the comfort factor of the community residents. Therefore, an alternative approach is proposed in this chapter where the community residents can set their respective essential loads to maintain the comfort factor. Bill sharing (BS) or mid-market rate (MMR) used in [168] is not encouraging enough to decide the proper payoff for peer-to-peer (P2P) energy transfer [169].

This thesis finds a way to balance energy demand optimization within the community, minimizing carbon footprint during electrical power generation and maximizing community payoff from green energy trading. Representation from the community ensures community interest, which is unfortunately absent in most works of literature. Therefore, this work proposes an approach of delegates from the community to look after community interests. The proposed model is almost energy-self-sufficient during sunshine hours. In the literature, most studies concentrated only on P2P energy trading, barely observing the community's social

welfare. In [170], the social behaviour of prosumers is modelled during winning and losing the game during trading, but it does not reflect the social responsibilities.

Therefore, the overall objective of this thesis is to

- **Apply** an adaptive control strategy for a plug-and-play DSTATCOM connected to non-conventional micro sources.

- **Employ** low-cost IoT-operated hardware prototypes for demand response management.

- **Search** the strategy for maximizing microgrid payoff while participating in energy trading.

2.12. Discussion

Increasing energy demand is characteristic of the modern era. The challenge is generating and consuming energy, reducing negative environmental impact and promoting cleaner and sustainable options. Renewable energy resources are a choice for a cleaner future. However, these energy sources suffer from certain drawbacks. Despite several limitations, renewable energy sources can solve this problem sustainably. However, this concept needs a more structured approach and effective legislation. This chapter inspects and reviews the strategies presented in the literature for energy demand optimization in AC microgrids.

.

Chapter 3

Voltage Regulation with Proportional-Integral-Derivative Controller DSTATCOM

3.0 Introduction

Renewable power generation is an important affair in the modern world. Renewable energy sources (RES) are smaller than conventional power generators. These small power networks are prone to power quality issues, which also affect the operation of the grid. FACTS controllers provide solutions for grid reliability, supporting the inclusion of renewable energy sources. DSTATCOM is a shunt compensator that looks after the consumer's reactive power demand and rectifies the distorted and unbalanced terminal voltage. The components of DSTATCOM are a voltage source inverter (VSI), a DC capacitor, a coupling transformer and a controller if it is only transferring the reactive power. For active power management a DC source is essential. The system's function and efficiency solely depend upon the proficiency of the controller. The controller responds to the system dynamics and provides a solution depending on the control algorithm written inside. The control algorithm of the DSTATCOM is applied for the reactive power exchange between the DSTATCOM bus and the bus at the point of common coupling (PCC). PCC is where consumers' loads are connected to the utility grid. Renewable energy resources are also connected to the PCC to feed excess generation to the grid. Fig.3.1(a) depicts the per-phase equivalent circuit to understand the DSTATCOM operation. If the compensator bus voltage is E and the PCC bus voltage is V, the device injects current to the grid if $|E| > |V|$. This mode of operation in known as capacitive mode. The equation of this mode is explained in (3.2), and the phasor diagram is shown in Fig.3.1 (b).
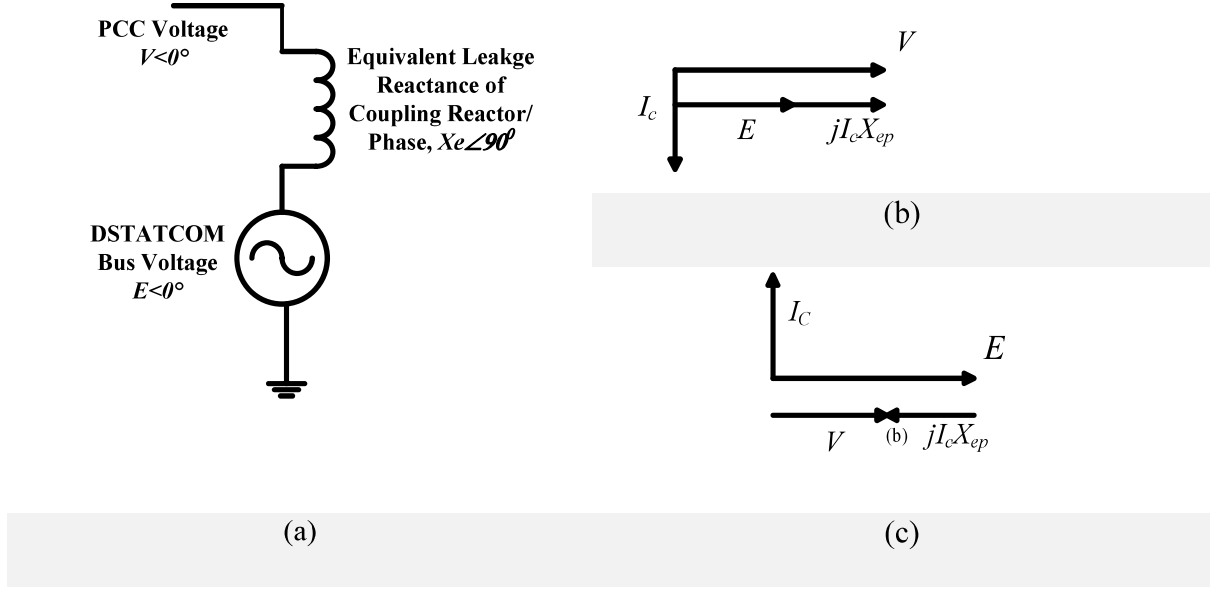
Fig.3.1 (a) Equivalent Circuit of Phasor Diagram of DSTATCOM operation
DSTATCOM per phase (b) inductive mode (Ic lagging) (c) capacitive
mode (Ic leading)

Applying Kirchoff's voltage law (KVL) in Fig. 3.1(a)

$$E\angle 0^0 - V\angle 0^0 = jI_c X_e$$

$$E\angle 0^0 + V\angle 180^0 = jI_c X_e \qquad (3.1)$$

$$\therefore I_c\angle\theta = \frac{E\angle 0^0 + V\angle 180^0}{X_e\angle 90^0} \qquad (3.2)$$

Ic is leading by $90^0$and DSTATCOM supplies leading reactive power.

Similarly, For $|E|<|V|$

DSTATCOM absorbs the reactive power and is in inductive mode, as expressed

$$V\angle 0^0 - E\angle 0^0 = jI_c X_e \qquad (3.3)$$

$$\therefore I_c\angle\theta = \frac{V\angle 0^0 - E\angle 0^0}{X_e\angle 90^0} \qquad (3.4)$$

Ic is lagging by $90^0$and DSTATCOM absorbs lagging reactive power.

29

3.1. Control Structure

Four sets of proportional, integral and derivative (PID) controllers are required to manage active and reactive power. In this chapter, only reactive power management is considered. Therefore, three sets of controllers have been used. The control algorithm is divided into two loops- the voltage regulator loop and the current regulator loop, as shown in Fig.3.2. The load current and the voltage at the point of common coupling (PCC) are converted from three phases (*a-b-c*) to two axis variables-direct and quadrature(*d-q*) components. The *d* component is responsible for the active power, and the *q* component is for reactive power. The setting of controller gains for all three controllers needs to be appropriately matched to get the desired response. This procedure is generally a trial and error approach, and it is necessary to re-tune the DSTATCOM controller when there is a substantial change in the distribution network parameter or load demand, such as switching off a line due to a fault condition, etc.
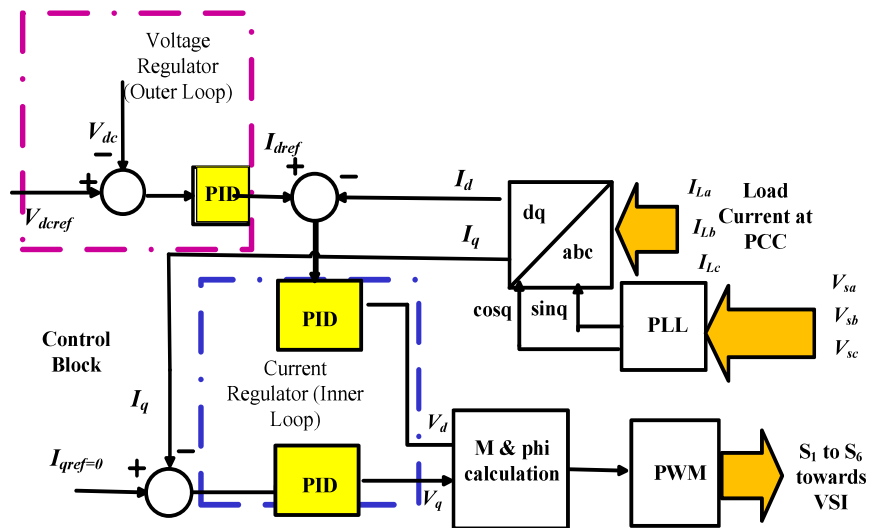
Fig.3.2 Control Structure of PID Controlled DSTATCOM for Reactive Power Management

3.2. System Configuration
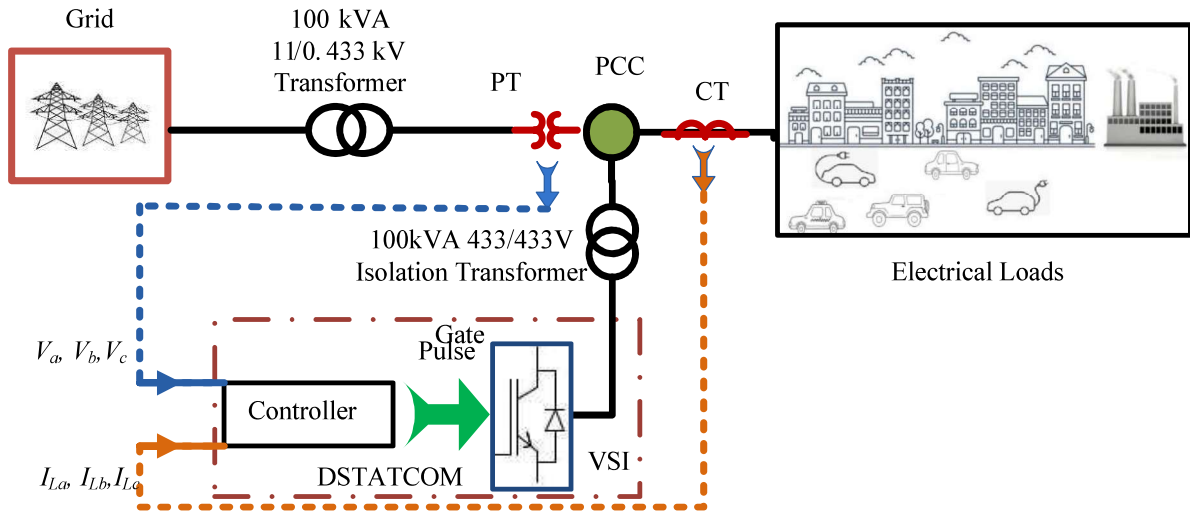
Fig. 3.3. DSTATCOM connected with system loads

A system network is designed with 11kV rms (line-line), 50Hz source, 100kVA, 11/0.433kV delta/star, 3 phase transformer as shown in Fig.3.3 in MATLAB Simulink. The shunt compensation device DSTATCOM is connected at the load end to deliver reactive power required by the load and to regulate PCC voltage at 433V (1pu). A rabbit conductor of 50 sq mm is taken as the distribution feeder at 433V in this case study. Feeder lengths are generally restricted to 2 km to avoid significant voltage drops in the aerial distribution system, per Indian Electricity Rules, 1956 [171]. Here, the DSTATCOM is 2 km away from the PCC. The resistance per km is about 0.5426 Ω/km at 20°C. In the transmission line, the inductance per conductor is calculated as

$$L = 2 \times 10^{-7} \ln \frac{D}{r'} \text{ H/m} \tag{3.5}$$

Where r' is the geometric mean radius and equal to 0.7788 times the conductor radius r, D is the space between two adjacent conductors.

Capacitance is calculated as

$$C = \frac{2\pi\varepsilon_0\varepsilon_r}{\ln(\frac{D}{r})} \text{ F/m}$$ (3.6)

Where permittivity of free space $\varepsilon_0 = 1/(4\pi \times 9 \times 10^9)$F/m and $\varepsilon_r = 1$.

Table 3.1 indicates the feeder's calculated resistive, inductive and capacitive effects under observation.

3.3. DSTATCOM Model

The system can be modelled as a 2nd order unity feedback system, as shown in Fig 3.3. $R(s)$, $E(s)$ and $C(s)$ represent the input signal, error signal and output signal respectively. The

Table 3. 1. 2 km Feeder Specification

Conductor	Area (sqm m)	Length (km)	Conductor span (m)	Resistance/ km at 20ºC	Resistance (ohm)	Inductance (mH)	Capacitance (nF)
Rabbit	50	2	0.15	0.5426	1.0852	1.2316	30
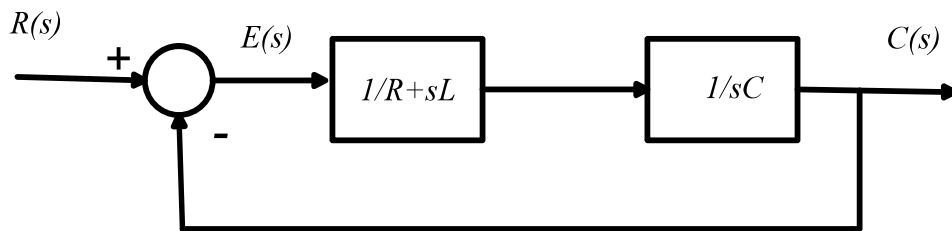
Fig. 3.4. 2nd order unity feedback system

primary component of a DSTATCOM is a voltage source inverter. The linear equivalent circuit of an inverter can be represented as an RLC circuit, as shown in Fig.3.4, with $R(s)$

considered as step voltage [172]. The standard 2nd order closed loop system transfer function, T(s), is:

$$T(s) = \frac{k\omega_n^2}{s^2 + 2\varsigma\omega_n s + \omega_n^2} \tag{3.7}$$

where k=DC gain; ς= damping ratio; ω_n= un-damped natural frequency of oscillation

RLC circuit can be modeled as 2nd order differential equation as follows:

$$L\frac{d\,i}{dt} + Ri + \frac{1}{C}\int i\,dt = v_x \tag{3.8}$$

where L= inductor value, R= resistance, C= the capacitance value and i= circuit current and v_x= step voltage.

Thus, the transfer function (TF) is given by:

$$\therefore T.F = \frac{1/LC}{s^2 + sR/L + 1/LC} \tag{3.9}$$

Comparing it with equation (3.5),

$$\omega = \sqrt{1/LC} \text{ and } \varsigma = (R/2)\sqrt{C/L}$$

3.4. Controller Tuning

The open loop approach or Cohen Coon method of controller parameter identification is not possible in this case as the DSTATCOM model is linear. It only shows a linear relationship with time if step voltage is applied in the input. The closed-loop response of the RLC system (with calculated values in table 3.1) with step input was obtained in MATLAB, as shown in Fig.3.4. This test is to identify the transient behaviour of the inverter model. The inverter model's open loop and closed loop transient response does not follow the curve patterns for any of the two methods for the Zeigler-Nicholes method. Other PID tuning methods also

have some limitations. Therefore, a PID controller is tuned in MATLAB to improve the dynamic stability with a trial and error approach.
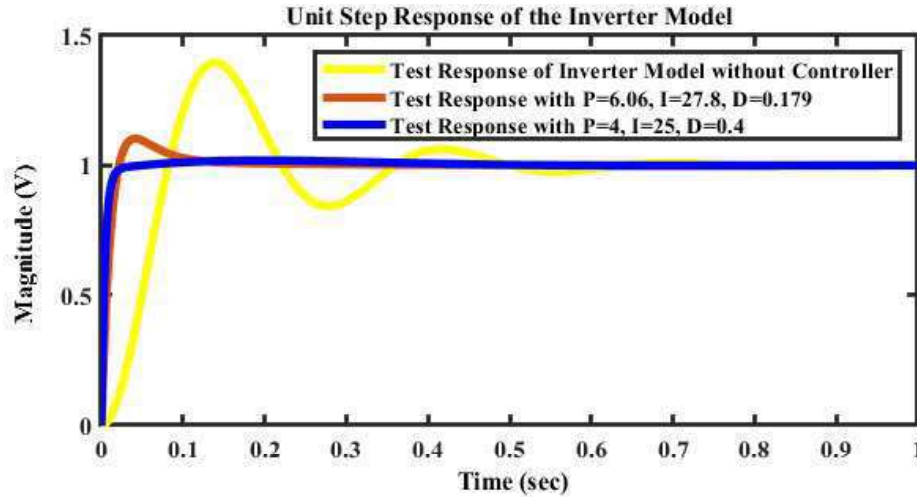
Fig.3.5. Step response of 2nd order DSTATCOM model

3.5. Results

Both tuned values determined from the DSTATCOM model, as shown in Fig.3.4, are applied to the current regulator loop of the system as indicated in Fig.3.2. PCC voltage response with simulated controller coefficients are shown in Fig.3.6. Fig. 3.5 shows the step response for a 2nd order system with and without controller. Two sets of PID gain of controller parameters are taken for desired responses. However, Fig. 3.6 indicate that PID controller values that give satisfactory results for the designed model may not give an acceptable response for the actual system. Improper tuning of the controllers can deteriorate power quality. The terminal voltages are calculated as

$$V_t = \sqrt{\frac{2}{3}(v_a^2 + v_b^2 + v_c^2)} \quad \text{or} \quad V_t = \sqrt{v_d^2 + v_q^2} \qquad (3.10a)$$

Where v_a, v_b, v_c are three phase voltages and v_d and v_q are the direct axis and quadrature axis component of voltage after $dq0$ transformation. PCC voltage is converter to the terminal voltage is shown in Fig. 3.6(b) and (d).
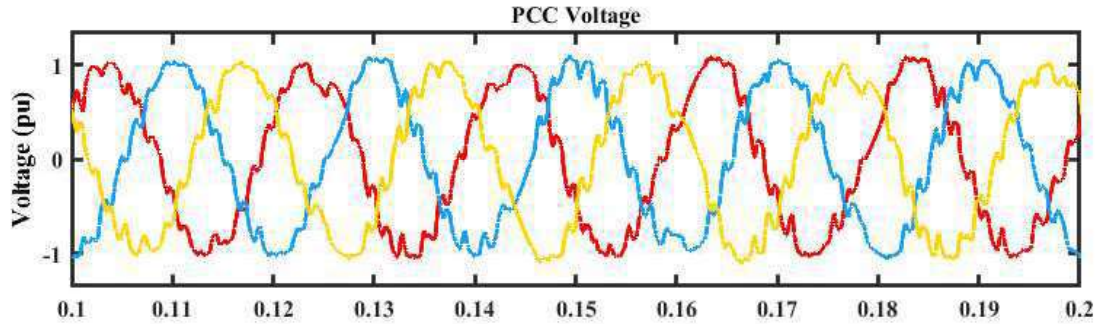
(a)
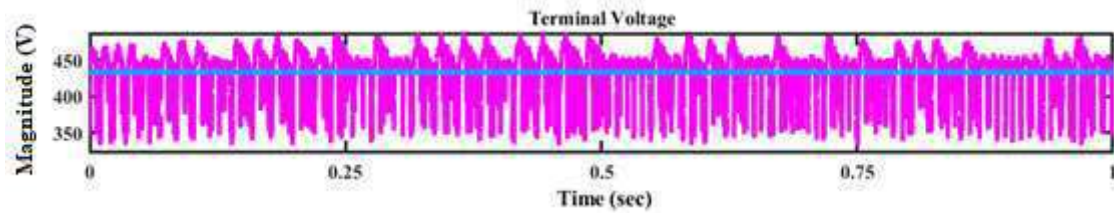
(b)
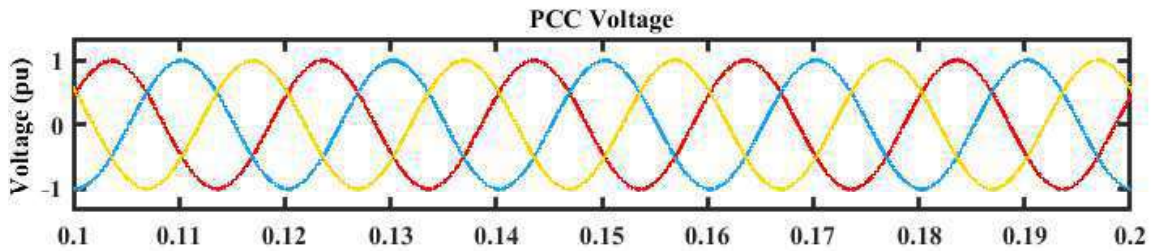
(c)
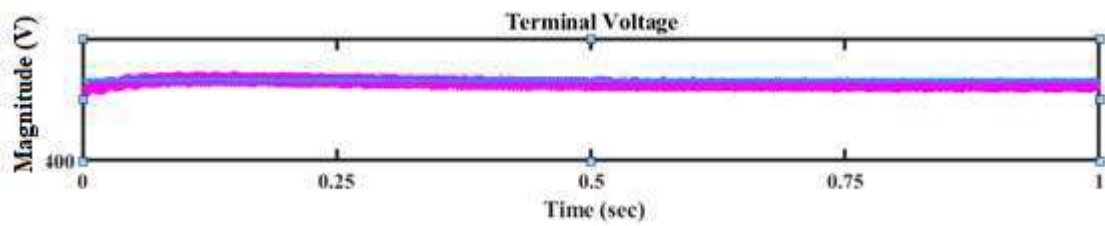
(d)

Fig.3.6. (a)Tuning using 2nd order system model with K_p=4, K_i=25, K_d=0.4 (b)plot of instantaneous voltage with modelled values K_p=4, K_i=25, K_d=0.4 (c) manual tuning using trial and error with K_p =6.06, K_i =27.8, K_d =0.179 (d) plot of instantaneous voltage with manually tuned values K_p =6.06, K_i =27.8, K_d =0.179

Fig 3.7 shows that K_p=4, K_i=25, K_d=0.4 produces total harmonic distortion (THD) of 13.2%, whereas K_p =6.06, K_i =27.8, K_d =0.179 causes THD of only 0.43%. The probable reason includes idealising parameters, excluding the system's intricacies. The transient also settles within 0.3 sec, as shown in Fig.3.6(d).

(a)   (b)
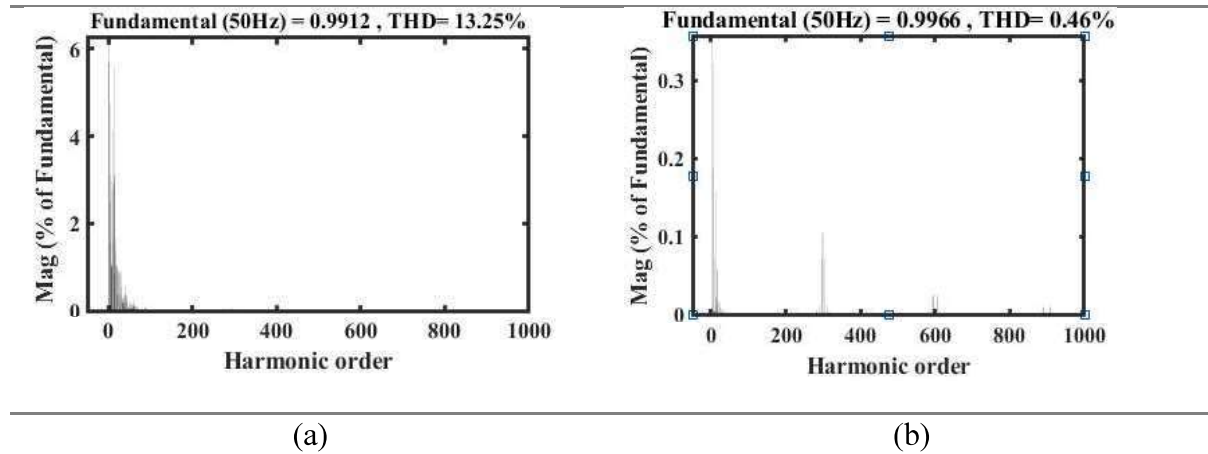
Fig.3.7. Discrete Fourier Transform of Phase 'a' Voltage waveform (a) with **K_p =4, K_i =25, K_d =0.4** & (b) **K_p =6.06, K_i =27.8, K_d =0.179**

3.6. Discussion

Renewable energies like photo voltaic (PV) are available and waiting to be harnessed. Renewable energy-based power systems are weaker than conventional ones and require reactive power generation close to load to unburden the source. DSTATCOM is a powerful device for power compensation, load levelling, balancing and harmonics elimination in a distribution system. The controller within this device is responsible for such functions. So, the control technique is essential to achieve satisfactory operation performance. DSTATCOM generally requires tuning of PI controllers by utility engineers during installation. This process is mostly a trial-and-error approach. It is necessary to re-tune the DSTATCOM controller when there is a change in operating condition. This chapter describes a tuning approach using a linear DSTATCOM model. However, it has been observed that the controller gain parameter that

gives good results for the designed model provides a poor response for the actual system. The

inappropriate value of controller gain also worsens the power quality.

Chapter 4

A Plug-&-Play DSTATCOM with Adaptive Neuro-Fuzzy Controller

4.0 Introduction

Proportional integral derivative(PID) controllers are robust and generally determine the controller action of DSTATCOM. The PID control action is determined by setting K_p, K_i, and K_d values. DSTATCOMs, received from the factory, require tuning of PI controllers (namely K_p, K_i settings) by utility engineers during installation in the power system. The trial and error approach is cumbersome as standard control strategies of this device require four (two for voltage regulator and two for current regulator) for PI controllers. It may require re-tuning the DSTATCOM controller when changes occur in network parameters or conditions [173]. Improper selection of controller gain constants makes the controller response slower, triggers oscillation in system response, and increases system overshoot [174]. In the literature, several control algorithms depict the use of PI controllers for DSTATCOM operations. However, they cannot add the plug-and-play feature to the device [175]. Researchers have adopted advanced control approaches for self-regulating PI or implementing Artificial Neural Network (ANN)or Predictive analysis to ensure adaptive operations for this device. The methods are classified briefly in the literature survey of this thesis. These methods are well accepted in terms of research suggestions; however, simple, robust, cost-effective and easy to implement in real-life situations without much change in design features is much needed.

Fuzzy set theory is a generalization of classical set theory. Fuzzy reasoning is known as approximate reasoning and is based on rules expressed using linguistic variables. Fuzzy logic is used as an operational technique for control in modern industries. Fuzzy logic easily blends with the classical PID control loop for DSTATCOM control and implements automatic PID controller tuning [176]. Fuzzy logic is very popular in literature due to its simple concepts, effective performance and easier amenability. Fuzzy logic algorithms are more accessible to implement because they resemble language. However, it ultimately depends upon human technical expertise, which limits its use to design a plug-and-play DSTATCOM. The use of supervised learning can be a solution to this problem. In supervised learning, input and output datasets train algorithms to predict output.

Artificial neural network (ANN) is a branch of artificial intelligence (AI) that learns the functional relationship between the system's inputs and outputs. Therefore, an ANN-featured adaptive controller for DSTATCOM can help implement the plug-and-play feature [177]. [178] describes a fuzzy PID controller with genetic algorithm for PID tuning. The training for ANFIS controllers for reactive compensation has not been focused in the literatures. This chapter applied this controller for reactive power management in a MG. It does not need tuning at the time of installation.

4.1. Fuzzy PID controller

Fuzzy logic is a rule-based control that provides the best responses per the stated rules. For fuzzy PID operation, the controller simulates PID-like action using a fuzzy interference system (FIS), and it is a combination of conventional PID controller with fuzzy rules. The controller structure is shown in Fig.4.1
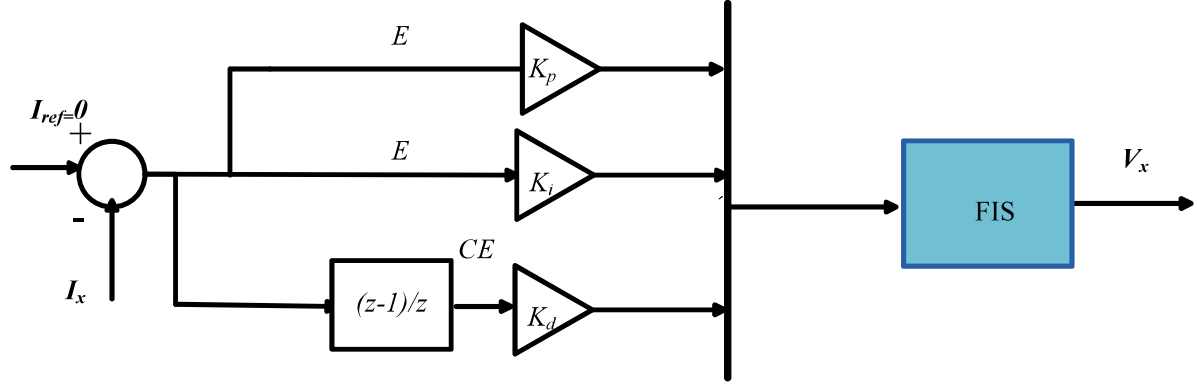
Fig.4.1. Fuzzy PID Control Action

V_{ref} is the reference input to the controller. Voltage and current at PCC are obtained using a potential transformer (PT) and current transformer (CT). It is then converted to d-q components. These d and q values are then fed to the controller. In Fig.4.1, the d or q value has been considered as I_x. K_p, K_i, and K_d are proportional, integral and derivative controller gain factors. Input to the Fuzzy PID is error (E) and change in error (CE). Input and outputs are normalized between [-1,1]. Fuzzy rules are constructed as follows:

1. Identification of input fuzzy variables

2. Identification of output fuzzy variables

3. Fuzzy variables membership functions determination for input-output mapping

4. Setting of fuzzy rules.

5. Determination of output following prescribed rules and using membership functions.

6. Getting a crisp output variable using the de-fuzzification method.

A fuzzy PID controller are an improved version of conventional PID controller with a rule base. It is suitable for non-linear input-output relationships. Moreover, a fuzzy system is less noise-sensitive and responds better to handling system uncertainty. Therefore, it retrieves quickly from system disturbance, and as long as perturbation resides in system performance, it effectively mitigates variations, thus enhancing performance. However, FIS needs technical knowledge to set the IF-THEN rules. Therefore, the controller's efficiency depends on the

control engineer's expertise. So, with immense potential, it is still a simple fuzzy PID controller that cannot be the choice for the controller for a plug-and-play DSTATCOM. Therefore, an adaptive neuro-fuzzy inference system (ANFIS) controller is a better approach than a simple FIS controller. In this controller structure, the neural network imparts intelligence to the FIS by supervised learning. Training with real-time input data and target value adjusts the membership function and the rule weights. This information helps the controller to predict the target value. The prediction accuracy largely depends upon the data set and the training epochs.

4.2. Adaptive Neuro-Fuzzy Inference System (ANFIS)

Neuro-fuzzy systems can be classified into three distinct categories: cooperative, concurrent, and hybrid [179]. The cooperative system neural network is initially used to tune the fuzzy membership functions. In this method the ANN and fuzzy logic works individually. After configuring the controller, only fuzzy system controls the operation.

. In concurrent and hybrid systems, both neural network (NN) and FIS work together. ANFIS comes under hybrid architecture and provides excellent flexibility while working online and offline. It uses a Sugeno-type fuzzy model. The main difference between the Mamdani and Sugento models is that the later output MFs are either linear or constant. The output in the Sugeno model can be obtained in the form as follows:

If input1 =x and input2=y then the output is z=ex+fy+g (4.1)

ANFIS has five layers, as shown in Fig. 4. 2. Layers 1 and 4 are adaptive layers, and other layers are fixed. The details of the ANFIS layers are described in the following section:

Layer 1: A_i and B_i ($i=1,2.....,m$) are the fuzzy MFs of inputs x and y, respectively. The nodes of this layer are adaptive. If the number of inputs and/ or the MFs changes then the number of adaptive nodes in layer 1 changes. The analytical expression of this layer is as follows:

41

$$l_{1,i} = \mu_{Ai}(x)$$
$$l_{1,i} = \mu_{Bi}(y)$$
(4.2)

Where l_{1i} denotes the output. μ_{Ai} and μ_{Bi} are the mapping values between MFs and respective inputs.
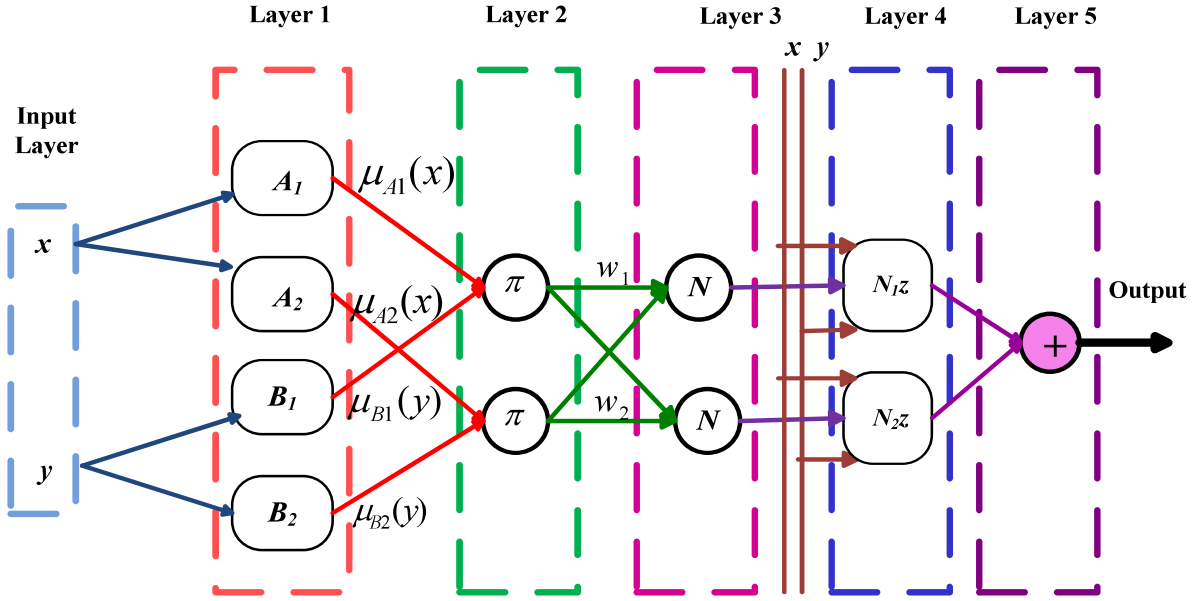
Fig. 4.2 ANFIS Architecture

Layer 2: The nodes of this layer have fixed properties. This layer performs fuzzy intersection or conjunction (AND) operation of the incoming input. The firing strength of the fuzzy AND selects the minimum of the incoming variable.

$$l_{2,i} = w_i = \min(\mu_{Ai}(x), \mu_{Bi}(y))$$
(4.3)

Layer 3: This layer performs the normalization process (N_i) on the previous layer's output. Every node in this layer is fixed in nature. The output of this layer indicates the normalized firing strength. The i_{th} node calculates the normalized value as follows:

$$l_{3,i} = N_i = \frac{w_i}{\sum\limits_{i=1}^{m} w_i}$$
(4.4)

42

Layer 4: This is an adaptive layer. It obtains the output following the Sugeno model. In this layer, the normalized firing strengths associate with (4.3) and produce output as follows:

$$l_{4,i} = N_i z = N_i(e_i x + f_i y + g_i)$$ (4.5)

Where e_i, f_i, g_i are the parameter sets of the node and are known as consequent parameters.

Layer 5: The last layer is the summation layer of all incoming values. The layer node is non-adaptive. The output of layer 5 is computed as follows:

$$l_{5,i} = \sum_{i=1}^{m} N_i z$$ (4.6)

The adaptive layers 2 and 4 update the premise and consequent parameters using a hybrid learning algorithm. Consequent parameters are updated during the forward pass by applying the least mean square (LMS) technique. Premise parameters are updated during the backpropagation by applying a gradient descent algorithm.

Here, the ANFIS controller is used for reactive power management. A time series of active (i_d) and reactive current (i_q) data was collected from the system described in the control structure of Chapter 3, Fig.3.2.

ANFIS is applied only in the current regulator loop. Data to train the ANFIS model is collected from the PID controller-based system. The system has two inputs and one output. Two inputs are error (E) and change in error (CE) to the controller. Output predicts direct and quadrature voltage components (V_d, V_q). Training is done using 70% of the data set, and testing is done with the rest of the data. The learning accuracy significantly depends upon the number of epochs. The correlation coefficient (R^2) between the system output (y) and predicted output ($\hat{y}$) is termed applied to measure network efficiency. The following relation describes the prediction error coefficient [180]:

$$R^2 = 1 - \frac{\sum\limits_{i=1}^{k} (y_i - \hat{y}_i)^2}{\sum\limits_{i=1}^{k} \hat{y}_i^{\;2}} \qquad\qquad (4.7)$$

4.3. Simulation Results

(a)   (b)
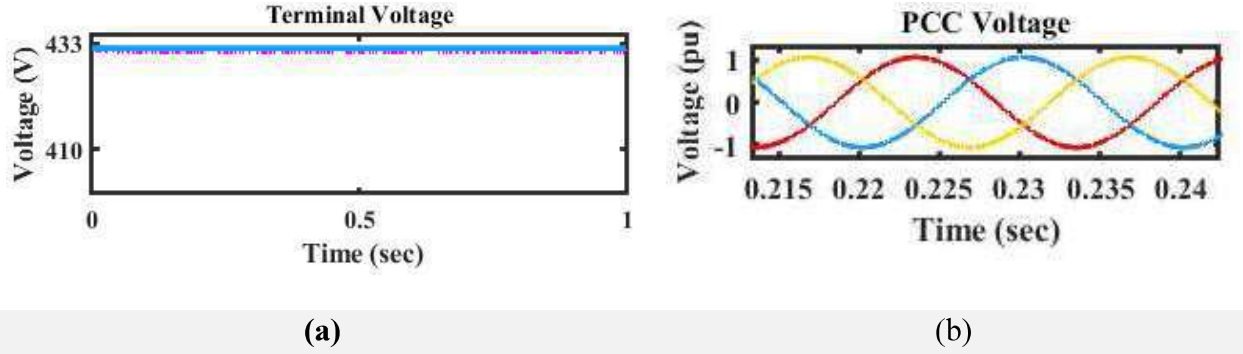
Fig.4.3. PCC voltage profile using the ANFIS controller (a) magnitude of terminal voltage (b) instantaneous voltages

(a)
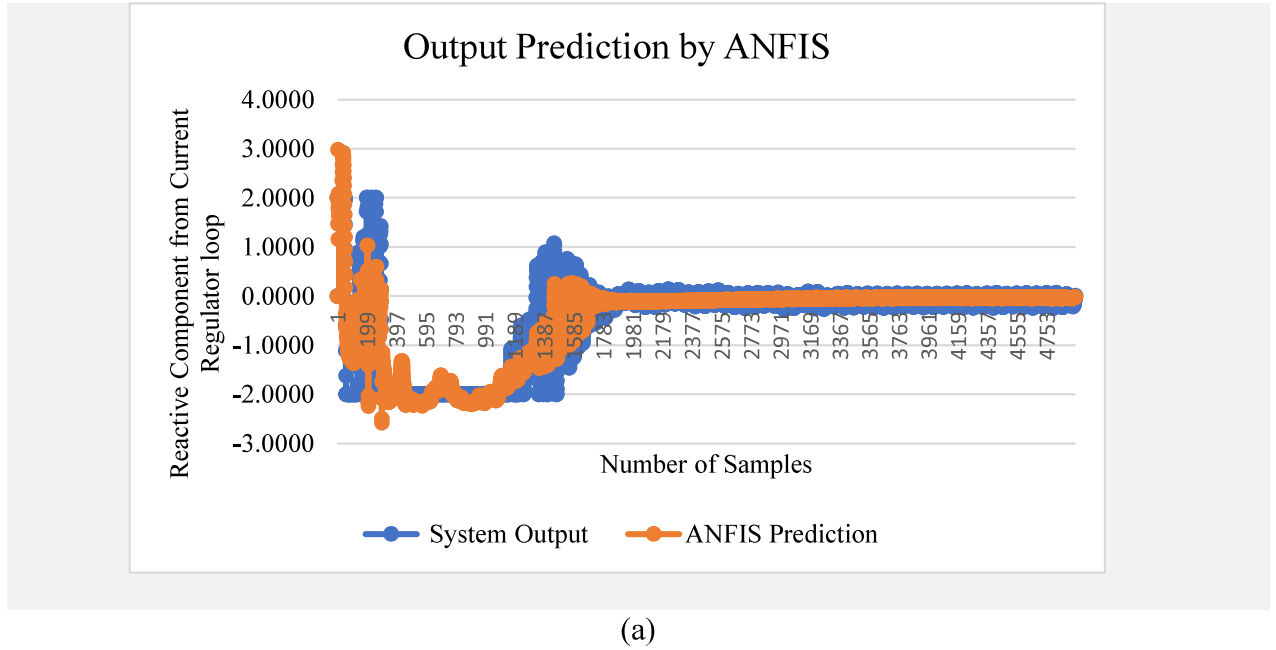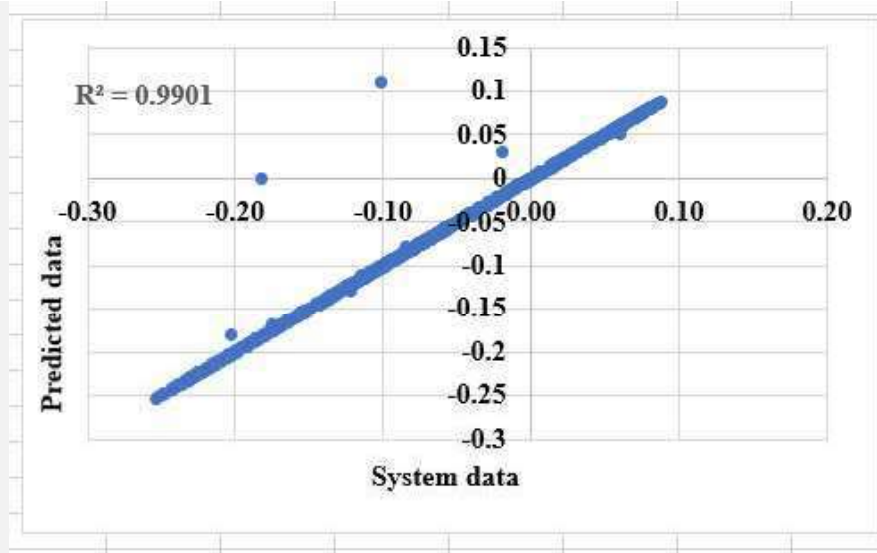
(b)

Fig.4.4. Output Prediction by ANFIS Controller

The training data for the ANFIS model is collected from a PID controller-based control structure, as shown in Fig.3.2. Fig.4.3(a) shows the magnitude of terminal voltage of the ANFIS controller. Fig. 4.3 (b) shows the three phase voltage profile with ANFIS controller. The output prediction from the ANFIS controller is then validated by providing a new set of inputs, as shown in Fig.4.4. (a) Fig 4.4 (b) indicates the R-square curve between actual output and ANFIS predicted output is 0.9901.
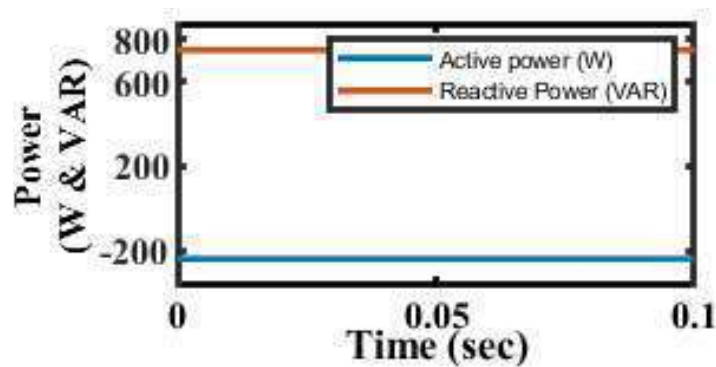
Fig.4.5. Active and reactive power absorbed and supplied by DSTATCOM

Fig.4.5 shows that the ANFIS-controlled DSTATCOM only supplies reactive power and absorbs active power. The reactive power supplied by the DSTATCOM is nearly equal to 800VAR. The negative value of the active power indicates absorption of the active power by the DSTATCOM. It takes power from the supply line for battery charging. Reactive power transfer depends upon the magnitude of bus voltages. The DSTATCOM bus voltage was kept in higher magnitude than the PCC bus to ensure the reactive power transfer. The phase angle of the DSTATCOM is kept slightly lagging than the phase angle of the PCC bus for active power absorption.

4.4. Discussion

This chapter describes a plug-and-play DSTATCOM with an adaptive neuro-fuzzy controller. It is a fuzzy-controlled DSTACOM with adaptive characteristics. Neural networks provide this feature through their supervised learning. Fuzzy logic control is robust and can also work on inaccurate data conditions. However, system accuracy may not be good in this situation. High technical skill is required for fuzzy logic controller to work with good accuracy and precision. But this limits the application of the FIS for being plug- and -play controller. ANFIS method can limit human interaction and install the DSTATCOM as a plug-and-play device.

Chapter 5

Model Predictive Controller for DSTATCOM

5.0 Introduction

DSTATCOM has a voltage source inverter (VSI) as the main component. The grid-tied inverter uses an insulated gate bipolar transistor (IGBT) with non-linear characteristics. Unfortunately, in most research papers, the inverter is modelled using RLC circuits, neglecting the nonlinearity of semiconductor switches. A grid-coupled inverter scheme with additional battery backup is proposed [181], which can also be performed during grid disconnection. The scheme also uses a PI controller. The grid-tied inverter is modelled using its RLC parameters, leading to a linear 2nd order transfer function[149][182]. However, inverters use semiconductor devices and exhibit nonlinear characteristics in the form of on-off, saturation, dead zone etc. Thus, a simple linearized model leads to erroneous results. This chapter introduces a continuous control set (CCS) model predictive control (MPC) method with sine pulse width modulation (SPWM) for better power quality. Inverter installation in an existing grid system is generally tied to several system factors. However, each inverter configuration must be independently programmed to minimize energy and time loss. The use of three-phase control needs tuning of coefficients of three phases. A terminal voltage control method is proposed here to optimize the controller setting for the VSI to achieve a plug-and-play feature in the MG. This method is used for the magnitude control of the voltage where a single variable needs to be controlled, which is more manageable and creates less burden on the controller.

Predictive control predicts the future output, considering previous details of a system or process and forecasting future input. A predictive deadbeat-controlled inverter supplies a doubly fed induction generator as proposed in [183]. Deadbeat controllers perform well without

overshoot but are comparatively slower than Model Predictive Control (MPC) [184]. MPC is also popular in literature because of its ability to predict a system's dependent variable from the measure of independent variables. An observer-recognized (MPC) [185]is used for grid voltage measurement to reduce the offset. MPC is also an essential method for operating grid-connected inverters [186]. A droop-controller assisted with the MPC technique is proposed [44] to reduce voltage variation in the wind farm. A Finite Control Set (FCS) MPC-driven grid-connected inverter switching is also presented [45], [187]. FCS-MPC does not require any modulator, yet complex calculations lead to variable switching of the inverter. An increased number of switching states causes harmonic penetration in voltage and current waveform, leading to power loss, audible noise etc. The authors use three-phase control, which needs tuning of coefficients of three phases [188]. A Continuous Control Set (CCS) MPC requires a modulator but produces a fixed switching frequency. A CCS-MPC based on a feedforward ANN-controlled VSI is described in [189]. Although a complex training method for the ANN is used to get the optimum voltage vector, which is difficult in real time, the CCS MPC performs well in steady-state operations [190].

This chapter describes a CCS MPC with sine pulse width modulation (SPWM) for better power quality. Inverter installation in an existing grid system is generally tied to several system factors. However, each inverter configuration must be independently programmed to minimize energy and time loss. Most of the research articles use three-phase control, which needs tuning of coefficients of three phases. The proposed approach optimizes the controller setting for the VSI to achieve a plug-and-play feature in the MG. Here, a terminal voltage control method is used for the magnitude control of the voltage where a single variable needs to be controlled, which is more manageable and creates less burden on the controller. This method is friendly for the user, and no tuning arrangement of the controller is required here, unlike the PI controllers [191], [192]. PSO is used in [189] to determine PI controller gains,

but this technique may be lost in the suboptimal region. Therefore, a backtracking line search algorithm is proposed with PSO for better results [193]. Therefore, a backtracking line search algorithm is used for optimization by the MPC. A descriptive function method analysis is used to observe the stability of the modelled non-linear inverter, which guarantees stable operation.

To demonstrate the characteristics mentioned above, a real-time distribution network in MATLAB Simulink, following the loading pattern of the network, demonstrates controller potential in terms of power quality. Power quality refers to quality index for system parameters present during transient and steady stare operation in power system [194]. An existing 11kV feeder (Elachi feeder) from a 33/11kV Sub-Station at Narendrapur, belonging to West Bengal State Electricity & Distribution Company Limited (WBSEDCL), India, is studied, where voltage control is only through the on-load tap changers of the power transformer (PTR1,2,3). The absence of dynamic voltage control causes fluctuation in the industrial loads which is detrimental to the plant, machinery and production. The salient features of the proposed controller actions are as follows:

● Terminal voltage magnitude method: The three-phase voltages are controlled using a single terminal voltage magnitude method in the proposed controller.

● The nonlinearity of the inverter: The Inverter has nonlinear dynamics, which research articles neglect to achieve simplicity. This chapter takes care of the nonlinear behaviour of the inverter.

● Plug and play feature: The proposed inverter control can be attached to any point of the MG network.

5.1 System Configuration

In this chapter a system is modelled in MATLAB SIMULINK following the loading pattern of a feeder. .Elechi feeder of Narendrapur substation in West Bengal is modelled in MATLAB SIMULINK. The architecture of the MG is depicted in Fig. 5.1. It has two distinct portions. The red dotted line on the right-hand side indicates the architecture of the MG. The left-hand part, surrounded by green dotted lines, shows the 33/11kV Narendrapur Substation of West Bengal State Electricity Distribution Company Limited (WBSEDCL). Sources of the substation are two incoming feeders (INC), 33kV INC-1 (from Sonarpur) and 33kV INC-2 (from Mahinagar). These feeders supply the 33kV bus at Narendrapur and then further step down to 11kV. This 11kV bus is the source of the Elachi feeder. This is a mixed feeder with most industrial loading and some households. Table 5.1 reveals the load characteristic of this feeder system. Following the loading pattern, a system is modelled in MATLAB SIMULINK.
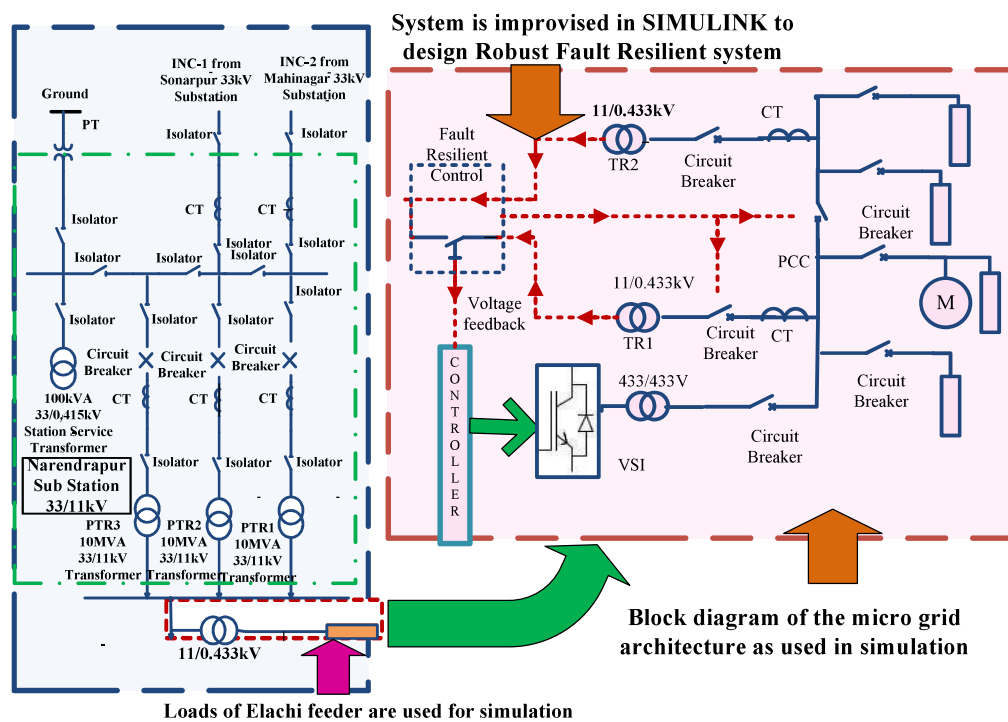
Fig.5.1. The architecture of the MG network

A 100kVA 11/0.433kV distribution transformer is supplying microgrid loads. The loads are simulated with induction motors and resistive and inductive loads in SIMULINK. Fig.5.2 reveals the MG connected to the main grid with the signal flow diagram between system to the proposed controller in. A microgrid may have several distributed energy resources (DERs) connected within it. Here a single inverter control is presented to illustrate the operation of the inverters within the microgrid. As the microgrid is spread over a small area, the IGBT based VSI with CCS-MPC control is assumed to be connected to the point of common coupling (PCC). Terminal voltage magnitude (V_t) is calculated from the three-phase voltages at the PCC end and fed back to the MPC. A second-order closed-loop transfer function with an on-off nonlinearity has been found to be a suitable model for the VSI system and used to train the ANN [195]. A non-linear autoregressive exogenous (NARX) series parallel based ANN is used to predict the plant output. The prediction horizon refers to the number of future control intervals the MPC controller evaluates by prediction at any instant. Optimization occurs based on the control horizon, but only the first variable, the modulation index (m), is applied to the system. Fig. 5.3 shows the typical highest loading pattern of the year for the 11kV Elachi feeder and Narendrapur 33/11kV substation as the study time is the month of June. The loading pattern considered for simulation is from 23.00 hrs of 06 June 2021 (Day1) to 06.00 hrs of 07 June 2021 (Day2), as marked in Fig. 5.3.

The DSTATCOM with CCS-MPC control is assumed to be connected to the point of common coupling (PCC). An IGBT-based VSI is the main component of it. Terminal voltage magnitude (V_t) is calculated from the three-phase voltages at the PCC end and fed back to the MPC. A second-order closed-loop transfer function with an on-off nonlinearity is a suitable model for the VSI system and is used to train the ANN [195]. A non-linear autoregressive exogenous (NARX) series parallel-based ANN is used to predict the plant output. The prediction horizon refers to the number of future control intervals the MPC controller

evaluates by prediction at any instant. Optimization occurs based on the control horizon, but only the first variable, the modulation index (m), is applied to the system.

Table 5.1. Load Pattern at 11kV Elachi feeder, Narendrapur

Date	Time	Hourly Loading of 11kV Elachi Feeder (A)	Set Current (A)	Bus Voltage (kV)	Ratio Load
06 June 2021	23.00hrs	250	300	10.9	0.833
07 June 2021	00.00hrs	240		10.9	0.8
	01.00hrs	218		10.9	0.727
	02.00hrs	202		11.0	0.673
	03.00hrs	186		11.1	0.62
	04.00hrs	172		11.2	0.573
	05.00hrs	156		11.3	0.52
	06.00hrs	160		11.4	0.533

Fig. 5.2. Signal flow diagram between system to the proposed controller	Fig.5.3. Load pattern of the feeder
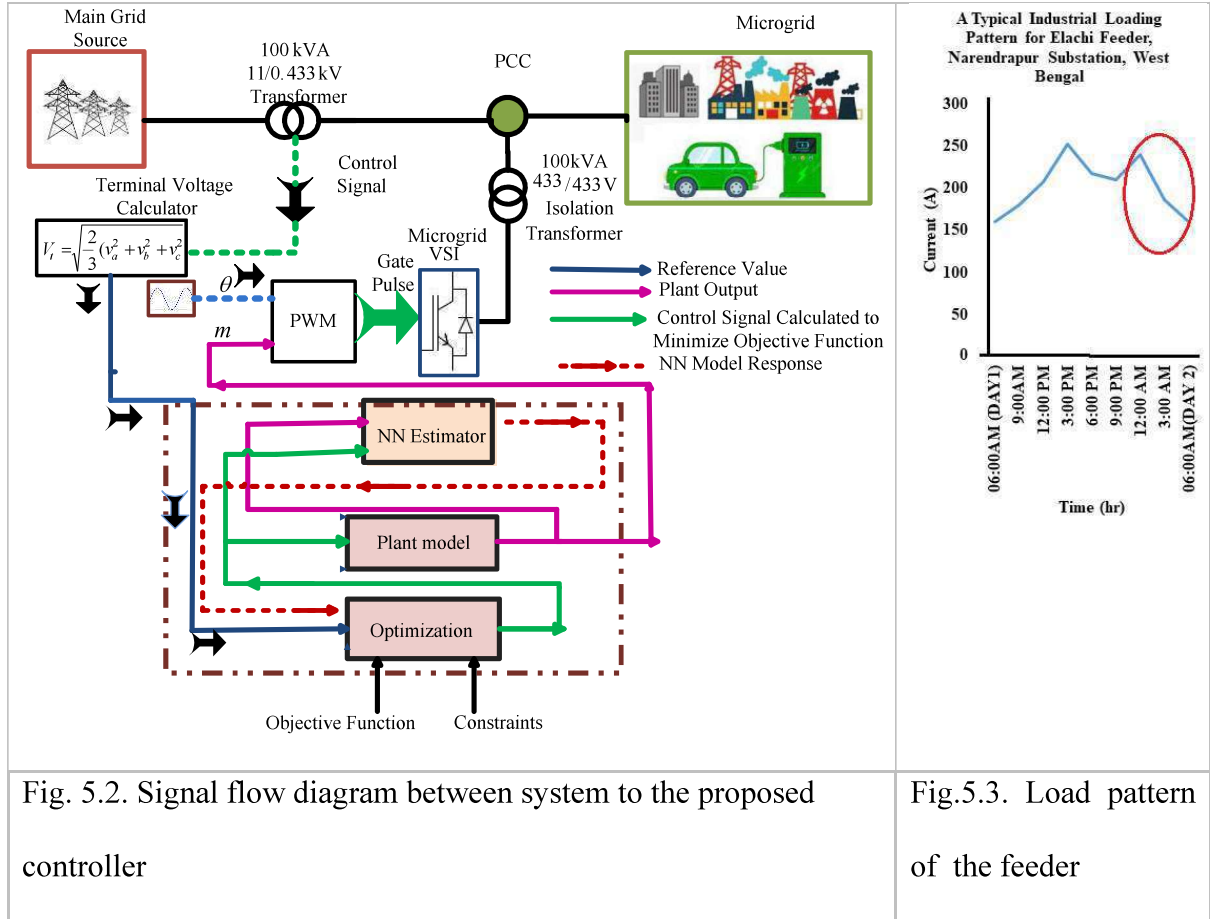
5.2 Proposed Controller Design

A CCS-MPC is applied on VSI to maintain the voltage regulation of the AC bus. The linear section of a VSI is modelled by the RLC filter part as discussed in Chapter 3 equation (3.9). MPC has a broader aspect as a controller. CCS MPC provides fixed switching frequency and maintains good response in steady-state operation. In the proposed control scheme, the ANN represents a plant model for output prediction by the MPC. The non-linear autoregressive exogenous (NARX) model in series-parallel architecture is used here to model the neural network (NN) model to predict output values. Autoregressive values predict future values from past observations. The proposed control avoids tuning PI controllers in multiple loops. The nonlinearity of the semiconductor switches has also been adopted in the system model to

53

minimize error. Describing function is applied for the stability of the designed nonlinear VSI model, which is a method for frequency response of a nonlinear system. The nonlinear VSI model is illustrated in Fig. 5.4. The nonlinearity is modelled using on-off, as shown in Fig. 5.4(a), where v_o is the voltage coming out from the circuit, and v_e is the driving voltage of the semiconductor switch. The linear portion of the inverter is represented here as a 2nd order transfer function ($G(s)$). $G(s)$ and nonlinear describing function ($N_f(A,\omega)$) with on-off nonlinearity are shown in Fig.

5.4(b).Fig. 5.4(c) shows the linear RLC model for the VSI.
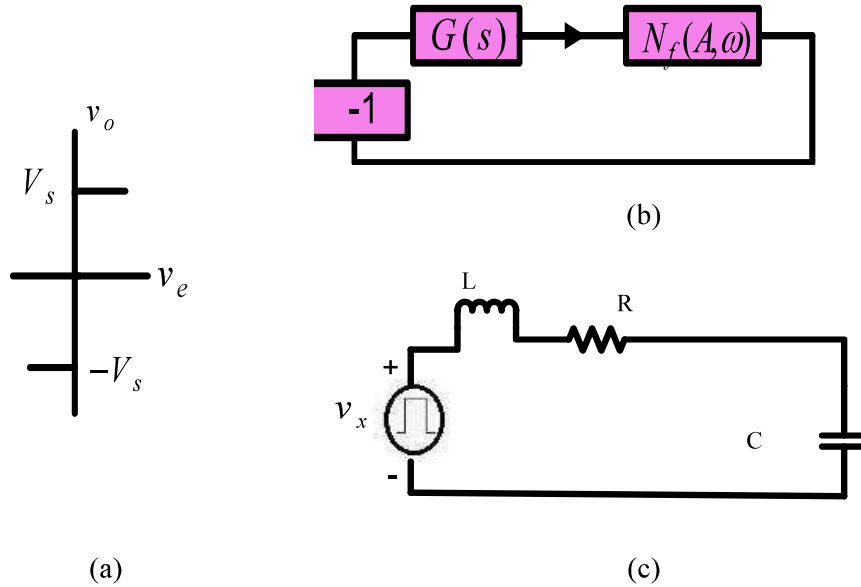
Fig.5.4. Inverter model with (a) on-off nonlinearity; (b) system structure represented by linear transfer function and nonlinear describing function; (c) linear equivalent circuit of inverter;

The neural network model is developed as a time series model. The terminal voltage magnitude is used as input to the plant. The input and output from the plant are fed to the neural network. The plant model generates output following the step response of a 2nd order slightly underdamped system. The inverter model is discussed in the next section. The output from the

plant transfer function with an on-off nonlinearity block in series is simulated with normalized applied voltage values. The output is considered as modulation index, *m*. Finally, the input voltage and *m* are applied to the neural network model. The ANN model is designed using a nonlinear auto-regressive exogenous series-parallel model [196]. This architecture is employed because the model is stable and a good predictor of time series value.

Further, it has a purely feedforward construction. Input and target variables are set for training. Bus voltage at PCC and bus loading factor time series values simulate the MG system for different loading conditions. These are taken as input data. Target values are obtained from the inverter model as *m*. Now, ANN is trained first, and the performance and regression values are checked. The training process is repeated until the regression values for training, validation, and testing are nearly equal to 1. After the training, the network is used for output prediction. ANN predicts the future value of *m*, which is then fed to the optimization block. MPC optimizes the value of output based on the ANN system model. It minimizes the cost function over a receding horizon using the modelled output. This minimization of cost function demands an optimization algorithm. Here it has been considered that the degree of optimization problem remains the same throughout different operating points, and a linear adaptive MPC is implemented as it would be able to identify the single global optimum of the convex optimization issue.

5.2.1 Nonlinear Plant Model

The nonlinear inverter output voltage are described using the following Describing Function (DF), which implies the application of dead time, hysteresis and relay [197]. It is a method for analyzing any nonlinear system with the best-suited linear time-invariant (LTI)

function. Thus, using the nonlinearity as mentioned earlier, describing the function of the inverter is modelled as:

$$N_d(A,\omega) = \frac{4}{\pi}\frac{V_d}{A}\sqrt{1-[\frac{r}{A}]^2} - j\frac{4}{\pi}\frac{rV_d}{A^2} \tag{5.1}$$

Where V_d denotes battery voltage, A is the peak value of sinusoidal current, and r is the threshold voltage of the semiconductor switch. In this work, the threshold voltage of the semiconductor switch is ignored in modelling for the sake of simplicity. Thus, the final describing function leads to the following equation:

$$N_f(A,\omega) \approx \frac{4}{\pi}\frac{V_d}{A} \tag{5.2}$$

Equation (5.1) leads to a model of an on-off nonlinearity. In Fig. 5.5, Γ_G is the representation of the Nyquist plot of $G(s)$ while Γ_N is used for the polar plot of $\{-1/[N_f(A,\omega)]\}$. Equation (3.9) and (5.2) indicates the linear transfer fuction and nonlinear describing function of the modelled inverter respectively. Fig. 5.5 presents the stability analysis of the inverter model using a Nyquist plot for the linear transfer function and a polar plot for describing the function. The modelled inverter design is stable as Γ_G and Γ_N of the modelled inverter do not intersect [198]. It means any oscillation that may occur in the system output due to disturbance dies out, and no sustained oscillation exists at a steady state. The objective of any feedback control system is to maintain the system goal, and it is done by measuring the output variable and permitting the actuating signal to achieve the desired system performance. The voltage at PCC is fed back to the control circuit of VSI. The three-phase instantaneous voltages are converted to the magnitude of terminal voltage, and the following transformation gives V_t:

$$V_t = \sqrt{(2/3)v_a^2 + v_b^2 + v_c^2} \tag{5.3}$$
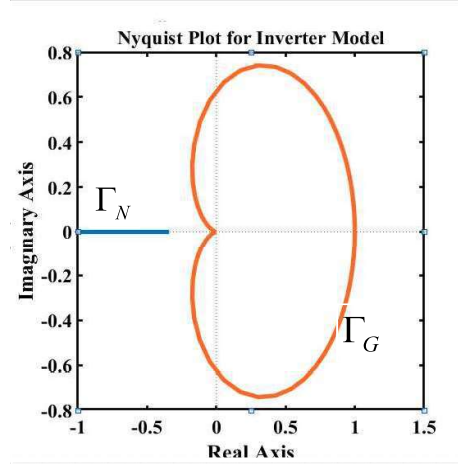
Fig. 5.5. Stability analysis of inverter model using Nyquist plot & describing function

5.2.2 Non-linear Auto Regressive Model

The prediction equation of NARX model with series-parallel structure as shown in Fig. 5.6.(a) is:

$$\hat{y} = f[u(k), u(k-d_1), u(k-d_2),....y(k), y(k-d_1), y(k-d_2),...]$$ (5.4)

Where u is the control inputs, d signifies the time delay and y is the output from the plant model. After initializing the parameters as mentioned above, the neural network is ready for training.
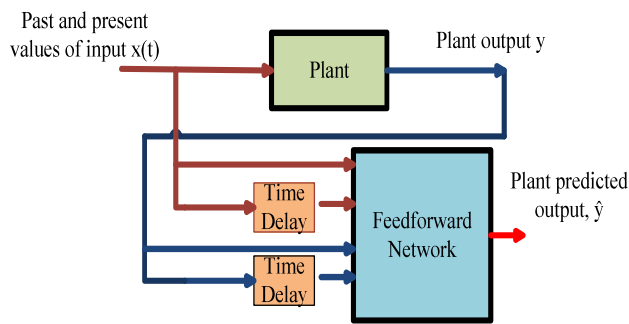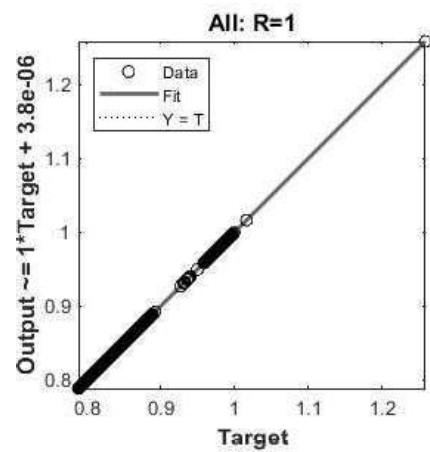
(a)   (b)

Fig. 5.6. Series Parallel NARX model (a) structure (b) regression response after training

This training process optimizes the network performance. Mean Square Error (MSE) governs the performance function.

$$MSE = \frac{1}{N} \sum_{i=1}^{N} (e_i)^2 = \frac{1}{N} \sum_{i=1}^{N} (\hat{y} - y)^2 \qquad (5.5)$$

Where e_i = error between the network output ($\hat{y}$) and target output (y).

The neural network is trained in batch mode. Levenberg-Marquardt (LM) algorithm is used here for backpropagation training for the minimization of cost function $J(\theta)$ [199]. For any fitting problem, the aim is to minimize the error between output data and the fitting function. The rule for LM is as follows:

$$\Delta\theta = (H + \mu I)^{-1} h_{lm} \qquad (5.6)$$

Where h_{lm} is the gradient vector ($J^T e$), H is the approximated Hessian matrix (J^{TJ}), I is the identity matrix and is the learning parameter. After repeated training, the regression response is shown in Fig. 5.6 (b). Mean normalization is applied to convert the input (u) and target data to be better applicable for training, as mentioned before:

$$u = u - M / s \qquad (5.7)$$

M is the mean of all feature values, and s is the standard deviation. After training, validation is done using the validation data set.

A continuous control set model predictive controller uses this ANN model to predict future performance. It calculates the control input to optimize plant performance over a specified future time horizon. Performance CCS-MPC with a receding horizon control (RHC), as DSTATCOM controller, is discussed in this chapter.

5.2.3 Receding Horizon Control

Receding Horizon Control (RHC) is also called Moving Horizon Control (MHC). The principle of the Receding Horizon Controller is shown in Fig 5.7. As per the principle of this technique, the future output is predicted over the future time step N, known as the future horizon. The current time, k, and current state x_k at k optimal control problem are solved over the future horizon, [k, $k+N-1$][200]. Though the whole future control trajectory is calculated, it only applies to the first step in the calculated optimal result. Next, the measure is taken at time $k+1$. This same procedure repeats itself in the next sampling instants over a fixed future horizon, i.e., between [$k+1$, $k+N$] at the current state [x_{k+1}]. The optimization process determines the control signal to minimize the cost function, J, over the set out horizon.

$$J = \sum_{i=N_1}^{N_2} [W(k+i) - \hat{y}(k+i)]^2 + \rho \sum_{i=1}^{Nu} [u'(k+i-1) - u'(k+i-2)]^2 \qquad (5.8)$$

Where N_1, N_2, and N_u describe the horizons. The tracking error and the control increments are evaluated on these horizons., and u' describes the tentative control variable. W is the reference, and $\hat{y}$ is the predicted output. The value of ρ determines the contribution of the sum of squares of the control increments on the performance index, J. The model predictive control performs an optimization procedure repeatedly to determine the best input condition within a specified horizon to meet the desired output response while maintaining the constraints. Here, a prediction horizon of N_2=7 and a control horizon of N_u=2 with control weight ρ=0.05 are used.
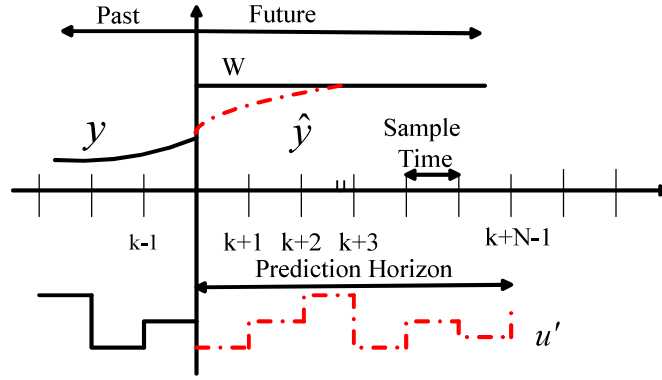
Fig.5.7. Receding Horizon Principle

The controller action performs optimization over and over again as follows:

Step 1. Minimization of open-loop control.

$$u_N(x_0) = \arg\min_{u_N \in U^N} J_N(x_{0,}u_N)$$

Subject to:

$$J_N(x_0, u_N) = \sum_{i=0}^{N-1} l(x_{uN}(i, x_0) - x_{ref}(i), u_N(x_0, i))$$

$$x_{uN}(i+1, x_0) = f(x_{uN}(i, x_0), u_N(x_0, i)) \ \forall_i \in \Im_u$$

$$x_{u_N}(0, x_0) = x_0$$

$$x_{u_N}(i, x_0) \in X \ \forall_i \in \Im_x$$

$$u_{u_N}(x_0, i) \in U \ \forall_i \in \Im_u$$

Where time set; $\Im_u = \{0, 1, ..., N-1\}$; Control function $u_{N:}\Im_u \to U$; State Space is X

Step 2. Solve for (5.8)

5.2.4 Online Optimizer

The optimization algorithm presented here uses a multilayer prescribed time horizon. The neural network reciprocates the plant dynamics, which has to be controlled. This ANN-based plant model estimates future responses based on control signals. An optimization routine is then set to optimize the control inputs for the original plant for effective output responses, maintaining the constraints over the input and following the prescribed path while moving towards the reference set value. The cost function is differentiable in nature. The optimizer determines u' to minimize the cost function. Then, the optimal input is fed to the plant. The computation of α_k is called the line search. The procedure for line search is as follows:

Step I. Choosing of initial state x_0, putting $k = 0$

Step II. Till convergence of x_k:

    a.   Search direction of ρ_k from x_k calculation considering

$$[g^k]^T \rho^k < 0 \text{ if } g^k \neq 0 \tag{5.9}$$

        (where g^k is Lipshitz continuous gradient)

    b.   Calculation of $\alpha_k > 0$ such that

$$f(x_k + \alpha_k \rho_k) < f^k \tag{5.10}$$

    c.   Setting

$$x_{k+1} = x_k + \alpha_k \rho_k \tag{5.11}$$

However, the challenge here is to get a good α_k to avoid step lengths from becoming too long or too short. Therefore, a backtracking line search algorithm is applied in this proposed controller. Backtracking line search starts with a relatively larger step size

but decreases the step size as required to obtain an optimized target. This chapter uses a search parameter of 0.1 to apply the backtracking line search algorithm to reach the Armijo-Goldstein inequality condition.

Backtracking Line Search Algorithm

1. Given $\alpha^{(init)} > 0$, let $\alpha_0 = \alpha^{(init)}$ and $l = 0$

   2.   Until $f(x_k + \alpha_l \rho_k) < f_k$

       a. $\alpha_{l+1} = \tau \alpha_l$ where $\tau \in (0,1)$

       b. $l = l + 1$

3. Set $\alpha_k = \alpha_l$

5.3 Simulation Result

The variation of load in terms of active power is given in Fig. 5.8(a). In the simulation, a 4kW squirrel cage induction motor and a 2kW resistive load get disconnected at 1.2sec and 1.5sec, respectively. Fig 5.8(b) shows the three-phase voltages during the entire period with the inverter connected to a microgrid. Fig. 5.9 compares the terminal voltage profile with and without the inverter connected to the microgrid system. Fig 5.9(a) depicts that since the grid-connected microgrid operates initially at peak load conditions without any inverter attached at PCC, the voltage at PCC drops from the reference value (433V). It has been mentioned initially that a real-time system is modelled in Simulink as a microgrid which has voltage control through only an online tap changer.

Therefore, during maximum loading conditions, the system is not able to maintain the voltage profile, and the voltage goes below the reference value. However, the inverter equipped with the proposed controller can instantly maintain the voltage profile at the reference value,

supplying reactive power to the grid without any tuning process, as shown in Fig. 5.9(b). The proposed ANN- MPC method controls the modulation index m. A phase-locked-loop (PLL) is used to create the phase angle ωt. m and ωt is used for a 50Hz sinusoidal signal. A 5kHz triangular carrier signal is compared with the modulating signal for gate pulse generation for the VSI. Fig. 5.10 describes the voltage profile of the PCC when an induction motor (IM) starts during peak load conditions with the inverter connected to the system. Fig. 5.10(a) shows that an induction motor is switched on at 0.05 sec, but the PCC voltage before and after switching displays a satisfactory result, with the other loads connected at PCC remaining unaffected.
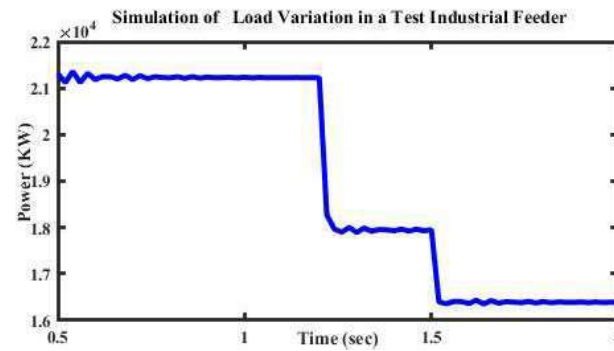
(a)
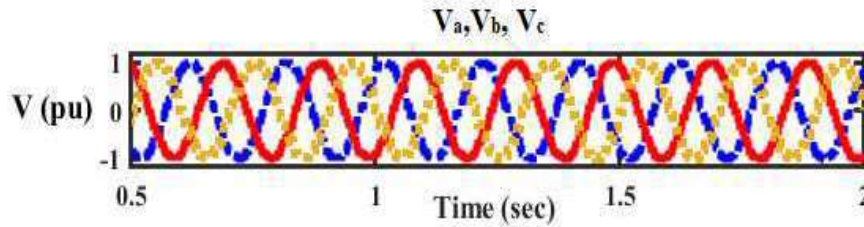
(b)

Fig. 5.8. The modelled system is under simulation with a solar-fed inverter connected to the MG network (a) Load variation; (b) System line voltages V_a, V_b, V_c
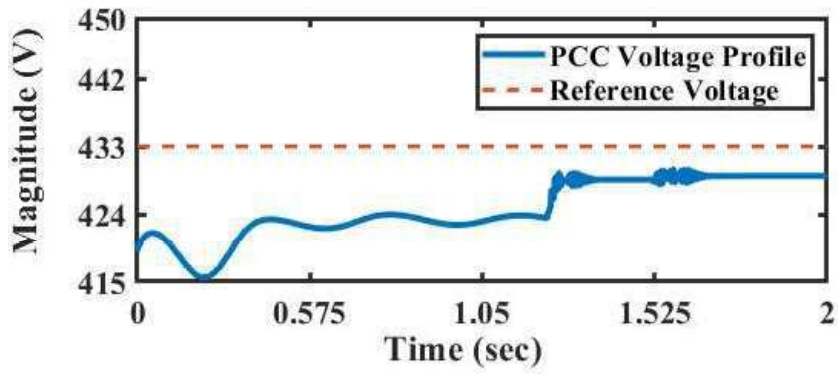
(a)
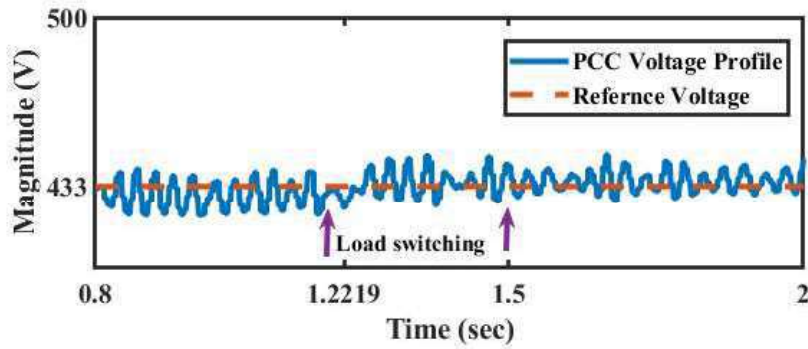
(b)

Fig 5.9. Control of the PCC voltage with load variation (a) with tap changer only (b) with DSTATCOM

Figure 5.8 (b) shows the magnitude of terminal voltage (V_t) during and after the switching of the induction motor. It indicates that after a drop at the switching instant, the terminal voltage again attains the reference value within 0.1 sec. The modelled VSI is a 2nd-order underdamped system that has overshoot in response. The MPC controller is fast but susceptible to overshooting. However, an optimized model design and an appropriate number of control variables resulted in no overshoot in the simulation.
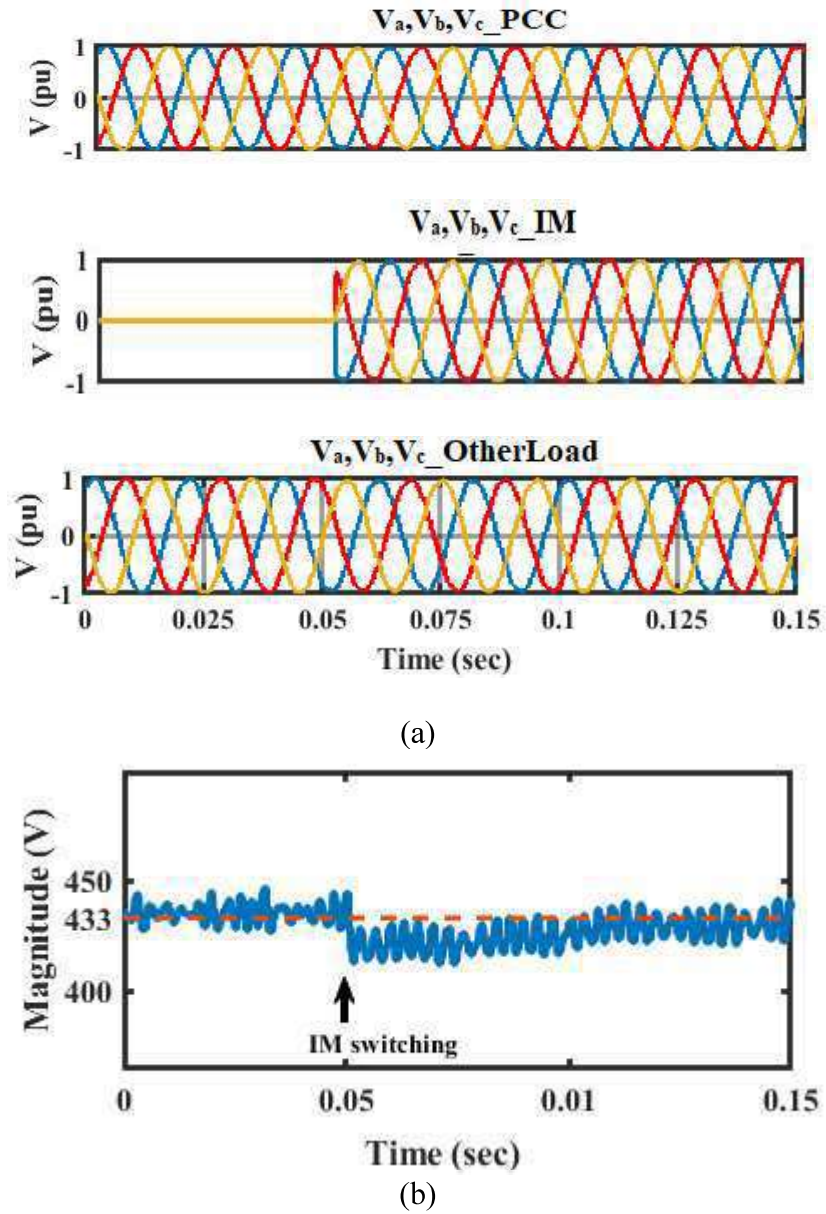
Fig. 5.10. Voltage profile of PCC at the time of induction motor starting (a) Voltage profile at the PCC during motor load switching at MG. (b) The magnitude of terminal voltage at PCC during switching.

The modulation index generated by the controller can maintain the PCC voltage. The magnitude of inverter voltage is kept more than PCC voltage to supply reactive power required by the MG loads. The phase angle of the VSI is set slightly leading.to supply the active power loss of the connecting the resistive losses in its own circuit.Fig.5.11(a) shows

the power supplied by the VSI.Fig.5.11(b) also indicates that the grid supplies mostly active power with a negligible reactive line loss.
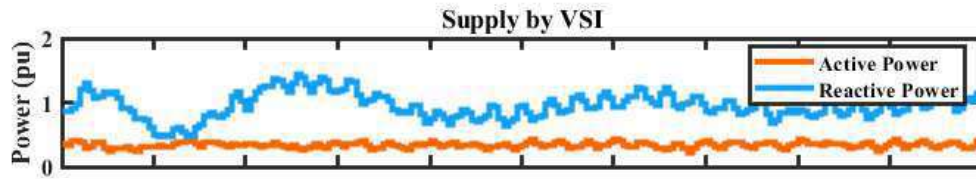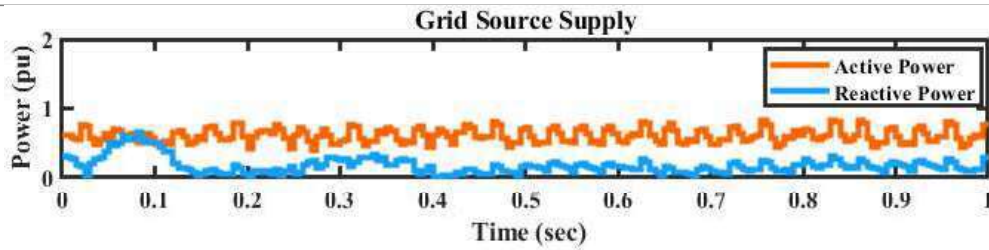
Fig.5.11 Active and reactive power supplied from (a) the inverter (b) grid source

5.4. Discussion

This chapter describes continuous control set model predictive control (CCS-MPC) on inverter for dynamic voltage regulation supplying reactive power to the load for a MG. The proposed method uses the terminal voltage magnitude, which reduces calculation time, sensor per phase, and the engagement burden of the controller. The controller uses a nonlinear model of the inverter as the system and a series-parallel NARX model for the ANN for future output prediction. The inverter model introduces on-off nonlinearity to include real-time semiconductor switch characteristics. The proposed control can introduce the VSI anywhere in the microgrid as a plug-and-play device.

Chapter 6

Open Source IoT-based Real-Time Monitoring in an AC Microgrid

6.0 Introduction

Electricity consumption in the residential sector has increased much in the last twenty years, which is also a cause of an increase in carbon dioxide (CO_2) emissions. Integrating distributed energy resources (DER) like solar can solve this problem and has gained popularity in the present era [201][202]. Consuming less power can contribute towards a greener environment by preserving the earth's natural resources and bringing down green house gases from the chimneys of the power plants. So, energy or power management is a relevant factor of the power systems in today's world. The power sector is advancing, employing digital devices and technologies to integrate with intelligent machines. These new technologies allow monitoring, analyzing, and controlling data in the smart devices along with power flow, making the existing system move gradually towards the smart grid system [203]. An Energy Management System (EMS) or Power Management System (PMS) is the intrinsic factor of a Smart Electric System (SES) [204]. Demand Side Management (DSM) is the measure to optimize energy consumption, providing incentives for less energy consumption, especially during peak demand. Advanced Metering systems are indispensable for two-way communication, making residential commercial or industrial consumers evolve as active entities or players in the new grid system. The demand side response (DSR) program can

67

significantly improve the dynamic stability of microgrids. Residential photo voltaic systems (RPVS) are becoming popular worldwide [205].

However, the power market needs to be flexible for green energy trading. Therefore, the penetration of these energy sources in the power market initiates changes in the price dynamics. However, a small rooftop solar photovoltaic system cannot individually participate in the energy market due to its small capacity and intermittent characteristics. Dynamic pricing (DP) or real-time pricing (RTP) and time of use (TOU) are the critical features of DSM [203]. The Internet of Things (IoT) refers to the cyber-physical system with several devices connected over the internet. DSM may be achieved using smart electrical gadgets over the internet. Moreover, passing clouds cause fluctuations in solar irradiation and power fluctuations affect power quality. Thus, power system operators regulate the change in solar power through a ramp rate limitation. Energy storage systems (ESS) like batteries thus serve as the solution to solar power fluctuations [206]. However, the storage unit adds to the cost and size; hence, storage optimization is also essential to reduce the economic burden of small energy producers.

6.1. System Configuration & Operation

The structure of the MG proposed in is shown in Fig 6.1. Each resident here possesses a rooftop solar photovoltaic with a battery backup system associated with a maximum power point tracking (MPPT) charge controller circuit and inverter. The prosumer creates an energy account in the energy management system (EMS) installed on the prosumer's computer. EMS predicts energy generation, battery management, and load patterns based on weather data, battery parameters, and previous load patterns. Every household connects through a common bus [149], MB, for P2P energy transfer among the community members. It has been assumed

that P2P transfer is only required in case of contingency. A community microgrid operator (MO) plays a significant role in the successful operation.
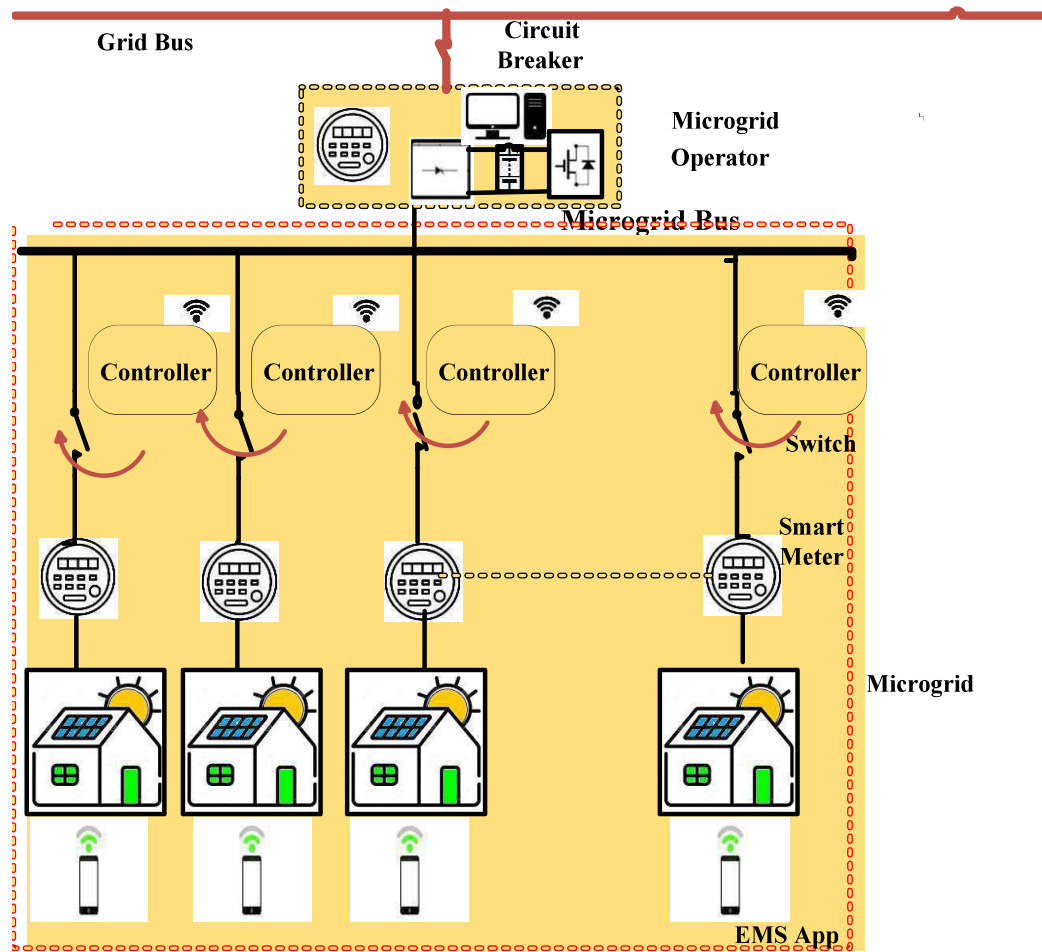
Fig. 6.1. A small residential microgrid system configuration

A small prototype has been developed to demonstrate interaction between two participants as shown in Fig.6.2. Open-source IoT applications are used for energy transfer between two residents. But instead of a PV panel with an inverter, a single AC source is used in the experimental setup for hardware simulation. The block diagram for the proposed IoT setup is shown in Fig.6.2. Experimental prototype of the real-time model has been set up to establish the battery management and P2P transaction to a limited extent. The real-time model has hardware and software components. Fig.6.3(a) and(b) represent the battery management circuit

and real-time P2P energy transfer experimental setup, respectively. Experimental results are shown in Fig 6.4(a),(b),(c) and (d). The components required are described below.
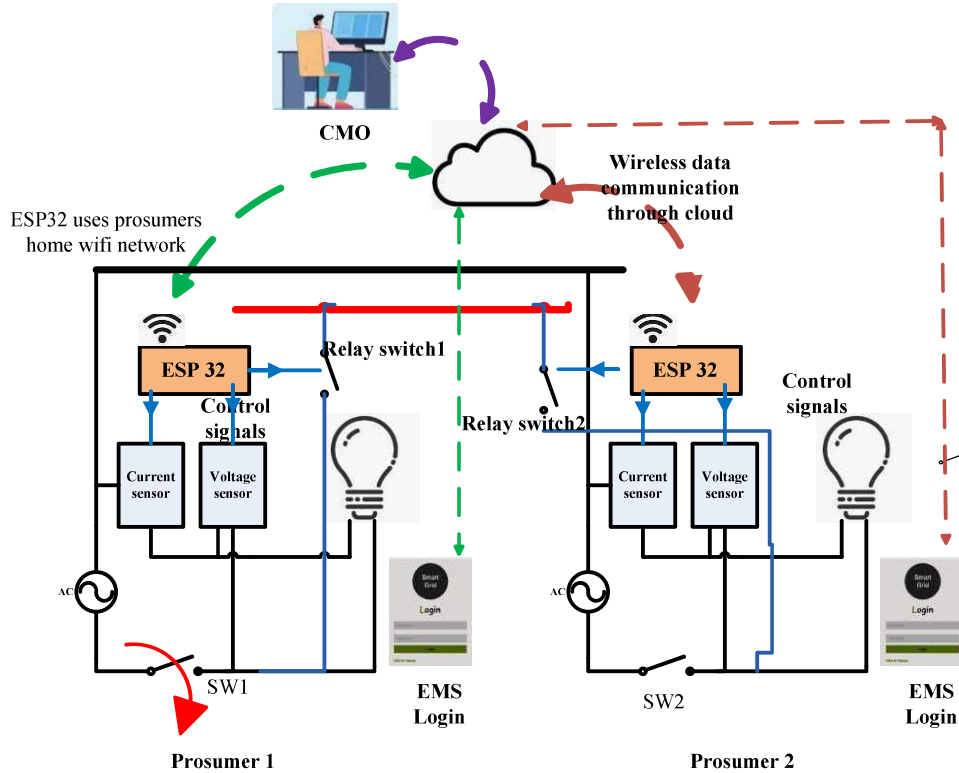
Fig.6.2.IoT based P2P energy transfer block diagram

Hardware: Fig.6.3(a) shows an IoT-operated battery management system prototype. A 3.7V 1800mA (maximum charging voltage 4.5V and cut-off voltage of 2.8V) lithium-ion battery is used with a TP4056 battery charger circuit. Each prosumer is provided with a battery management circuit. The battery management circuit measures the voltage and SOC of the battery.

In Fig 6.3(b), this experimental setup uses a single-phase AC source with two switches. Each prosumer is connected to the common bus through the respective switch. Hardware simulation of energy transfer between two prosumers is done when the command is sent to the

respective switches (relay switch 1 and relay switch 2) to close. The local load of each prosumer is simulated with the help of a bulb load. P2P energy transfer from the first prosumer to the second prosumer is demonstrated in this experiment. A contingency is created for the second prosumer by disconnecting the switch, SW2, providing power to its load. The P2P energy transfer is made by the first prosumer to the second prosumer to supply its load.

ESP32 sends the prosumers' voltage and current data to the microgrid operator, which operates on the Thinkspeak platform. The MO then commands an energy transfer from Prosumer 1 to Prosumer 2 by sending commands to each ESP 32 to close the relay switches 1 and 2. ESP32 transfers the energy transfer data to the MO on the Thinkspeak platform.

Software: Thinkspeak is an open-source IOT application. It stores and instantly shows the sensor-transferred data on the cloud. It stores data in a central location in the cloud. Here, ESP 32 is used to send data to the cloud with a scanning rate of 1 sec. Arduino Integrated Development Environment (Arduino IDE) is a platform to upload programs on microcontroller memory. Here, the ESP32 add-on is installed to Arduino IDE to initialize the software for ESP32. The Thinkspeak Aurdino library is installed to send the current and voltage sensor readings to the cloud. Authority to program interface (API) determines the user's right to the stored data. The community's residents have viewing rights, whereas MO has control rights. This platform arranges the data in charts for better observation.

Communication: ESP32 uses Message Queuing Telemetry Transmission to communicate with Thinkspeak.It is a lightweight Transmission Control Protocol / Internet Protocol (TCP/IP). It uses publish and subscribe modes. The ThingSpeak platform provides clients access to updating and receiving information from channel feeds via the ThingSpeak MQTT broker. MQTT broker acts as the mediator among its subscribers. When a client sends a message, it

acts as the publisher; when it receives the message, it acts as the receiver [207]. This bi-directional communication is better than the famous unidirectional Hypertext Transfer Protocol (HTTP). [208] uses MQTTv5 for communication in smart grid.

6.2. Results

The hardware simulation experiment is performed for P2P energy transfer using open-source IOT applications among two prosumers. Since a contingency restricts the supply of the second prosumer, he requests for supply from the first prosumer through EMS. Therefore, energy transfer occurs among two community residents. The information on the operation is fully available on the Thinkspeak server, as shown in Fig. 6.4. Fig.6.4(a) reveals state of charge (SOC) and battery voltage of a particular prosumer. Information on the time response can also be obtained from the server through the EMS portal. Fig.6.4(b) indicates the lithium-ion battery response with time which was used in the hardware prototype. Fig 6.4(c) describes the current profile on the sender's end, supplying its local load and the neighbour's load. The time t_1 indicates it. Other times, only the local local-load of the sender is shown. Fig6.4(d) reveals the sender's supply voltage profile. MO also observes the profile in the Thinkspeak cloud platform. The application program interface (API) decides the access to the channel data.
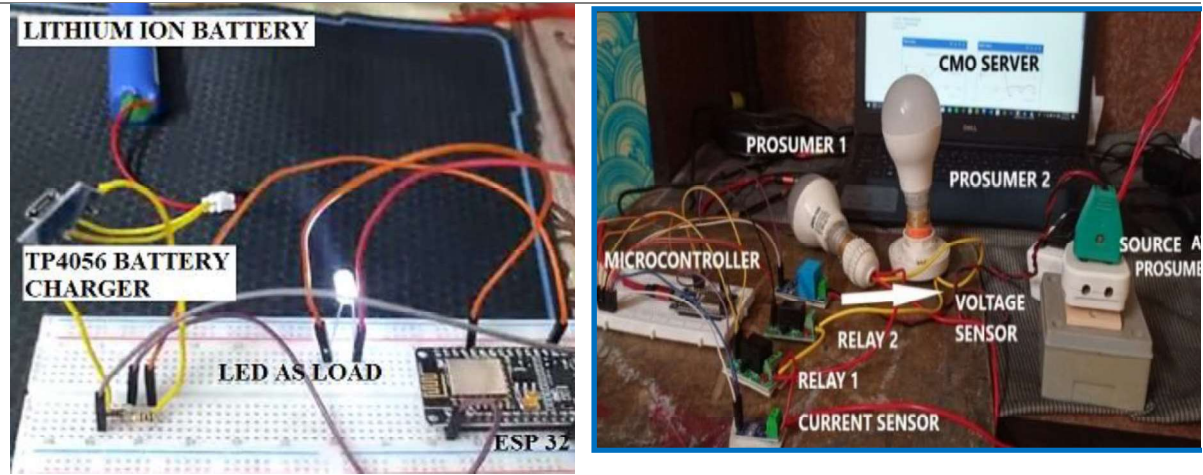
Fig.6.3 Hardware setup (a) Battery voltage monitoring setup (b) P2P energy transfer setup

(a)

(b)

(c)

(d)
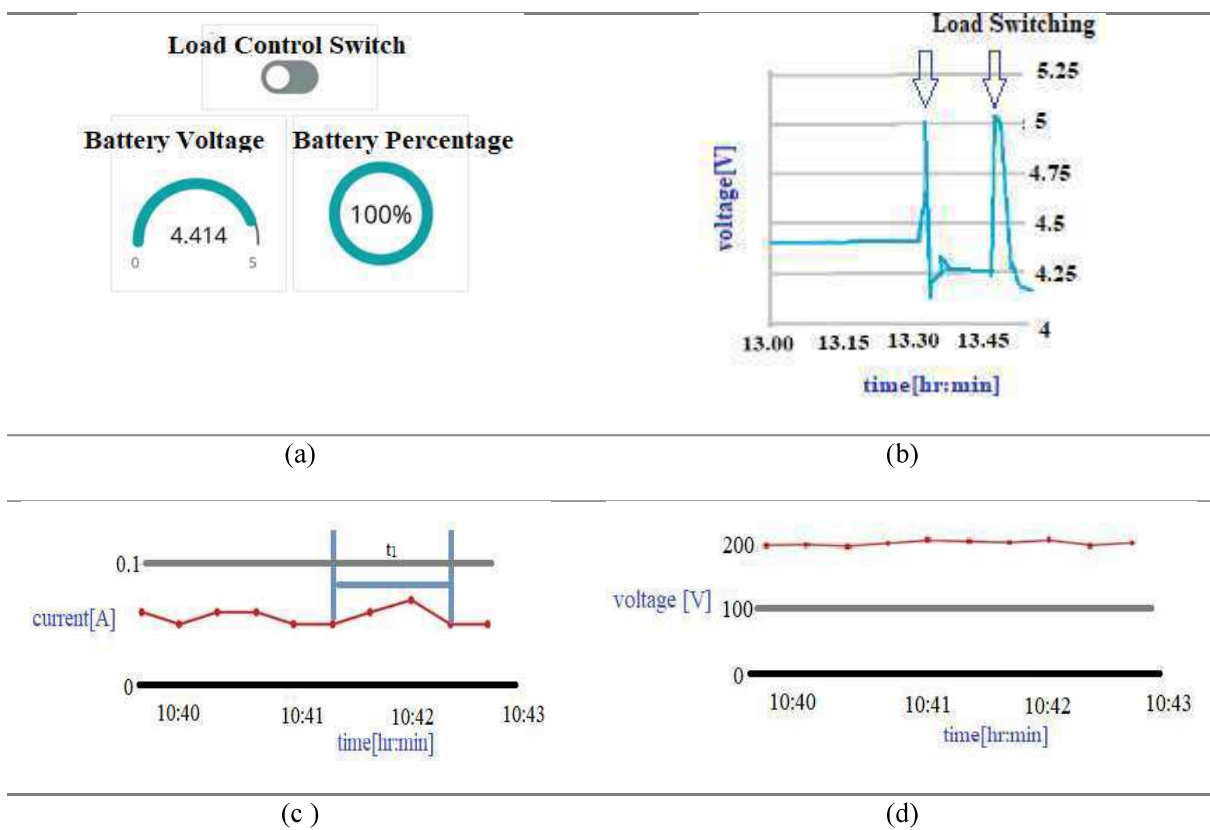
Fig. 6.4.Sensor data in Thinkspeak cloud (a) battery voltage and percentage SOC (b) time

response of battery circuit (c) sender's current profile (d) sender's voltage profile

6.3. Discussion

Real-time monitoring, control, and two-way communication are the built-in parts of any smart grid system. A smart grid monitoring system consists of a communication system that connects all devices with remote monitoring capabilities, utility and end-user to a central data collection location. IoT provides an excellent solution for emulating a traditional power grid into a modern smart grid. This system collects energy information via dedicated hardware, software and communication mechanisms. This chapter uses a low-cost open-source controller with an open-source software application.

Chapter 7

Economic Strategy for a Self-Sufficient Small Residential Microgrid

7.0. Introduction

This chapter explores a strategic approach for an economically sustainable small residential community. The community is powered by rooftop solar photovoltaics. This community plays the role of a microgrid (MG) with a microgrid operator (MO). It operates in two distinct modes: within the MG (peer-to-peer or P2P) and with the utility grid. In this chapter, P2P transfer is experimentally performed with open-source Internet of Things (IoT) applications from the cloud. This application will enable a low-cost MG operation for developing countries.

Few residents from the community who support community welfare are elected. They are considered as delegates. The MO, with delegates, control the energy transfer operation. This approach distributes generated energy among community members at low prices if there is energy demand, minimizing carbon footprint. Selling energy by a prosumer to fellow residents' during their needs is considered as a token of social service towards the community. A social service counter (SSC) is chosen to identify services for each prosumer in the MG. When a seller sells energy within the community, the SSC increases. This count rewards the prosumer in several ways. Delegates allow only the prosumers, with an SSC count above the threshold value, to participate in energy trading with the grid during the high-demand hours of

the day. Delegates are essential in protecting the community's interest while selling energy outside the community. They try to form a coalition among participants to reduce installed capacity and maximize the cumulative payoff.

7.1. System Configuration & Operation

The structure of the MG is configured in Chapter 6 Fig.6.1. Each resident possesses a rooftop solar photovoltaic with a battery backup system associated with a maximum power point tracking (MPPT) charge controller circuit and inverter. The prosumer creates an energy account in the energy management system (EMS) installed on the prosumer's computer. EMS is assumed to predict energy generation, battery management, and load patterns based on weather data, battery specifications, and previous load patterns. Every household connects through a common bus, MB, for P2P energy transfer among the community members. It has been assumed that P2P transfer is only required in case of contingency. A community microgrid operator plays a significant role in the successful operation.

The problem statement addressed in this chapter is shown in Fig.7.1. The MO supervises the energy transfer operations in the community. It also acts as an energy trading aggregator for energy trading to the grid and a validator during energy trading. In this proposed model, a new concept of delegate is introduced. Community benefits largely depend upon
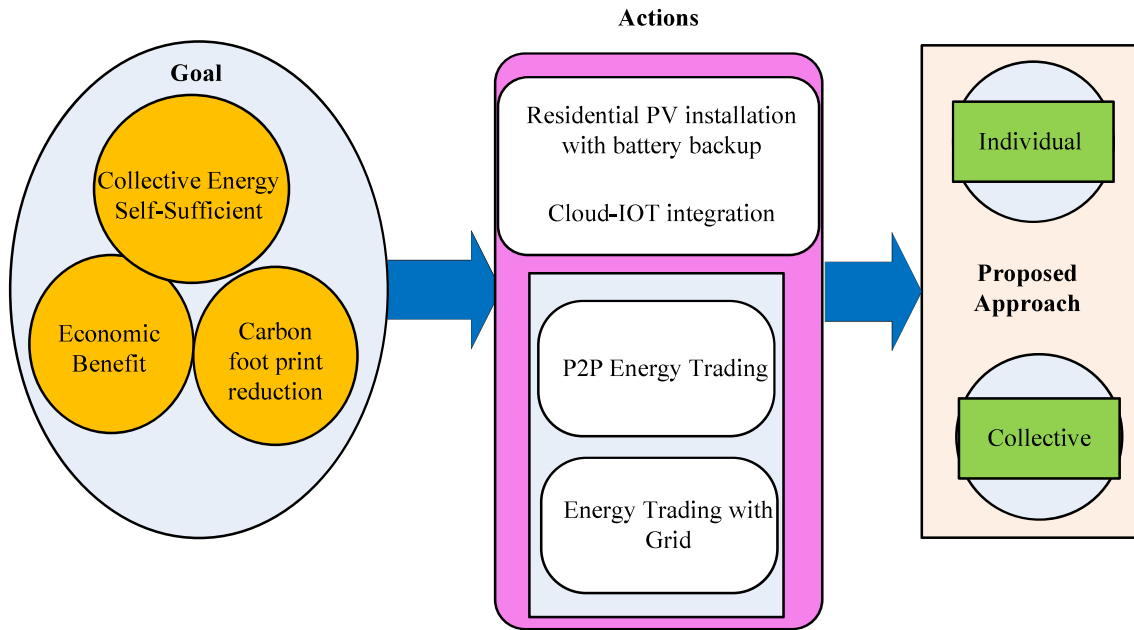
Fig.7.1. Problem Identification

their actions. The Shapley value index is used to determine delegates' contributions. The concept of delegate and the Shapley value is described as follows:

Delegates-Delegates are chosen from community members by all the residents through election. They are responsible for the energy-efficient, economically viable community. The economic benefit of the community largely depends upon their activity. Delegates are accountable for the cumulative benefit of the community. They also get monetary benefits from the community depending upon their actions. Profit maximization of the community determines their payoffs. Community residents set up regulations for energy transfer operations. The delegates monitor the rules. Therefore, validation from the delegates is necessary for every energy transfer operation. If there is consensus among the delegates for an energy transfer operation, then the MO validates the transaction and attaches it to the ledger.

77

Shapley value-Shapley value is named after Lloyd Stowell Shapley, an American economist. This concept is used in cooperative game theory to identify the distribution of money among the players playing the game. It indicates the contribution of one considering all of the possible relative moves by others. In this approach, Shapley's value is used to determine the contribution of the respective delegates to form a grand coalition, and the delegate with the most contributions gets more payoff. Therefore, for a coalition S_c, the payoff distribution among players, j shall receive payoff x_j where payoff vector $x=(x_1,x_2,...x_n)$ where $N=\{1,2,...n\}$ are the sets of players and $n=|N|$ is the total number of players. Games gained for each coalition or characteristic function are denoted with $v(S_c)$ and can be expressed as $v: 2^n \rightarrow \mathbb{R}$. The Shapley value ϕ_j can be expressed as

$$\phi_j = \sum_{S_c \subseteq N \setminus \{j\}} \frac{|S|!(n-|S|-1)!}{n!}(v(S_c \cup \{j\}) - v(S_c)) \tag{7.1}$$

The community operates in two distinct modes of energy transfer operation as follows:

   i)   P2P energy transfer during the day

   ii)   Trading with the grid with stored energy in a battery during peak demand hours in the evening

Buying electricity from the grid during low tariff hours is only allowed if the community collectively cannot support its demand. The rules by the community residents are set as follows:

7.1.1.Rules

i.   The price of unit energy ($Pc\tau$) for P2P transfer is determined by MO is kept less than the grid buying price for unit energy ($P_{g\tau}$) at that time,τ, i.e $P_{c\tau} < P_{g\tau}$

ii.   Before asking for energy transfer, the buyer must minimize his demand as much as possible.

iii. The resident buying energy cannot trade with the grid for next 24 hrs. This regulation avoids making a profit by buying energy from the community at a lower rate and selling it to the grid at a high price during peak demand hours.

iv. The seller can only sell a maximum set percentage of its installed capacity.

v. If the community cannot fulfil the demand, then only a consumer can buy electrical energy from the grid.

vi. Seller must pay a network cost (P_{nc}) or wheeling charge for each transaction to MO.

vii. Social service counter, SSC: SSC counter value (Σ_p) is considered a token of service offered to the community. With each P2P transaction Σ_p for the seller is increased by one. If Σ_p reaches a set value as below, then one resident can participate in electrical energy trading with the grid. Considering the SSC with the number of days of a week is applied to allow trading with the grid as follows:

$$w_p \geq (\Sigma_p/number\ of\ days\ in\ a\ week) * 100\% \tag{7.2}$$

A minimum set value (w_p) of 20% is mandatory for trading with the grid.

Residents of the community or prosumers generate power during the daytime, depending on their respective solar panel capacity. Due to various quantities of energy generation and load requirements, energy demand may arise within the MG. This situation establishes the peer-to-peer (P2P) power transfer between two residents. The procedure involved in the trading operation is described below.

Power from each prosumer is fed to the bus through a smart meter (SM) and a normally open (NO) switch. MO control the switching action through the IoT cloud. A wi-fi-enabled microcontroller unit receives the command from the cloud and controls the switches through general-purpose input-output (GPIO) pins. MO sells green energy (trapped solar energy) to the grid during high demand. The battery stores energy during the daytime for load levelling at

peak demand in the real-time market. Real-time active and reactive power dispatch from the prosumer is supplied, controlling the MB voltage and individual prosumer's phase angle, respectively, as expressed in (7.3), (7.4) and shown in Fig. 7.2 (a) and 7.2(b).
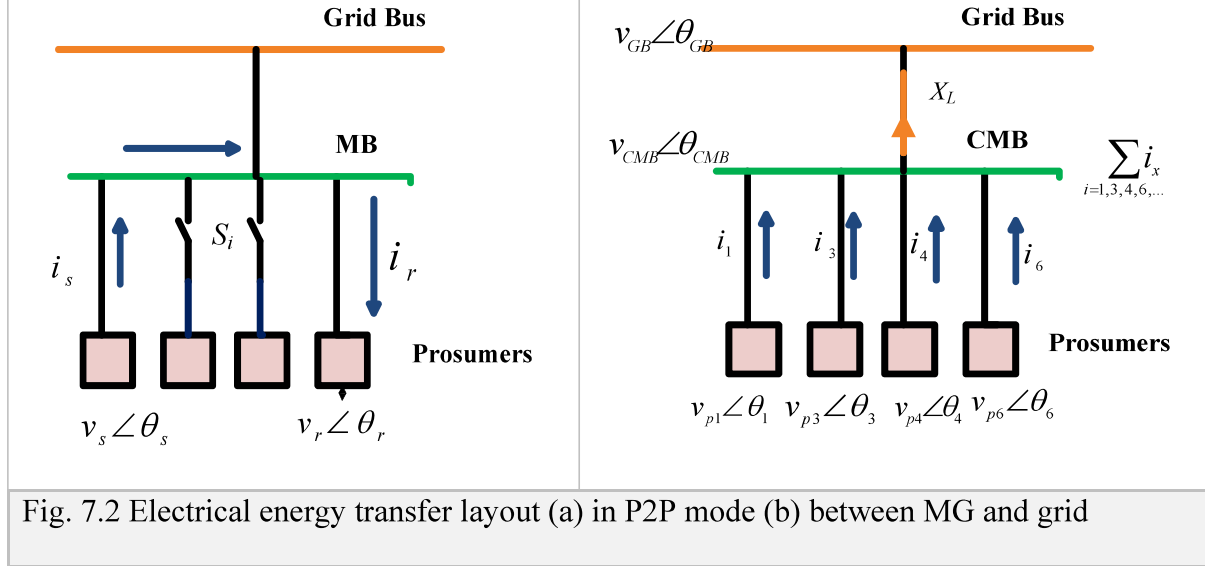
Fig. 7.2 Electrical energy transfer layout (a) in P2P mode (b) between MG and grid

7.2. Mathematical Model

This section's system model parameters are based on energy transfer. It is divided into two sections. One is associated with P2P energy transfer within MG, and the other is for energy trading with the utility grid.

7.2.1 P2P Energy Sharing Within Community

v_{MB} is the community microgrid bus voltage. A switch (S_i) links each prosumer and MB. S_i is an on-off switch with $S_i \in \{0,1\}$. The number of S_i is equal to the number of prosumers, i.e., $S_i \in \{0, 1, 2....., n\}$. During P2P energy transfer within the community, the states of switches except the participants' switches are S_i=0. Agreement between electrical energy sender and receiver initiates P2P energy transfer. As a result of their agreement, two switches, S_s (sender switch) and S_r (receiver switch) will be on, i.e.,

$S_s, S_r = 1$ when $\left| v_s \right| > \left| v_r \right|$ or $\angle \theta_s$ leading and $\angle \theta_r$ lagging

Where $v_s \angle \theta_s$ is the sender voltage, $v_r \angle \theta_r$ is the receiver voltage, $\angle \theta_s$ is the sender's phase angle and $\angle \theta_r$ is the receiver's phase angle.

$$i_{sr} > \frac{v_s \angle \theta_s - v_r \angle \theta_r}{Z_{sr} + Z_{Lr}} \qquad (7.3)$$

Where i_{sr} is the current from the sender's source to the receiver's load. Z_{sr} is the output impedance between the sender and receiver end, Z_{Lr} is the load impedance of the receiver. Members of the community and the MO are connected through the web-based energy account. If a resident has excess energy generation, he can log in to his account and request energy sales. Similarly, for demand, one can request energy buying. The MO allows transfer of energy between buyer and seller at a pre-determined rate. The rules for energy transfer are made considering service to the community and an independent energy society with green energy participation in the energy market.

7.2.2. Energy Trading Model with Grid

The community redirects the power flow from the battery towards the grid in the late evening when the grid tariff is at its maximum and sunlight is absent. The community bus is connected to the grid bus through a feeder having inductance X_L. Tariff becomes maximum when the power demand of the grid is high. There is demand of power on the grid. The microgrid bus phase angle ($\angle \theta_{MB}$) leads the grid bus phase angle. Active power flows from the microgrid bus to grid bus [17]. Fig. 7.2(b) indicates if any prosumer voltage is v_{px} where $\angle \theta_x$ is his generation phase angle, Z_{px} is his impedance, and his MB switch S_x is ON, then

current will flow from the prosumer towards MB if $\angle\theta_{MB}$ lags $\angle\theta_x$. Therefore, the total current flow from prosumer ends to MB, (i_{CM2G}), with 'l' number of switches are ON, ($l \leq n$) is:

$$i_{CM2B} = \sum_{x=2,5,8,11,\ldots} i_x = \sum_{x=2,5,8,11,\ldots} (v_{px}\angle\theta_x - v_{CMB}\angle\theta_{CMB})/Z_{px} \qquad (7.4)$$

This current flows towards the grid bus if $\angle\theta_{GB}$ is more lagging than $\angle\theta_{MB}$:

$$i_{CM2G} = (v_{CMB}\angle\theta_{CMB} - v_{GB}\angle\theta_{GB})/X_L \qquad (7.5)$$

where X_L is the grid-side power network impedance.

7.3.   Energy Transfer Economics

7.3.1. P2P energy transfer during the day

Every member or node creates an Externally Owned Account (EOA) for energy transfer. The account is provided with an account number (η) and a private key (K). After creating an account, a node must ask for entry permission to the network. After getting permission, a node can participate in a P2P power transfer. Buyers and sellers place demand and quantity through EMS. Then, the power balance equation for demand and supply is compared in (7.6). The power balance equation compares the bided generation and consumption of the prosumer and decides the possibility of transfer. Let us suppose that at any instant, a request for q_{dp} energy demand comes from the buyer and q_0 energy is offered by the seller. Therefore, the power balance equation becomes

$$q_0 \geq q_{gp} - q_{dp} - q_{lp} \qquad (7.6)$$

where q_{gp} refers to the overall generation of the prosumer, and q_{lp} refers to the local load demand of the prosumer.

The phenomenon invokes a smart contract action. Smart contracts are digital directives stored to check if certain conditions are met or differ as follows:

i.   It checks for equation (7.6)

ii.   Delegates validate the status of seller and buyer

iii.   TRUE condition initiates the contract between buyer and seller with the mentioned price and time of transfer.

iv.   EMS triggers a control circuit which switches on the power transfer between buyer and seller at the times mentioned in the contract.

Transaction sends the details to a shared, accessible, immutable ledger in the cloud. The participants can observe past transactions through their respective EMS accounts. The ledger includes the following information:

     a. Supplier Account Address

     b. Receiver Account Address

     c. Transaction Details

     d. Hash ID

     e. Date and Time

In this energy transfer within the community, the buyers' spending amount

$$C_b = P_{C\tau} \times q_{dp} \tag{7.7}$$

Where Pcr is the energy price per unit and q_{dp} energy demand comes from the buyer .

And seller's gain

$$G_S = P_{C\tau} \times q_o - P_{nc} \tag{7.8}$$

Where q_0 energy is offered by the seller and P_{nc} is the cost for unit energy production of the seller

7.3.2. Trading with the grid

As the demand for the primary grid is at its maximum in the evening, MO decides to sell power then. Thus, participants having a battery backup system can sell power. For trading with the grid, the MO declares the market demand function (*MD*) and invites a quote for the amount of energy for selling and the price per unit of energy. MO is an intermediary organization between an MG and the electricity market. More than one MG operates under one MO. MO is an independent entity and does not care about MG's structure and economic welfare; instead, it tries to increase its profit margin. Delegates are MG representatives who look after the welfare and community profit from energy selling to the grid. Delegates take an essential role in identifying participants and maximizing the profit from the trading for the community.

a. If SSC Σ_p reaches the minimum set value, then only delegates allow one resident to participate in electrical energy trading with the grid.

b. Sellers are small domestic RES-dependent prosumers; they produce limited energy. Cooperation among themselves leads to reliable operation because this would

      i.   decreases the individual installed capacity of residents

      ii.   increases reliability

      iii.   escalates the community profit

Residents of the MG participating in trading are forming a coalition. If several small groups within the community interact with MO for trading and impart competition among themselves, it hinders community interest. The coalition of all players is called a grand coalition. Grand Coalition decreases the quantity of energy each resident delivers and can store the rest in its battery and use it during peak hours, thereby increasing its profits. Delegates tries

to maximize the number of participants in the grand coalition to increase community profit. An increase in community profit economically benefits the delegates. Their respective contributions pay them. The contributions of delegates are calculated from the Shapley value index.

7.3.2.1.   Cooperative Game

If at any instant the number of participants towards energy selling with the grid is l. The energy produced by l numbers of participants are $\{q_1, q_2, \ldots, q_l\}$ respectively. Let Q be the total electric energy the community produces, which is the aggregated sum of the outputs from each prosumer participating.

$$Q = \sum_{i=1}^{l} q_i \qquad (7.9)$$

Now, to optimize the electric energy quantity and maximize the payoff

$$\max\{i\} \text{ for } i=1,\ldots\ldots N \qquad (7.10)$$

Where N is the total number of community residents.

The produced electric energy (Q) and unit price (P) have a relationship:

$$Q = -\sigma P + \kappa \qquad (7.10a)$$

Where σ is the slope of the demand curve and κ is the quantity intercept of the demand. Price is expressed as:

$$P = -(Q/\sigma) + (\kappa/\sigma) \qquad (7.10b)$$

Cost Function:

$$\psi_1 = f(q_1)$$
$$\psi_2 = f(q_2)$$
.
$$\psi_l = f(q_l)$$

Where the above are the costs borne by the prosumers depending upon the amount of electrical energy sold by each prosumer.

Individual maximization occurs when $\partial \psi_i / \partial q_i = 0$

The cumulative cost function is

$$\psi = \sum_{i=1}^{i} \psi_i \tag{7.11}$$

Payoff

$$U = \Re - \psi \tag{7.12}$$

where $\Re$ is total revenue

Marginal Revenue:

$$\Re_m = d\Re / dQ \tag{7.13}$$

Marginal cost function

$$\psi_m = d\psi / dq \tag{7.14}$$

Equilibrium reaches when:

$$\psi_m = \Re_m \tag{7.15}$$

Shapley's value decides the pay-off to the delegates as per (7.1). It is considering the case of two delegates in the community. Therefore, it will be a two-player game. In two two-player games, i.e., only two permutations are possible *{1,2}* and *{2,1}*. *{1,2}* If for player 1 gets *v{1}* then player *2* will get *v{L}-v{1}*. Similarly, for *{2,1}* if player 2 gets *v{2}* then player 1 will get *v{L}-v{2}*. Considering total residents as 30 and *80%* of residents, i.e.*v{L}= 24* taking part in trading, then Shapley value for each delegate can be obtained as shown in the following Table 7.1:

Table 7.1. Case Study: Shapley Value Calculation

Probability	Order of arrival	1st delegates contribution	2nd delegates contribution
1/2	{1,2}	10	24-10=14
1/2	{2.1}	11	24-11=13
Overall contribution per player		10+11=21	14+13=27
Shapley value for delegates		½*21=**10.5**	½*27=**12.5**

7.3.2.2. Competitive Game

If the community residents act individually to sell energy to MO, they can either make simultaneous decisions or observe one another's move sequentially. It is called a simultaneous game if the players select a game plan simultaneously without following other players' activities. However, if one player observes the opponent's strategy before selecting his move, it is called a sequential game.

Simultaneous Game-Cournot's duopoly model is a simultaneous game is described below. Let us assume the game between two players, $i= x, y$, with cost ψ_m. The game can be modelled following the equations from 7.12 to 7.14. From the marginal cost function, the reaction curve for two players, x and y, can be obtained as follows

$$q^*_x = q^*_y = \frac{(\kappa/\sigma) - \psi_m}{(l+1)/\sigma} \quad [l=2] \tag{7.16a}$$

Therefore, the market price becomes from (7.10b)

$$P^* = P_C = -\frac{(q_x + q_y)}{\sigma} + \frac{\kappa}{\sigma} = \frac{(\kappa/\sigma) + 2\psi}{(l+1)} \tag{7.16b}$$

And overall quantity to be produced by the community

$$Q^* = \frac{2(\kappa/\sigma) - 2\psi_m}{(l+1)}$$

(7.16c)

For $l \to \alpha$ Cournot equilibrium tends towards perfect competition and $P^* \to \Sigma\psi_m$.

The profit become

$$U_x = U_y = \frac{[(\kappa/\sigma) - \psi_m]^2}{9/\sigma}$$

(7.16d)

Sequential Game- Another choice can be a sequential move game represented by the Stackelberg competition. In this game, the leading firm chooses its quantity on the reaction curve of the other firm. Suppose x has a larger battery bank capacity; therefore, x is the leader among the two players. In the Stackelberg game, x will observe the reaction function of y. The same linear demand function is also applied here. Therefore, the revenue for the second player can be expressed as

$$\Re_y = \{-(\frac{q_x + q_y}{\sigma}) + \frac{\kappa}{\sigma}\} \times p_y$$

(7.17a)

$\dfrac{\partial \Re_y}{\partial q_y} = 0$ gives reaction function as

$$q^*_y = \frac{\dfrac{\kappa}{\sigma} - \dfrac{1}{\sigma}q_x - \psi_m}{\dfrac{2}{\sigma}}$$

(7.17b)

Putting the value of q^*_y in $\dfrac{\partial \Re_x}{\partial q_x} = 0$ and solving

$$q^*_x = \frac{\dfrac{\kappa}{\sigma} - \psi_m}{\dfrac{2}{\sigma}}$$

(7.17c)

and $q^*_y = \dfrac{\dfrac{\kappa}{\sigma} - \psi_m}{\dfrac{4}{\sigma}}$ (7.17d)

$$Q^* = \frac{3[(\kappa/\sigma) - \psi_m]}{4/\sigma}$$ (7.17e)

$$P^* = P_s = \frac{(\kappa/\sigma) + 3\psi_m}{4}$$ (7.17f)

The profit becomes

$$U_x = \frac{[(\kappa/\sigma) - \psi_m]^2}{8/\sigma}$$ (7.17g)

$$U_y = \frac{[(\kappa/\sigma) - \psi_m]^2}{16/\sigma}$$ (7.17h)

It is obtained from the relationships that the leader has more profit than the follower; however, he needs to produce more energy.

7.4. Algorithms for energy trading with the grid

Community trades with the grid through MO during high tariff hours from their battery storage. Community rule allows participation depending upon Σ_p. Delegates communicate with all participants to form a grand coalition to maximize community profit. Fig.7.3(a) indicates the approaches while trading with the grid. The steps are as follows:

1)   The overall marginal cost of the MG is determined by adding cost functions horizontally, also known as lateral summation.

2)   From the market demand, market revenue is obtained

3)   The intersection point of the market revenue with the overall cost function provides the equilibrium point or lowest selling price to avoid loss.

4) Cumulative energy produced by the community with maximum selling price is also obtained from the equilibrium point, as explained in Fig.7.4(a).

Apart from cooperation, participants can compete with each other. A comparative study is performed with two competitive strategies (simultaneous and sequential) in this thesis. The algorithms for two competitive games is described in Fig. 7. 3(b.)

t=0 Query generated by CMO for Q	t++;t=T Request placed by Prosumers $\sum P_i$ $i=1,3,4,$ $6,9.15.....$	If Σ_p Is true	Predict q_i and P	Accept calls Trading Contract

Collusive Model Prediction Algorithm

1. Find lateral summation of $\Lambda = \Sigma MC_i$

2. Get Q from (7.10a)

3. Generate Cumulative Market Revenue $\Re$ and $\Re_m$ from (7.12) & (7.13)

4. Get Equilibrium, E, at intersection of Λ & $\Re_m$ as (Q_T, P_e)

5. Co-ordinate Q_T= total energy to be supplied

6. Extrapolate P_e to demand function to get selling price P

Return (Q_T, P)

(a)

Cournot Model

1.   Get Demand Function from (7.10a)

2.   Get the Best Responses of the players from from (7.16a)

3.   Calculate Payoff of Prosumers $U_{Cx}(q_x, q_y)$ and $U_{Cy}(q_y, q_x)$ from (7.16d)

4.   Get Cournot Equilibrium (q_{xC}, q_{yC}) & Predicted Price (P_C)

End

Stackelberg Model

Start:

1.   Get Demand Function from (7.10a)

2.   Get the Demand Function for Stackelberg from (7.17b)

4.   Calculate Payoff of Leader Prosumers $U_{Sx}(q_x, q_y)$ from (7.17g)

5.   Get Best Responses of the Leader, Follower (q_{xS}, q_{yS}) and Predicted Price (P_S) using

(7.17c) (7.17d)

6.   Return (P_C, q_{xC}, q_{yC}) and (P_S, q_{xS}, q_{yS})

(b)

Fig.7.3. Algorithms for Energy Trading (a) Cooperative (b) Competitive

7.5.   Results

Fig 7.4 describes the energy trading results for community residents' distinct conducts. Fig 7.4(a) indicates a case study when the sellers cooperate. Fig7.4(b) and (c) indicate if they decide to go for individual decisions that would inward them towards competition. Competitive actions among two residents are simulated here. Two methods of popular competitive games, the Cournot and Stackelberg model, are used for comparison. The coordination algorithm works on proportionate marginal cost (MC) functions of prosumers as per the battery sizing.

The market survey observed that the larger battery capacity price given per unit is comparatively less.Therefore, the seller with higher battery ratings gets an advantage as a leader. In the case study analysis, 150Ah and 120Ah C10 batteries are used. When the prosumer's battery charges from his solar panel, the battery charging cost is almost zero; therefore seller's MC is chosen, treating installation cost, maintenance cost etc. A network cost is added for the MO for each successful transaction. Assumptions for ψ_{m1} and ψ_{m2} are the MC functions of two prosumers; MC_T represents the cumulative MC of the prosumers, i.e. lateral summation of MC. Equilibrium reaches when MC_T reaches cumulative marginal revenue, as shown in Fig. 7.4(a). **The price is expressed in US Cent equivalent from data collected in Indian Rupees.** The price at the equilibrium point is 7.83 US cents per unit of energy, as estimated in India, and the total energy produced by the community is 13.6839 kWh. The projection of the equilibrium point on the MD predicts the selling price of unit energy. Here, it is 20.05 US cents per unit of energy

On the other hand, non-cooperative game theory creates competition, which burdens them regarding energy production to fulfil the agreement with MO. Moreover, classical non-cooperative games generally did not consider the interdependences of the participants. However, in small groups, interdependences reflect in each player's action, leading to collusion among players. Therefore a collusive model with a proportional cost-sharing approach is proposed for the domestic prosumers of the small residential microgrid. A comparative study between the proposed technique and two non-collusive models in the restricted domain, like the Cournot and Stackelberg algorithm, reveals that the proposed method is more suitable for a small residential community microgrid.

The cost of the overall production is 7.83 US cents. The amount of electric energy required from each prosumer depends upon the equilibrium point obtained and the prosumer's respective MC. Here, the equilibrium price intersecting with ψ_{m1} gives almost 7.6 kWh from

one prosumer, and intersecting with ψ_{m2} gives 6.083 kWh of energy from another prosumer. From the law of the market, increased participation reduces MC_T and increases the capacity to fulfil more demand. Therefore, although the selling price may decrease with increased participation, the community's payoff increases with more participants. Now, if residents want to bid individually, then competition comes between them. In Fig7.4(b) and (c), the determination of energy quantity produced by the same prosumers and demand function is illustrated by applying Cournot and Stackelberg model. Fig7.4(b) shows that the Cournot model determines energy production of 10.74 kWh and 8.56 kWh from leader and follower, respectively. As per the demand function, the price per unit of energy comes out to be 15.56 US cents (P_C). In Fig7.4(c), as per the Stackelberg algorithm, the leader prosumer firm makes the production decision by observing the intersection of the follower firm's reaction function (orange line) and own profit curve. The quantity produced by the leader prosumer is 16.1125 kWh (q_{1S}), and by the other, it is 5.88125 kWh ($q_{2S.}$). The price function is 13.405 US cents (P_s).

Fig.7.5 compares the game approaches regarding production cost, selling price, the overall electrical energy produced and quantity produced by each prosumer. This thesis chapter takes the distinct MC function for two prosumers. In the collusive model, the cumulative marginal cost (MC_T)is calculated by the horizontal addition of individual players MC. The value of MC_T is in between the individual player's MC. Therefore, the individual profit of the players above the MC_T (P2 in this chapter) will get less profit. However, the profit of P2 is still more significant for simultaneous or sequential competition.

Additionally, both the players need to produce electrical energy much less than in competitive games. The study reveals that prosumer 1, a leader in the Stackelberg model, needs to produce the highest quantity among all the methods, which may burden domestic prosumers. However, the proposed method demands the least generation from a prosumer, which benefits
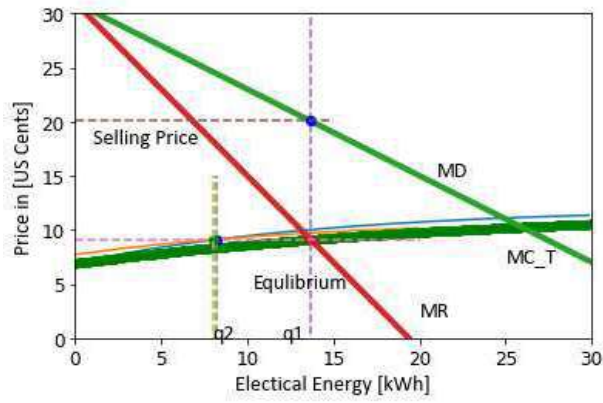
(a)
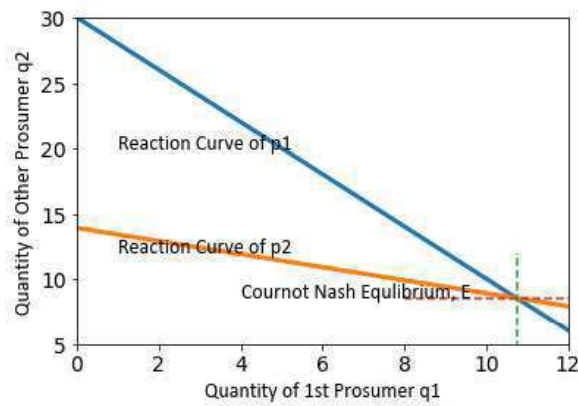
(b)
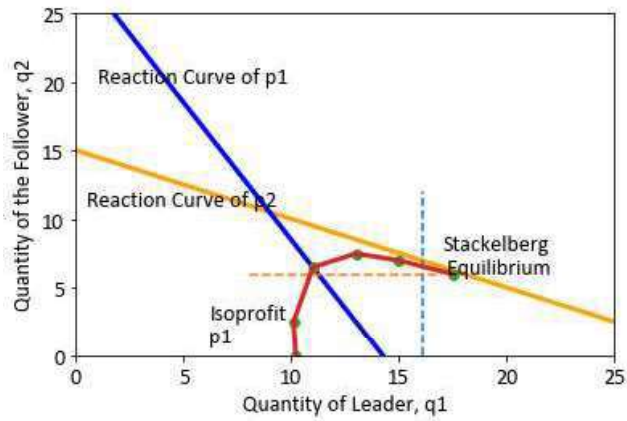
(c)

Fig. 7.4 (a) Selling quantity and price prediction using proportionate cost collusive model;

(b) Quantity equilibrium determination for non-collusive Cournot model (c) Quantity

equilibrium determination for non-collusive Stackelberg model

94
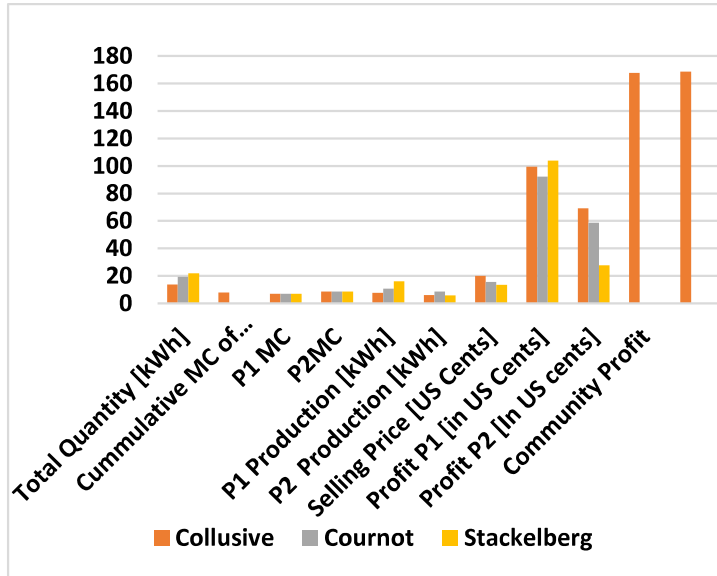
Fig.7.5. Comparative analysis between proportionate cost sharing collusive model, Cournot and Stackelberg model for two prosumers

7.6.   Discussion

This chapter proposes a MG concept with a rooftop solar and battery backup system for households where prosumers can actively participate in energy trading using IoT cloud applications for a sustainable future. The MG residents participate in P2P energy transfer during the daytime to create energy balance within the community, reducing carbon footprint. Transaction details, sender and receiver account details and energy transfer amount are kept in a distributed ledger validated with the dPOS consensus algorithm by the MO and a witness board. Service towards the community is made essential unless residents cannot participate in business like selling electricity to the grid. Witnesses try to obtain the Pareto optimal condition in the game to maximize community profit, increasing their payoffs. The players in this trading are small domestic electrical energy suppliers; therefore, the proposed method yields good

results. The author has also observed that the non-cooperative game theory creates competition, which may burden them regarding energy production to fulfil the agreement with MO.

Moreover, classical non-cooperative games generally did not consider the interdependences of the participants. However, in small groups, interdependences reflect in each player's action, leading to collusion among players. Therefore, a collusive model with a proportional cost-sharing approach is proposed for the domestic prosumers of the small residential microgrid. A comparative study between the proposed technique and two non-collusive models in the restricted domain, like the Cournot and Stackelberg algorithm, reveals that the proposed method is more suitable for a small residential community microgrid.

Chapter 8

Conclusion

Modern generation trends through renewable energy-based distributed energy resources have made microgrids vital to the power system. Robust control techniques and quality power have become essential microgrid (MG) requirements. This thesis searches for the control algorithms for DSTATCOM that take care of MG's voltage profile and supply reactive power to the MG loads. Even today, the installation of these devices needs sufficient technical expertise and time from utility engineers. Artificial intelligence can solve this problem and save human labour and time incorporating plug-and-play features to the DSTATCOM. This thesis proposed a continuous control set model predictive control (CCS-MPC) on an inverter for dynamic voltage regulation supplying reactive power to the load for the MG. The proposed method uses the terminal voltage magnitude, which reduces calculation time, sensor per phase, and the engagement burden of the controller. This chapter applies a nonlinear DSTATCOM model and a series-parallel structure nonlinear autoregressive exogenous (NARX) model of artificial neural network (ANN) to predict future output, which CCS-MPC optimizes. The proposed VSI with CCS MPC is applied to a case study of a real system as a plug-and-play device.

The renewable energy sources of MG are intermittent and require energy storage. This thesis proposes a concept of energy self-sufficient MG with a rooftop solar and battery backup system for each household where prosumers can actively participate in energy trading using low-cost IoT cloud applications for a sustainable future. The MG residents participate in P2P energy transfer during the daytime to create energy balance within the community, and thereby reducing the carbon footprint. Transaction details, sender and receiver account details and energy transfer amount are kept in a distributed ledger

validated with the dPOS consensus algorithm by MO and a group of delegates. Service towards the community is made an essential qualification cannot participate in business like selling electricity to the grid. Delegates try to maximize community profit, increasing their payoffs. Marginal contributions of the delegates are calculated by using an index called the Shapley value. The players in this trading are small domestic electrical energy suppliers. Cooperative method yields better results with respect to profit and energy production than the non-cooperative games.

References

[1]   D. H. Nguyen, "Electric vehicle-wireless charging-discharging lane decentralized peer-to-peer energy trading," *IEEE Access*, vol. 8, pp. 179616–179625, 2020, doi: 10.1109/ACCESS.2020.3027832.

[2]   X. Fang, Q. Zhao, J. Wang, Y. Han, and Y. Li, "Multi-agent Deep Reinforcement Learning for Distributed Energy Management and Strategy Optimization of Microgrid Market," *Sustain. Cities Soc.*, vol. 74, no. July, p. 103163, 2021, doi: 10.1016/j.scs.2021.103163.

[3]   E. A. Bhuiyan, M. Z. Hossain, S. M. Muyeen, S. R. Fahim, S. K. Sarker, and S. K. Das, "Towards next generation virtual power plant: Technology review and frameworks," *Renew. Sustain. Energy Rev.*, vol. 150, no. July, p. 111358, 2021, doi: 10.1016/j.rser.2021.111358.

[4]   K. Mahmud, B. Khan, J. Ravishankar, A. Ahmadi, and P. Siano, "An internet of energy framework with distributed energy resources, prosumers and small-scale virtual power plants: An overview," *Renew. Sustain. Energy Rev.*, vol. 127, no. April, p. 109840, 2020, doi: 10.1016/j.rser.2020.109840.

[5]   K. O. Adu-Kankam and L. M. Camarinha-Matos, "Towards collaborative Virtual Power Plants: Trends and convergence," *Sustain. Energy, Grids Networks*, vol. 16, pp. 217–230, 2018, doi: 10.1016/j.segan.2018.08.003.

[6]   A. A. Alkahtani *et al.*, "Power Quality in Microgrids including Supraharmonics: Issues, Standards, and Mitigations," *IEEE Access*, vol. 8, pp. 127104–127122, 2020, doi: 10.1109/ACCESS.2020.3008042.

[7]   M. M. Hashempour and T. L. Lee, "Integrated power factor correction and voltage fluctuation mitigation of microgrid using STATCOM," *2017 IEEE 3rd Int. Futur.*

Energy Electron. Conf. ECCE Asia, IFEEC - ECCE Asia 2017, no. 3, pp. 1215–1219, 2017, doi: 10.1109/IFEEC.2017.7992215.

[8]   R. An, Z. Liu, and J. Liu, "Successive-Approximation-Based Virtual Impedance Tuning Method for Accurate Reactive Power Sharing in Islanded Microgrids," *IEEE Trans. Power Electron.*, vol. 36, no. 1, pp. 87–102, 2021, doi: 10.1109/TPEL.2020.3001037.

[9]   W. Deng, N. Y. Dai, K. W. Lao, and J. M. Guerrero, "A Virtual-Impedance Droop Control for Accurate Active Power Control and Reactive Power Sharing Using Capacitive-Coupling Inverters," *IEEE Trans. Ind. Appl.*, vol. 56, no. 6, pp. 6722–6733, 2020, doi: 10.1109/TIA.2020.3012934.

[10]   L. Ahmethodzic and M. Music, "Comprehensive review of trends in microgrid control," *Renew. Energy Focus*, vol. 38, no. September, pp. 84–96, 2021, doi: 10.1016/j.ref.2021.07.003.

[11]   C. Hu, Z. Liu, R. Li, P. Hu, T. Xiang, and M. Han, "Smart Contract Assisted Privacy-Preserving Data Aggregation and Management Scheme for Smart Grid," *IEEE Trans. Dependable Secur. Comput.*, vol. PP, pp. 1–17, 2023, doi: 10.1109/TDSC.2023.3300749.

[12]   G. Shahgholian, "A brief review on microgrids: Operation, applications, modeling, and control," *Int. Trans. Electr. Energy Syst.*, vol. 31, no. 6, pp. 1–28, 2021, doi: 10.1002/2050-7038.12885.

[13]   R. Majumder, "Some aspects of stability in microgrids," *IEEE Trans. Power Syst.*, vol. 28, no. 3, pp. 3243–3252, 2013, doi: 10.1109/TPWRS.2012.2234146.

[14]   G. Jóos, B. T. Ooi, D. McGillis, F. D. Galiana, and R. Marceau, "The potential of distributed generation to provide ancillary services," *Proc. IEEE Power Eng. Soc. Transm. Distrib. Conf.*, vol. 3, no. d, pp. 1762–1767, 2000, doi:

10.1109/pess.2000.868792.

[15] G. D. Marques, "Comparison of active power filter control methods in unbalanced and non-sinusoidal conditions," *IECON Proc. (Industrial Electron. Conf.*, vol. 1, pp. 444–449, 1998, doi: 10.1109/iecon.1998.724284.

[16] S. Panda and N. P. Padhy, "Optimal location and controller design of STATCOM for power system stability improvement using PSO," *J. Franklin Inst.*, vol. 345, no. 2, pp. 166–181, 2008, doi: 10.1016/j.jfranklin.2007.08.002.

[17] G. C. Keerthana and B. Vidyasagar, "Adaptive Back Propagation Control Algorithm for PQ Improvement Using STATCOM," *J. Curr. Trends Electr. Eng.*, vol. 4, no. 3, pp. 12–26, 2019.

[18] G. Kumaravel and C. Kumar, "Design of self-tuning PI controller for STATCOM using bats echolocation algorithm," *Eur. J. Sci. Res.*, vol. 54, no. 3, pp. 473–483, 2011.

[19] U. R. Babu, V. V. K. Reddy, and S. Tarakalyani, "Notice of Removal: Design and simulation of Genetic algorithm for DSTATCOM," *Int. Conf. Electr. Electron. Signals, Commun. Optim. EESCO 2015*, pp. 6–9, 2015, doi: 10.1109/EESCO.2015.7253991.

[20] P. Mitra and G. K. Venayagamoorthy, "An adaptive control strategy for DSTATCOM applications in an electric ship power system," *IEEE Trans. Power Electron.*, vol. 25, no. 1, pp. 95–104, 2010, doi: 10.1109/TPEL.2009.2024152.

[21] B. B. Bukata and Y. Li, "A novel model-free prediction of power quality problems via DSTATCOM," *ICAC 12 - Proc. 18th Int. Conf. Autom. Comput. Integr. Des. Eng.*, no. September, pp. 37–42, 2012.

[22] A. Rashad, S. Kamel, F. Jurado, M. Abdel-Nasser, and K. Mahmoud, "ANN-Based STATCOM Tuning for Performance Enhancement of Combined Wind Farms," *Electr. Power Components Syst.*, vol. 47, no. 1–2, pp. 10–26, 2019, doi:

10.1080/15325008.2019.1570052.

[23]   H. Li, Y. Huang, and J. Lu, "Reactive power compensation and DC link voltage
control using Fuzzy-PI on grid-connected PV system with d-STATCOM," *Asia-
Pacific Power Energy Eng. Conf. APPEEC*, vol. 2016-Decem, pp. 1240–1244, 2016,
doi: 10.1109/APPEEC.2016.7779691.

[24]   J. Shi, A. Noshadi, A. Kalam, and P. Shi, "Fuzzy logic control of DSTATCOM for
improving power quality and dynamic performance," *2015 Australas. Univ. Power
Eng. Conf. Challenges Futur. Grids, AUPEC 2015*, pp. 2–7, 2015, doi:
10.1109/AUPEC.2015.7324796.

[25]   J. Ansari, A. R. Abbasi, M. H. Heydari, and Z. Avazzadeh, "Simultaneous design of
fuzzy PSS and fuzzy STATCOM controllers for power system stability enhancement,"
Alexandria Eng. J., vol. 61, no. 4, pp. 2841–2850, 2022, doi:
10.1016/j.aej.2021.08.007.

[26]   M. Srinivas, I. Hussain, and B. Singh, "Combined LMS-LMF-Based Control
Algorithm of DSTATCOM for Power Quality Enhancement in Distribution System,"
IEEE Trans. Ind. Electron., vol. 63, no. 7, pp. 4160–4169, 2016, doi:
10.1109/TIE.2016.2532278.

[27]   A. Bhattacharya and C. Chakraborty, "Adaline controlled 3-phase 3-wire shunt active
power filter with enhanced performance using the capacitor voltage feedback," *Proc.
IEEE Int. Conf. Ind. Technol.*, 2009, doi: 10.1109/ICIT.2009.4939726.

[28]   M. Sujith and S. Padma, "Optimization of harmonics with active power filter based on
ADALINE neural network," *Microprocess. Microsyst.*, vol. 73, p. 102976, 2020, doi:
10.1016/j.micpro.2019.102976.

[29]   B. Singh and J. Solanki, "Load compensation for diesel generator-based isolated
generation system employing DSTATCOM," *IEEE Trans. Ind. Appl.*, vol. 47, no. 1,

pp. 238–244, 2011, doi: 10.1109/TIA.2010.2090847.

[30] B. Singh, R. Niwas, and S. K. Dube, "Load leveling and voltage control of permanent magnet synchronous generator-based DG Set for standalone supply system," *IEEE Trans. Ind. Informatics*, vol. 10, no. 4, pp. 2034–2043, 2014, doi: 10.1109/TII.2014.2341952.

[31] A. Kumar and P. Kumar, "Power Quality Improvement for Grid-connected PV System Based on Distribution Static Compensator with Fuzzy Logic Controller and UVT/ADALINE-based Least Mean Square Controller," *J. Mod. Power Syst. Clean Energy*, vol. 9, no. 6, pp. 1289–1299, 2021, doi: 10.35833/MPCE.2021.000285.

[32] A. Y. Cherif, S. El Islam Remache, K. Barra, and P. Wira, "Adaptive Model Predictive Control for Three Phase Voltage Source Inverter using ADALINE estimator," *Proc. - 2019 IEEE 1st Glob. Power, Energy Commun. Conf. GPECOM 2019*, pp. 164–169, 2019, doi: 10.1109/GPECOM.2019.8778544.

[33] C. Mittal and S. Srivastava, "Comparison of ANN and ANFIS Controller Based Hysteresis Current Control Scheme of DSTATCOM for Fault Analysis to Improve Power Quality," *Proc. Int. Conf. Electron. Sustain. Commun. Syst. ICESC 2020*, no. Icesc, pp. 149–156, 2020, doi: 10.1109/ICESC48915.2020.9155619.

[34] M. A. Bhayo *et al.*, "An Experimental Hybrid Control Approach for Wind Turbine Emulator," *IEEE Access*, vol. 11, no. June, pp. 58064–58077, 2023, doi: 10.1109/ACCESS.2023.3283420.

[35] M. Elsisi, M. Q. Tran, K. Mahmoud, M. Lehtonen, and M. M. F. Darwish, "Robust design of ANFIS-based blade pitch controller for wind energy conversion systems against wind speed fluctuations," *IEEE Access*, vol. 9, pp. 37894–37904, 2021, doi: 10.1109/ACCESS.2021.3063053.

[36] X. Sun, J. Cao, G. Lei, Y. Guo, and J. Zhu, "A Robust Deadbeat Predictive Controller

with Delay Compensation Based on Composite Sliding-Mode Observer for PMSMs," *IEEE Trans. Power Electron.*, vol. 36, no. 9, pp. 10742–10752, 2021, doi: 10.1109/TPEL.2021.3063226.

[37]   J. Long, M. Yang, Y. Chen, K. Liu, and D. Xu, "Current-Controller-Free Self-Commissioning Scheme for Deadbeat Predictive Control in Parametric Uncertain SPMSM," *IEEE Access*, vol. 9, pp. 289–302, 2021, doi: 10.1109/ACCESS.2020.3043751.

[38]   P. Viarouge, "Analvsis and Imdementation of a Real-Time Predictive Current Controller for Permanent-Magnet Synchronous Servo Drives," vol. 41, no. 1, pp. 110–117, 1994.

[39]   M. J. Duran *et al.*, "Predictive Current Control of Dual Three-Phase Drives Using Restrained Search Techniques," vol. 58, no. 8, pp. 3253–3263, 2011.

[40]   P. Cortés, S. Member, J. Rodríguez, S. Member, D. E. Quevedo, and C. Silva, "Imposed Load Current Spectrum," vol. 23, no. 2, pp. 612–618, 2008.

[41]   J. Rodríguez *et al.*, "Predictive Current Control of a Voltage Source Inverter," vol. 54, no. 1, pp. 495–503, 2007.

[42]   L. Guo, Y. Li, N. Jin, Z. Dou, and J. Wu, "Sliding mode observer-based AC voltage sensorless model predictive control for grid- connected inverters," 2020, doi: 10.1049/iet-pel.2019.1075.

[43]   H. Zhao, Q. Wu, Q. Guo, H. Sun, S. Huang, and Y. Xue, "Coordinated voltage control of a wind farm based on model predictive control," *IEEE Trans. Sustain. Energy*, vol. 7, no. 4, pp. 1440–1451, 2016, doi: 10.1109/TSTE.2016.2555398.

[44]   X. Chen, W. Wu, N. Gao, H. S. H. Chung, M. Liserre, and F. Blaabjerg, "Finite Control Set Model Predictive Control for LCL-Filtered Grid-Tied Inverter with Minimum Sensors," *IEEE Trans. Ind. Electron.*, vol. 67, no. 12, pp. 9980–9990, 2020,

doi: 10.1109/TIE.2019.2962444.

[45] F. Sebaaly, M. Sharifzadeh, H. Y. Kanaan, and K. Al-Haddad, "Multilevel Switching-Mode Operation of Finite-Set Model Predictive Control for Grid-Connected Packed E-Cell Inverter," *IEEE Trans. Ind. Electron.*, vol. 68, no. 8, pp. 6992–7001, 2021, doi: 10.1109/TIE.2020.3003627.

[46] M. Darabian, A. Jalilvand, A. Ashouri, and A. Bagheri, "Stability improvement of large-scale power systems in the presence of wind farms by employing HVDC and STATCOM based on a non-linear controller," *Int. J. Electr. Power Energy Syst.*, vol. 120, no. March, p. 106021, 2020, doi: 10.1016/j.ijepes.2020.106021.

[47] J. Wei *et al.*, "Coordinated droop control and adaptive model predictive control for enhancing HVRT and post-event recovery of large-scale wind farm," *IEEE Trans. Sustain. Energy*, vol. 12, no. 3, pp. 1549–1560, 2021, doi: 10.1109/TSTE.2021.3053955.

[48] R. Chakrabarty and R. Adda, "DSTATCOM implementation using Reduced Switch Single DC Source Cascaded H-bridge Multilevel Inverter," *Electr. Power Syst. Res.*, vol. 199, no. June, p. 107373, 2021, doi: 10.1016/j.epsr.2021.107373.

[49] R. O. Ramirez, C. R. Baier, F. Villarroel, J. R. Espinoza, J. Pou, and J. Rodriguez, "A Hybrid FCS-MPC with Low and Fixed Switching Frequency without Steady-State Error Applied to a Grid-Connected CHB Inverter," *IEEE Access*, vol. 8, pp. 223637–223651, 2020, doi: 10.1109/ACCESS.2020.3044226.

[50] S. Bella *et al.*, "FCS-MPC current control of parallel photovoltaic grid connected inverter with common AC and DC Buses," *2019 6th Int. Conf. Control. Decis. Inf. Technol. CoDIT 2019*, no. April, pp. 1138–1143, 2019, doi: 10.1109/CoDIT.2019.8820314.

[51] S. P. Pimentel, O. Husev, D. Vinnikov, C. Roncero-Clemente, and S. Stepenko, "An

indirect model predictive current control (CCS-MPC) for grid-connected single-phase three-level NPC quasi-Z-source PV inverter," *2018 IEEE 59th Annu. Int. Sci. Conf. Power Electr. Eng. Riga Tech. Univ. RTUCON 2018 - Proc.*, pp. 4–9, 2018, doi: 10.1109/RTUCON.2018.8659840.

[52]   A. T. Nguyen, S. W. Ryu, A. U. Rehman, H. H. Choi, and J. W. Jung, "Improved Continuous Control Set Model Predictive Control for Three-Phase CVCF Inverters: Fuzzy Logic Approach," *IEEE Access*, vol. 9, pp. 75158–75168, 2021, doi: 10.1109/ACCESS.2021.3081718.

[53]   P. Kumkratug, "STATCOM control strategy based on Lyapunov energy function and fuzzy logic control for improving transient stability of multimachine power system," *WSEAS Trans. Circuits Syst.*, vol. 11, no. 5, pp. 159–168, 2012.

[54]   M. Čerňan, Z. Müller, J. Tlustý, and V. Valouch, "An improved SVC control for electric arc furnace voltage flicker mitigation," *Int. J. Electr. Power Energy Syst.*, vol. 129, 2021, doi: 10.1016/j.ijepes.2021.106831.

[55]   N. C. Sahoo, B. K. Panigrahi, P. K. Dash, and G. Panda, "Application of a multivariable feedback linearization scheme for STATCOM control," *Electr. Power Syst. Res.*, vol. 62, no. 2, pp. 81–91, 2002, doi: 10.1016/S0378-7796(02)00011-1.

[56]   K. Wang and M. L. Crow, "Power system voltage regulation via STATCOM internal nonlinear control," *IEEE Trans. Power Syst.*, vol. 26, no. 3, pp. 1252–1262, 2011, doi: 10.1109/TPWRS.2010.2072937.

[57]   W. Chao and Z. Yao, "Approach on nonlinear control theory for designing: STATCOM controller," *Proc. 2007 IEEE Int. Conf. Grey Syst. Intell. Serv. GSIS 2007*, pp. 871–875, 2007, doi: 10.1109/GSIS.2007.4443398.

[58]   V. Spitsa, A. Alexandrovitz, and E. Zeheb, "Design of a robust state feedback controller for a STATCOM using a zero set concept," *IEEE Trans. Power Deliv.*, vol.

25, no. 1, pp. 456–467, 2010, doi: 10.1109/TPWRD.2009.2034828.

[59] R. Chilipi, N. Al Sayari, and J. Y. Alsawalhi, "Control of single-phase solar power generation system with universal active power filter capabilities using least mean mixed-norm (LMMN)-based adaptive filtering method," *IEEE Trans. Sustain. Energy*, vol. 11, no. 2, pp. 879–893, 2020, doi: 10.1109/TSTE.2019.2911852.

[60] Y. Jin *et al.*, "A Dual-Layer Back-Stepping Control Method for Lyapunov Stability in Modular Multilevel Converter Based STATCOM," *IEEE Trans. Ind. Electron.*, vol. 69, no. 3, pp. 2166–2179, 2022, doi: 10.1109/TIE.2021.3063973.

[61] J. W. Smith, W. Sunderman, R. Dugan, and B. Seal, "Smart Inverter Volt / Var Control Functions for High Penetration of PV on Distribution Systems," pp. 1–6, 2011.

[62] S. Inverters, M. Microgrids, and M. S. Pilehvar, "Frequency and Voltage Supports by Battery-Fed," 2020.

[63] A. R. Malekpour and A. Pahwa, "A Dynamic Operational Scheme for Residential PV Smart Inverters," pp. 1–10, 2016.

[64] L. A. Paredes, "Improvements in the Voltage Stability of a Microgrid due to Smart FACTS – an Approach from Resilience," 2020.

[65] T. Hossen and F. Sadeque, "On Stability , Ancillary Services , Operation , and Security of Smart Inverters," pp. 1–8.

[66] I. Exhibition, E. Management, and D. Version, "Smart Inverters for Utility and Industry Applications," 2015.

[67] A. Aktas, K. Erhan, S. Ozdemir, and E. Ozdemir, "Experimental investigation of a new smart energy management algorithm for a hybrid energy storage system in smart grid applications," *Electr. Power Syst. Res.*, vol. 144, pp. 185–196, 2017, doi: 10.1016/j.epsr.2016.11.022.

[68]   Q. Jiang, M. Xue, and G. Geng, "Energy management of microgrid in grid-connected and stand-alone modes," *IEEE Trans. Power Syst.*, vol. 28, no. 3, pp. 3380–3389, 2013, doi: 10.1109/TPWRS.2013.2244104.

[69]   M. S. Mahmoud, S. Azher Hussain, and M. A. Abido, "Modeling and control of microgrid: An overview," *J. Franklin Inst.*, vol. 351, no. 5, pp. 2822–2859, 2014, doi: 10.1016/j.jfranklin.2014.01.016.

[70]   S. Mashayekh and K. L. Butler-Purry, "A novel deterministic and probabilistic dynamic security assessment approach for isolated microgrids," *2017 19th Int. Conf. Intell. Syst. Appl. to Power Syst. ISAP 2017*, pp. 0–5, 2017, doi: 10.1109/ISAP.2017.8071403.

[71]   D. D. Le, A. Berizzi, and C. Bovo, "A probabilistic security assessment approach to power systems with integrated wind resources," *Renew. Energy*, vol. 85, pp. 114–123, 2016, doi: 10.1016/j.renene.2015.06.035.

[72]   S. A. Alavi, A. Ahmadian, and M. Aliakbar-Golkar, "Optimal probabilistic energy management in a typical micro-grid based-on robust optimization and point estimate method," *Energy Convers. Manag.*, vol. 95, no. February, pp. 314–325, 2015, doi: 10.1016/j.enconman.2015.02.042.

[73]   T. Niknam, F. Golestaneh, and A. Malekpour, "Probabilistic energy and operation management of a microgrid containing wind/photovoltaic/fuel cell generation and energy storage devices based on point estimate method and self-adaptive gravitational search algorithm," *Energy*, vol. 43, no. 1, pp. 427–437, 2012, doi: 10.1016/j.energy.2012.03.064.

[74]   S. K. Elsayed, S. Al Otaibi, Y. Ahmed, E. Hendawi, N. I. Elkalashy, and A. Hoballah, "Probabilistic modeling and equilibrium optimizer solving for energy management of renewable micro-grids incorporating storage devices," *Energies*, vol. 14, no. 5, 2021,

doi: 10.3390/en14051373.

[75] G. E. Constante-Flores and M. S. Illindala, "Data-driven probabilistic power flow analysis for a distribution system with renewable energy sources using Monte Carlo simulation," *IEEE Trans. Ind. Appl.*, vol. 55, no. 1, pp. 174–181, 2019, doi: 10.1109/TIA.2018.2867332.

[76] H. Wang, Z. Yan, X. Xu, and K. He, "Probabilistic power flow analysis of microgrid with renewable energy," *Int. J. Electr. Power Energy Syst.*, vol. 114, no. June 2019, p. 105393, 2020, doi: 10.1016/j.ijepes.2019.105393.

[77] J. D. Mina-Casaran, D. F. Echeverry, C. A. Lozano, and A. Navarro-Espinosa, "On the value of community association for microgrid development: Learnings from multiple deterministic and stochastic planning designs," *Appl. Sci.*, vol. 11, no. 14, 2021, doi: 10.3390/app11146257.

[78] N. Holjevac, T. Capuder, and I. Kuzle, "Adaptive control for evaluation of flexibility benefits in microgrid systems," *Energy*, vol. 92, pp. 487–504, 2015, doi: 10.1016/j.energy.2015.04.031.

[79] D. Tenfen and E. C. Finardi, "A mixed integer linear programming model for the energy management problem of microgrids," *Electr. Power Syst. Res.*, vol. 122, pp. 19–28, 2015, doi: 10.1016/j.epsr.2014.12.019.

[80] M. B. Sigalo, A. C. Pillai, S. Das, and M. Abusara, "An energy management system for the control of battery storage in a grid-connected microgrid using mixed integer linear programming," *Energies*, vol. 14, no. 19, 2021, doi: 10.3390/en14196212.

[81] S. H. Mirbarati, N. Heidari, A. Nikoofard, M. S. S. Danish, and M. Khosravy, "Techno-Economic-Environmental Energy Management of a Micro-Grid: A Mixed-Integer Linear Programming Approach," *Sustain.*, vol. 14, no. 22, 2022, doi: 10.3390/su142215036.

[82] A. C. Luna, N. L. Diaz, M. Graells, J. C. Vasquez, and J. M. Guerrero, "Mixed-integer-linear-programming-based energy management system for hybrid PV-wind-battery microgrids: Modeling, design, and experimental verification," *IEEE Trans. Power Electron.*, vol. 32, no. 4, pp. 2769–2783, 2017, doi: 10.1109/TPEL.2016.2581021.

[83] M. Dashtdar, M. Bajaj, and S. M. S. Hosseinimoghadam, "Design of Optimal Energy Management System in a Residential Microgrid Based on Smart Control," *Smart Sci.*, vol. 10, no. 1, pp. 25–39, 2022, doi: 10.1080/23080477.2021.1949882.

[84] M. A. Mosa and A. A. Ali, "Energy management system of low voltage dc microgrid using mixed-integer nonlinear programing and a global optimization technique," *Electr. Power Syst. Res.*, vol. 192, no. November, p. 106971, 2021, doi: 10.1016/j.epsr.2020.106971.

[85] Y. Yoldas, S. Goren, and A. Onen, "Optimal Control of Microgrids with Multi-stage Mixed-integer Nonlinear Programming Guided Q-learning Algorithm," *J. Mod. Power Syst. Clean Energy*, vol. 8, no. 6, pp. 1151–1159, 2020, doi: 10.35833/MPCE.2020.000506.

[86] S. Chakraborty and M. G. Simoes, "PV-microgrid operational cost minimization by neural forecasting and heuristic optimization," *Conf. Rec. - IAS Annu. Meet. (IEEE Ind. Appl. Soc.*, pp. 1–8, 2008, doi: 10.1109/08IAS.2008.147.

[87] A. U. Haque, M. H. Nehrir, P. Mandal, and S. Member, "Solar PV Power Generation Forecast Using a Hybrid Intelligent Approach," no. D, pp. 1–5, 2013.

[88] S. Chapaloglou *et al.*, "Smart energy management algorithm for load smoothing and peak shaving based on load forecasting of an island ' s power system," *Appl. Energy*, vol. 238, no. January, pp. 627–642, 2019, doi: 10.1016/j.apenergy.2019.01.102.

[89] A. Stoppato, G. Cavazzini, G. Ardizzon, and A. Rossetti, "A PSO (particle swarm

optimization) -based model for the optimal management of a small PV (Photovoltaic) -pump hydro energy storage in a rural dry area," *Energy*, pp. 1–7, 2014, doi: 10.1016/j.energy.2014.06.004.

[90] T. Kerdphol, Y. Qudaih, and Y. Mitani, "Electrical Power and Energy Systems Optimum battery energy storage system using PSO considering dynamic demand response for microgrids," *Int. J. Electr. POWER ENERGY Syst.*, vol. 83, pp. 58–66, 2016, doi: 10.1016/j.ijepes.2016.03.064.

[91] Q. Zhang *et al.*, "PSO-LSSVM-based Online SOC Estimation for Simulation Substation Battery," 2022, doi: 10.32604/sdhm.2022.018422.

[92] J. M. G. Alvarez and P. E. Mercado, "Online inference of the dynamic security level of power systems using fuzzy techniques," *IEEE Trans. Power Syst.*, vol. 22, no. 2, pp. 717–726, 2007, doi: 10.1109/TPWRS.2007.895161.

[93] Z. Zhao, P. Yang, J. M. Guerrero, Z. Xu, and T. C. Green, "Multiple-time-scales hierarchical frequency stability control strategy of medium-voltage isolated microgrid," *IEEE Trans. Power Electron.*, vol. 31, no. 8, pp. 5974–5991, 2016, doi: 10.1109/TPEL.2015.2496869.

[94] Y. Zhang and L. Xie, "Online Dynamic Security Assessment of Microgrid Interconnections in Smart Distribution Systems," *IEEE Trans. Power Syst.*, vol. 30, no. 6, pp. 3246–3254, 2015, doi: 10.1109/TPWRS.2014.2374876.

[95] X. Li, Z. Li, L. Guo, J. Zhu, Y. Wang, and C. Wang, "Enhanced dynamic stability control for low-inertia hybrid AC/DC microgrid with distributed energy storage systems," *IEEE Access*, vol. 7, pp. 91234–91242, 2019, doi: 10.1109/ACCESS.2019.2926814.

[96] H. Peng, M. Su, S. Li, and C. Li, "Static Security Risk Assessment for Islanded Hybrid AC/DC Microgrid," *IEEE Access*, vol. 7, pp. 37545–37554, 2019, doi:

10.1109/ACCESS.2019.2899347.

[97]   F. Samadi Gazijahani and J. Salehi, "Optimal Bilevel Model for Stochastic Risk-Based Planning of Microgrids under Uncertainty," *IEEE Trans. Ind. Informatics*, vol. 14, no. 7, pp. 3054–3064, 2018, doi: 10.1109/TII.2017.2769656.

[98]   C. Deng, Y. Wang, C. Wen, Y. Xu, and P. Lin, "Distributed Resilient Control for Energy Storage Systems in Cyber-Physical Microgrids," *IEEE Trans. Ind. Informatics*, vol. 17, no. 2, pp. 1331–1341, 2021, doi: 10.1109/TII.2020.2981549.

[99]   V. Bolgouras, C. Ntantogian, E. Panaousis, and C. Xenakis, "Distributed Key Management in Microgrids," *IEEE Trans. Ind. Informatics*, vol. 16, no. 3, pp. 2125–2133, 2020, doi: 10.1109/TII.2019.2941586.

[100] A. Kavousi-Fard, W. Su, and T. Jin, "A Machine-Learning-Based Cyber Attack Detection Model for Wireless Sensor Networks in Microgrids," *IEEE Trans. Ind. Informatics*, vol. 17, no. 1, pp. 650–658, 2021, doi: 10.1109/TII.2020.2964704.

[101] T. L. Nguyen, H. T. Nguyen, Y. Wang, O. A. Mohammed, and E. Anagnostou, "Distributed Secondary Control in Microgrids Using Synchronous Condenser for Voltage and Frequency Support," *Energies*, vol. 15, no. 8, pp. 1–15, 2022, doi: 10.3390/en15082968.

[102] Z. Wang, B. Chen, J. Wang, and J. Kim, "Decentralized Energy Management System for Networked Microgrids in Grid-Connected and Islanded Modes," *IEEE Trans. Smart Grid*, vol. 7, no. 2, pp. 1097–1105, 2016, doi: 10.1109/TSG.2015.2427371.

[103] A. Krishna, J. Schiffer, and J. Raisch, "Distributed secondary frequency control in microgrids: Robustness and steady-state performance in the presence of clock drifts," *Eur. J. Control*, vol. 51, pp. 135–145, 2020, doi: 10.1016/j.ejcon.2019.08.003.

[104] M. B. Abdelghany, M. F. Shehzad, D. Liuzza, V. Mariani, and L. Glielmo, "Optimal operations for hydrogen-based energy storage systems in wind farms via model

predictive control," *Int. J. Hydrogen Energy*, vol. 46, no. 57, pp. 29297–29313, 2021, doi: 10.1016/j.ijhydene.2021.01.064.

[105] L. Meng, F. Tang, M. Savaghebi, J. C. Vasquez, and J. M. Guerrero, "Tertiary control of voltage unbalance compensation for optimal power quality in islanded microgrids," *IEEE Trans. Energy Convers.*, vol. 29, no. 4, pp. 802–815, 2014, doi: 10.1109/TEC.2014.2363687.

[106] S. Wang, S. Bi, and Y. J. A. Zhang, "Demand response management for profit maximizing energy loads in real-time electricity market," *IEEE Trans. Power Syst.*, vol. 33, no. 6, pp. 6387–6396, 2018, doi: 10.1109/TPWRS.2018.2827401.

[107] S. Kujur, H. M. Dubey, and S. R. Salkuti, "Demand Response Management of a Residential Microgrid Using Chaotic Aquila Optimization," *Sustain.*, vol. 15, no. 2, 2023, doi: 10.3390/su15021484.

[108] S. Maharjan, Q. Zhu, Y. Zhang, S. Gjessing, and T. Başsar, "Dependable demand response management in the smart grid: A stackelberg game approach," *IEEE Trans. Smart Grid*, vol. 4, no. 1, pp. 120–132, 2013, doi: 10.1109/TSG.2012.2223766.

[109] L. P. Qian, Y. Wu, Y. J. A. Zhang, and J. Huang, "Demand response management via real-time electricity price control in smart grids," *Smart Grid Networking, Data Manag. Bus. Model.*, vol. 31, no. 7, pp. 169–192, 2017, doi: 10.1201/b19664.

[110] N. Altin and S. E. Eyimaya, "A Review of Microgrid Control Strategies," *10th IEEE Int. Conf. Renew. Energy Res. Appl. ICRERA 2021*, no. September, pp. 412–417, 2021, doi: 10.1109/ICRERA52334.2021.9598699.

[111] N. D. Hatziargyriou and A. G. Tsikalakis, "Centralized Control for Optimizing Microgrids Operation Central Controller Strategy to Optimize Microgrids Operation," *IEEE Trans. Energy Convers.*, vol. 23, no. 1, pp. 241–248, 2008.

[112] X. Feng, A. Shekhar, F. Yang, R. E. Hebner, and P. Bauer, "Comparison of

Hierarchical Control and Distributed Control for Microgrid," *Electr. Power Components Syst.*, vol. 45, no. 10, pp. 1043–1056, 2017, doi: 10.1080/15325008.2017.1318982.

[113] A. Mehrizi-Sani, "Distributed Control Techniques in Microgrids," *Microgrid Adv. Control Methods Renew. Energy Syst. Integr.*, no. May, pp. 43–62, 2017, doi: 10.1016/B978-0-08-101753-1.00002-4.

[114] S. Chen, Z. Wu, and P. D. Christofides, "Cyber-security of centralized, decentralized, and distributed control-detector architectures for nonlinear processes," *Chem. Eng. Res. Des.*, vol. 165, pp. 25–39, 2021, doi: 10.1016/j.cherd.2020.10.014.

[115] L. Li, Y. Sun, Z. Liu, X. Hou, G. Shi, and M. Su, "A Decentralized Control with Unique Equilibrium Point for Cascaded-Type Microgrid," *IEEE Trans. Sustain. Energy*, vol. 10, no. 1, pp. 324–326, 2019, doi: 10.1109/TSTE.2018.2871641.

[116] H. J. Jabir, J. Teh, D. Ishak, and H. Abunima, "Impacts of demand-side management on electrical power systems: A review," *Energies*, vol. 11, no. 5, pp. 1–19, 2018, doi: 10.3390/en11051050.

[117] Q. Jia, S. Member, and S. Chen, "Optimal Incentive Strategy in Cloud-Edge Integrated Demand Response Framework for Residential Air Conditioning Loads," *IEEE Trans. Cloud Comput.*, vol. 10, no. 1, pp. 31–42, 2022, doi: 10.1109/TCC.2021.3118597.

[118] H. Zhong, S. Member, L. Xie, Q. Xia, and S. Member, "Coupon Incentive-Based Demand Response : Theory and Case Study," *IEEE Trans. Power Syst.*, vol. 28, no. 2, pp. 1266–1276, 2013, doi: 10.1109/TPWRS.2012.2218665.

[119] A. Fraija, K. Agbossou, N. Henao, S. Kelouwani, M. Fournier, and S. S. Hosseini, "A Discount-Based Time-of-Use Electricity Pricing Strategy for Demand Response with Minimum Information Using Reinforcement Learning," *IEEE Access*, vol. 10, pp. 54018–54028, 2022, doi: 10.1109/ACCESS.2022.3175839.

[120] H. K. Hwang, A. Y. Yoon, H. K. Kang, and S. Il Moon, "Retail Electricity Pricing Strategy via an Artificial Neural Network-Based Demand Response Model of an Energy Storage System," *IEEE Access*, vol. 9, pp. 13440–13450, 2021, doi: 10.1109/ACCESS.2020.3048048.

[121] R. Yu, W. Yang, and S. Rahardja, "A statistical demand-price model with its application in optimal real-time price," *IEEE Trans. Smart Grid*, vol. 3, no. 4, pp. 1734–1742, 2012, doi: 10.1109/TSG.2012.2217400.

[122] H. Algarvio and F. Lopes, "Bilateral Contracting and Price-Based Demand Response in Multi-Agent Electricity Markets: A Study on Time-of-Use Tariffs," *Energies*, vol. 16, no. 2, 2023, doi: 10.3390/en16020645.

[123] F. Alfaverh, M. Denai, and Y. Sun, "Demand Response Strategy Based on Reinforcement Learning and Fuzzy Reasoning for Home Energy Management," *IEEE Access*, vol. 8, pp. 39310–39321, 2020, doi: 10.1109/ACCESS.2020.2974286.

[124] D. Fuselli *et al.*, "Action dependent heuristic dynamic programming for home energy resource scheduling," *Int. J. Electr. Power Energy Syst.*, vol. 48, no. 1, pp. 148–160, 2013, doi: 10.1016/j.ijepes.2012.11.023.

[125] D. Liu, Y. Xu, Q. Wei, and X. Liu, "Residential energy scheduling for variable weather solar energy based on adaptive dynamic programming," *IEEE/CAA J. Autom. Sin.*, vol. 5, no. 1, pp. 36–46, 2018, doi: 10.1109/JAS.2017.7510739.

[126] B. M. Nejad, M. Vahedi, M. Hoseina, and M. S. Moghaddam, "Economic Model for Coordinating Large-Scale Energy Storage Power Plant With Demand Response Management Options in Smart Grid Energy Management," *IEEE Access*, vol. 11, no. June 2022, pp. 16483–16492, 2023, doi: 10.1109/ACCESS.2022.3184733.

[127] S. Y. Feb, D. Zhu, B. Yang, Y. Liu, and Z. Wang, "Energy Management Based on Multi-Agent Deep Reinforcement Learning for A Multi-Energy Industrial".

[128] R. Lu, Z. Jiang, H. Wu, and S. Member, "Reward Shaping-Based Actor − Critic Deep Reinforcement Learning for Residential Energy Management," vol. 19, no. 3, pp. 2662–2673, 2023.

[129] X. Huang, S. H. O. Hong, and S. Member, "Demand Response Management for Industrial Facilities : A Deep Reinforcement Learning Approach," *IEEE Access*, vol. 7, pp. 82194–82205, 2019, doi: 10.1109/ACCESS.2019.2924030.

[130] X. Zhang, T. Bao, T. Yu, B. Yang, and C. Han, "Deep transfer Q-learning with virtual leader-follower for supply-demand Stackelberg game of smart grid," *Energy*, 2017, doi: 10.1016/j.energy.2017.05.114.

[131] S. Chen, W. Chiu, and W. Liu, "User Preference-Based Demand Response for Smart Home Energy Management Using Multiobjective Reinforcement Learning," *IEEE Access*, vol. 9, pp. 161627–161637, 2021, doi: 10.1109/ACCESS.2021.3132962.

[132] D. P. Gradient, "Residential Demand Response Strategy Based on Deep Deterministic Policy Gradient," pp. 1–16, 2021.

[133] R. A. Residential, D. Response, and P. G. Learning, "Real-Time Autonomous Residential Demand Response Policy Gradient Learning," 2021.

[134] "A Stochastic Model for Energy Resources Management in Smart Grids".

[135] H. Karimi and S. Jadid, "Optimal energy management for multi-microgrid considering demand response programs : A stochastic multi-objective framework," *Energy*, vol. 195, p. 116992, 2020, doi: 10.1016/j.energy.2020.116992.

[136] H. Gong and S. Member, "Peak Reduction and Long Term Load Forecasting for Large Residential Communities Including Smart Homes With Energy Storage," pp. 19345–19355, 2021, doi: 10.1109/ACCESS.2021.3052994.

[137] X. Ding, W. Zhang, S. Wei, and Z. Wang, "Optimization of an energy storage system for electric bus fast-charging station," *Energies*, vol. 14, no. 14, pp. 1–17, 2021, doi:

10.3390/en14144143.

[138] T. Terlouw, T. Alskaif, C. Bauer, and W. Van Sark, "Multi-objective optimization of energy arbitrage in community energy storage systems using di ff erent battery technologies," *Appl. Energy*, vol. 239, no. February, pp. 356–372, 2019, doi: 10.1016/j.apenergy.2019.01.227.

[139] M. Jang, H. Choi, C. Lim, B. An, and J. Sim, "Optimization of ESS Scheduling for Cost Reduction in Commercial and Industry Customers in Korea," pp. 1–16, 2022.

[140] X. Bao, X. Xu, Y. Zhang, Y. Xiong, and C. Shang, "Optimal Sizing of Battery Energy Storage System in a Shipboard Power System with considering Energy Management Optimization," vol. 2021, 2021.

[141] S. Wen, H. Lan, Y. Hong, D. C. Yu, L. Zhang, and P. Cheng, "Allocation of ESS by interval optimization method considering impact of ship swinging on hybrid PV / diesel ship power system," *Appl. Energy*, vol. 175, pp. 158–167, 2016, doi: 10.1016/j.apenergy.2016.05.003.

[142] M. A. Sheba, D. A. Mansour, and N. H. Abbasy, "A new low-cost and low-power industrial internet of things infrastructure for effective integration of distributed and isolated systems with smart grids," no. August, pp. 4554–4573, 2023, doi: 10.1049/gtd2.12951.

[143] E. Sorin, L. Bobo, and P. Pinson, "Consensus-Based Approach to Peer-to-Peer Electricity Markets with Product Differentiation," *IEEE Trans. Power Syst.*, vol. 34, no. 2, pp. 994–1004, 2019, doi: 10.1109/TPWRS.2018.2872880.

[144] M. Khorasany, Y. Mishra, and G. Ledwich, "Auction based energy trading in transactive energy market with active participation of prosumers and consumers," *2017 Australas. Univ. Power Eng. Conf. AUPEC 2017*, vol. 2017-Novem, pp. 1–6, 2018, doi: 10.1109/AUPEC.2017.8282470.

[145] G. Belgioioso, W. Ananduta, S. Grammatico, and C. Ocampo-Martinez, "Operationally-Safe Peer-to-Peer Energy Trading in Distribution Grids: A Game-Theoretic Market-Clearing Mechanism," *IEEE Trans. Smart Grid*, vol. 13, no. 4, pp. 2897–2907, 2022, doi: 10.1109/TSG.2022.3158442.

[146] X. Wang, J. Yang, K. Zhang, S. Zhang, and L. Wu, "Game-theoretic analysis of market-based operation mechanism for demand response resources," *Int. J. Electr. Power Energy Syst.*, vol. 134, p. 107456, 2022, doi: 10.1016/j.ijepes.2021.107456.

[147] M. Yu *et al.*, "Assessing the Feasibility of Game-Theory-Based Demand Response Management by Practical Implementation," *IEEE Access*, vol. 9, pp. 8220–8232, 2021, doi: 10.1109/ACCESS.2021.3049768.

[148] M. Nykyri, T. J. Karkkainen, S. Annala, and P. Silventoinen, "Review of Demand Response and Energy Communities in Serious Games," *IEEE Access*, vol. 10, no. August, pp. 91018–91026, 2022, doi: 10.1109/ACCESS.2022.3202013.

[149] B. Cornélusse, I. Savelli, S. Paoletti, A. Giannitrapani, and A. Vicino, "A community microgrid architecture with an internal local market," *Appl. Energy*, vol. 242, no. March, pp. 547–560, 2019, doi: 10.1016/j.apenergy.2019.03.109.

[150] L. T. N. J. C.Long,J.Wu.C.Zhang, "Peer-to-Peer energy Trading a Community Microgrid," pp. 3–7, 2020.

[151] K. Anoh, M. Ieee, S. Maharjan, M. Ieee, A. Ikpehai, and M. Ieee, "Energy Peer-to-Peer Trading in Virtual Microgrids in Smart Grids : A Game-Theoretic Approach," *IEEE Trans. Smart Grid*, vol. PP, no. c, p. 1, 2019, doi: 10.1109/TSG.2019.2934830.

[152] Q. He, Z. Lin, H. Chen, X. Dai, Y. Li, and X. Zeng, "Bi - level optimization based two - stage market clearing model considering guaranteed accommodation of renewable energy generation," *Prot. Control Mod. Power Syst.*, 2022, doi: 10.1186/s41601-022-00253-y.

[153] F. Luo, Z. Y. Dong, G. Liang, J. Murata, and Z. Xu, "A Distributed Electricity Trading System in Active Distribution Networks Based on Multi-Agent Coalition and Blockchain," *IEEE Trans. Power Syst.*, vol. 34, no. 5, pp. 4097–4108, 2019, doi: 10.1109/TPWRS.2018.2876612.

[154] J. Wang, J. Wu, and X. Kong, "Multi-agent Simulation for Strategic Bidding in electricity markets using reinforcement learning," vol. 9, no. 3, pp. 1051–1065, 2023, doi: 10.17775/CSEEJPES.2020.02820.

[155] A. Anees, T. Dillon, and Y. P. Chen, "A novel decision strategy for a bilateral energy contract," *Appl. Energy*, vol. 253, no. December 2018, p. 113571, 2019, doi: 10.1016/j.apenergy.2019.113571.

[156] P. Producer, H. Rashidizadeh-kermani, M. Vahedipour-dahraie, M. Shafie-khah, and S. Member, "Evaluating the Impact of Bilateral Contracts on the Offering Strategy of a Price Maker Wind Evaluating the Impact of Bilateral Contracts on the Offering Strategy of a Price Maker Wind Power Producer," vol. 18, pp. 4331–4341, 2022.

[157] M. Aziz and H. Dagdougui, "A Decentralized Game Theoretic Approach for Virtual Storage System Aggregation in a Residential Community," *IEEE Access*, vol. 10, pp. 34846–34857, 2022, doi: 10.1109/ACCESS.2022.3162143.

[158] R. Roofegari Nejad and S. M. Moghaddas Tafreshi, "Operation Planning of a Smart Microgrid Including Controllable Loads and Intermittent Energy Resources by Considering Uncertainties," *Arab. J. Sci. Eng.*, vol. 39, no. 8, pp. 6297–6315, 2014, doi: 10.1007/s13369-014-1267-4.

[159] C. Bekara, "Security Issues and Challenges for the IoT-based Smart Grid," *Procedia - Procedia Comput. Sci.*, vol. 34, pp. 532–537, 2020, doi: 10.1016/j.procs.2014.07.064.

[160] A. Akkad, G. Wills, and A. Rezazadeh, "An information security model for an IoT-enabled Smart Grid in the Saudi energy sector," *Comput. Electr. Eng.*, vol. 105, no.

March 2022, p. 108491, 2023, doi: 10.1016/j.compeleceng.2022.108491.

[161] A. A. Khan, A. A. Laghari, P. Li, M. A. Dootio, and S. Karim, "The collaborative role of blockchain , artificial intelligence , and industrial internet of things in digitalization of small and medium - size enterprises," *Sci. Rep.*, no. 0123456789, pp. 1–13, 2023, doi: 10.1038/s41598-023-28707-9.

[162] O. Dzobo, B. Malila, and L. Sithole, "Proposed framework for blockchain technology in a decentralised energy network," *Prot. Control Mod. Power Syst.*, 2021, doi: 10.1186/s41601-021-00209-8.

[163] K. Thirugnanam *et al.*, "Energy Management of Grid Interconnected Multi-Microgrids based on P2P Energy Exchange :," vol. 8950, no. c, 2020, doi: 10.1109/TPWRS.2020.3025113.

[164] B. Dey, S. Basak, and B. Bhattacharyya, "Demand-Side-Management-Based Bi-level Intelligent Optimal Approach for Cost-Centric Energy Management of a Microgrid System," *Arab. J. Sci. Eng.*, vol. 48, no. 5, pp. 6819–6830, 2023, doi: 10.1007/s13369-022-07546-2.

[165] H. Ming, B. Xia, K. Lee, A. Adepoju, S. Shakkottai, and L. Xie, "Prediction and assessment of demand response potential with coupon incentives in highly renewable power systems," 2020.

[166] A. Aghmadi, H. Hussein, K. H. Polara, and O. Mohammed, "A Comprehensive Review of Architecture, Communication, and Cybersecurity in Networked Microgrid Systems," *Inventions*, vol. 8, no. 4, p. 84, 2023, doi: 10.3390/inventions8040084.

[167] M. Grimley and J. Farrell, "Mighty Microgrids," *ILSR's Energy Democr. Initiat.*, no. March, p. 38, 2016, [Online]. Available: https://ilsr.org/wp-content/uploads/downloads/2016/03/Report-Mighty-Microgrids-PDF-3_3_16.pdf

[168] M. Grzanic, J. M. Morales, S. Pineda, and T. Capuder, "Electricity Cost-Sharing in

Energy Communities under Dynamic Pricing and Uncertainty," *IEEE Access*, vol. 9, pp. 30225–30241, 2021, doi: 10.1109/ACCESS.2021.3059476.

[169] J. Li, Y. Ye, D. Papadaskalopoulos, and G. Strbac, "Computationally Efficient Pricing and Benefit Distribution Mechanisms for Incentivizing Stable Peer-to-Peer Energy Trading," *IEEE Internet Things J.*, vol. 8, no. 2, pp. 734–749, 2021, doi: 10.1109/JIOT.2020.3007196.

[170] L. Chen, N. Liu, C. Li, J. Wang, and S. Member, "Peer-to-peer Energy Sharing with Social Attributes : A Stochastic Leader-follower Game Approach," vol. 3203, no. c, pp. 1–11, 2020, doi: 10.1109/TII.2020.2999328.

[171] Section-37, "the Indian Electricity Rules , 1956," pp. 45–48, 2000.

[172] P. K. W. Chan, H. S. H. Chung, and S. Y. Hui, "A generalized theory of boundary control for a single-phase multilevel inverter using second-order switching surface," *IEEE Trans. Power Electron.*, vol. 24, no. 10, pp. 2298–2313, 2009, doi: 10.1109/TPEL.2009.2028630.

[173] Y. Xu and F. Li, "Adaptive PI control of STATCOM for voltage regulation," *IEEE Trans. Power Deliv.*, vol. 29, no. 3, pp. 1002–1011, 2014, doi: 10.1109/TPWRD.2013.2291576.

[174] S. Eshtehardiha, M. B. Poodeh, and A. Kiyoumarsi, "Optimized performance of STATCOM with PID controller based on genetic algorithm," *ICCAS 2007 - Int. Conf. Control. Autom. Syst.*, pp. 1639–1644, 2007, doi: 10.1109/ICCAS.2007.4406596.

[175] A. Lorduy, A. Lázaro, C. Fernández, I. Quesada, and A. Barrado, "Novel Simplified Controller for Three Phase Grid Connected Inverter Based on Instantaneous Complex Power," *Conf. Proc. - IEEE Appl. Power Electron. Conf. Expo. - APEC*, vol. 2, no. 5, pp. 1306–1312, 2009, doi: 10.1109/APEC.2009.4802833.

[176] S. Arockiaraj, B. . Manikandan, and A. Bhubanesh, "Fuzzy logic controlled

STATCOM with a series compensated transmission line analysis," in *REVUE ROUMAINE DES SCIENCES TECHNIQUES—SÉRIE ÉLECTROTECHNIQUE ET ÉNERGÉTIQUE*, 2023, p. pp.307-312.

[177] K. Muralikumar and P. Ponnambalam, "Comparison of Fuzzy and ANFIS Controllers for Asymmetrical 31-Level Cascaded Inverter with Super Imposed Carrier PWM Technique," *IEEE Access*, vol. 9, pp. 82630–82646, 2021, doi: 10.1109/ACCESS.2021.3086674.

[178] C. T. Chao, N. Sutarna, J. S. Chiou, and C. J. Wang, "An optimal fuzzy PID controller design based on conventional PID control and nonlinear factors," *Appl. Sci.*, vol. 9, no. 6, 2019, doi: 10.3390/app9061224.

[179] E. Vlamou and B. Papadopoulos, "Fuzzy logic systems and medical applications," *AIMS Neurosci.*, vol. 6, no. 4, pp. 266–272, 2019, doi: 10.3934/Neuroscience.2019.4.266.

[180] B. Khoshnevisan, S. Rafiee, M. Omid, and H. Mousazadeh, "Development of an intelligent system based on ANFIS for predicting wheat grain yield on the basis of energy inputs," *Inf. Process. Agric.*, vol. 1, no. 1, pp. 14–22, 2014, doi: 10.1016/j.inpa.2014.04.001.

[181] D. Venkatramanan, S. Member, V. John, and S. Member, "IEEE TRANSACTIONS ON INDUSTRIAL ELECTRONICS A Reconfigurable Solar Photovoltaic Grid-Tied Inverter Architecture for Enhanced Energy Access in Backup Power Applications," 2018.

[182] R. M. Milasi, "A Nonlinear Adaptive Control for a Bidirectional DC–AC Converter With Parameter Uncertainties," *IEEE Trans. Ind. Electron.*, vol. PP, pp. 1–8, 2023, doi: 10.1109/tie.2023.3323703.

[183] M. Bouderbala, B. Bossoufi, H. A. Aroussi, M. Taoussi, and A. Lagrioui, "Novel

deadbeat predictive control strategy for DFIG's back to back power converter," *Int. J. Power Electron. Drive Syst.*, vol. 13, no. 1, pp. 139–149, 2022, doi: 10.11591/ijpeds.v13.i1.pp139-149.

[184] J. Peng and M. Yao, "Overview of Predictive Control Technology for Permanent Magnet Synchronous Motor Systems," *Appl. Sci.*, vol. 13, no. 10, 2023, doi: 10.3390/app13106255.

[185] I. M. Alsofyani and L. M. Halabi, "Unidirectional Finite Control Set-Predictive Torque Control of IPMSM Fed by Three-Level NPC Inverter with Simplified Voltage-Vector Lookup Table," *Electron.*, vol. 12, no. 1, 2023, doi: 10.3390/electronics12010252.

[186] N. Ahmed, Z. Soraya, and C. Abdelkader, "Model predictive control of high voltage direct current based on voltage source converter transmission system," *Int. J. Power Electron. Drive Syst.*, vol. 14, no. 1, pp. 244–255, 2023, doi: 10.11591/ijpeds.v14.i1.pp244-255.

[187] J. C. U. Peña, L. P. Sampaio, M. A. G. de Brito, and C. A. Canesin, "RLC passive damped LCL single-phase voltage source inverter with capability to operate in grid-connected and islanded modes: design and control strategy," *Electr. Eng.*, vol. 102, no. 4, pp. 2509–2519, 2020, doi: 10.1007/s00202-020-01045-z.

[188] J. Yang, Y. Liu, and R. Yan, "A Comparison of Finite Control Set and Continuous Control Set Model Predictive Control Schemes for Model Parameter Mismatch in Three-Phase APF," *Front. Energy Res.*, vol. 9, no. August, pp. 1–12, 2021, doi: 10.3389/fenrg.2021.727364.

[189] I. S. Mohamed, S. Rovetta, T. D. Do, T. Dragicevic, and A. A. Z. Diab, "A neural-network-based model predictive control of three-phase inverter with an output LC Filter," *IEEE Access*, vol. 7, pp. 124737–124749, 2019, doi: 10.1109/ACCESS.2019.2938220.

[190] R. P. Aguilera, P. Lezana, and D. E. Quevedo, "Switched Model Predictive Control for Improved Transient and Steady-State Performance," *IEEE Trans. Ind. Informatics*, vol. 11, no. 4, pp. 968–977, 2015, doi: 10.1109/TII.2015.2449992.

[191] A. K. Mishra, S. R. Das, P. K. Ray, R. K. Mallick, A. Mohanty, and D. K. Mishra, "PSO-GWO Optimized Fractional Order PID Based Hybrid Shunt Active Power Filter for Power Quality Improvements," *IEEE Access*, vol. 8, pp. 74497–74512, 2020, doi: 10.1109/ACCESS.2020.2988611.

[192] M. S. Djebbar, A. Boukadoum, and A. Bouguerne, "Performances of a wind power system based on the doubly fed induction generator controlled by a multi-level inverter," *Int. J. Power Electron. Drive Syst.*, vol. 14, no. 1, pp. 100–110, 2023, doi: 10.11591/ijpeds.v14.i1.pp100-110.

[193] S. Nama, A. K. Saha, S. Chakraborty, A. H. Gandomi, and L. Abualigah, "Boosting particle swarm optimization by backtracking search algorithm for optimization problems," *Swarm Evol. Comput.*, vol. 79, no. August 2022, p. 101304, 2023, doi: 10.1016/j.swevo.2023.101304.

[194] R. Comfort, M. Gonzalalez, A. Mansoor, P. Barker, T. Short, and A. Sundaram, "Power Quality Impact of Distributed Generation: Effect on Staedy state voltage regulation." pp. 35–42.

[195] M. Wang, X. Xu, Z. Yan, and H. Wang, "An online optimization method for extracting parameters of multi-parameter PV module model based on adaptive Levenberg-Marquardt algorithm," *Energy Convers. Manag.*, vol. 245, no. 52077136, p. 114611, 2021, doi: 10.1016/j.enconman.2021.114611.

[196] Z. Boussaada, O. Curea, A. Remaci, H. Camblong, and N. M. Bellaaj, "A nonlinear autoregressive exogenous (NARX) neural network model for the prediction of the daily direct solar radiation," *Energies*, vol. 11, no. 3, 2018, doi: 10.3390/en11030620.

[197] M. C. Kang, S. H. Lee, and Y. D. Yoon, "Compensation for inverter nonlinearity considering voltage drops and switching delays of each leg's switches," *ECCE 2016 - IEEE Energy Convers. Congr. Expo. Proc.*, pp. 0–6, 2016, doi: 10.1109/ECCE.2016.7854946.

[198] M. Vidyasagar, *Nonlinear systems analysis*, vol. 42. 2002. doi: 10.1137/1.9780898719185.

[199] J. D. J. Rubio, "Stability Analysis of the Modified Levenberg-Marquardt Algorithm for the Artificial Neural Network Training," *IEEE Trans. Neural Networks Learn. Syst.*, vol. 32, no. 8, pp. 3510–3524, 2021, doi: 10.1109/TNNLS.2020.3015200.

[200] P. Grieder, M. Lüthi, P. A. Parrilo, and M. Morari, "Stability & feasibility of constrained receding horizon control," *Eur. Control Conf. ECC 2003*, vol. 38, no. 10, pp. 701–706, 2003, doi: 10.23919/ecc.2003.7085038.

[201] F. Dincer and E. Ozer, "Assessing the Potential of a Rooftop Grid-Connected Photovoltaic System for Gaziantep Islamic Science and Technology University/ Turkey," *Jordan J. Electr. Eng.*, vol. 9, no. 2, pp. 149–165, 2023, doi: 10.5455/jjee.204-1670146602.

[202] A. Yasin and O. Draidi, "Techno-Economic Assessment of Implementing Concentrated Solar Power Technology in Palestinian Territories," *Jordan J. Electr. Eng.*, vol. 6, no. 3, p. 253, 2020, doi: 10.5455/jjee.204-1586112414.

[203] E. Das, S. Roy, S. R. Chowdhury, B. Ambarnath, and B. Sujit, "Cloud-based P2P Energy Transfer in a Residential Photovoltaic System Community," in *Energy Systems, Drives, Power Electronics, Measurement and Sensors (ESDPEMS -2023)*, Kolkata: Department of Electrical Engineering, Narula Institute of Technology, 2023, pp. 4–7.

[204] A. Elmouatamid, R. Ouladsine, M. Bakhouya, N. El Kamoun, K. Zine-Dine, and M.

Khaidar, "A Model Predictive Control Approach for Energy Management in Micro-Grid Systems," *SEST 2019 - 2nd Int. Conf. Smart Energy Syst. Technol.*, pp. 1–6, 2019, doi: 10.1109/SEST.2019.8848995.

[205] X. Li, R. Chang, J. Zuo, and Y. Zhang, "How does residential solar PV system diffusion occur in Australia?-A logistic growth curve modelling approach," *Sustain. Energy Technol. Assessments*, vol. 56, no. October 2022, p. 103060, 2023, doi: 10.1016/j.seta.2023.103060.

[206] S. Liu *et al.*, "Operational optimization of a building-level integrated energy system considering additional potential benefits of energy storage," vol. 0, 2021.

[207] H. H. Alshammari, "The internet of things healthcare monitoring system based on MQTT protocol," *Alexandria Eng. J.*, vol. 69, pp. 275–287, 2023, doi: 10.1016/j.aej.2023.01.065.

[208] S. Blechmann, I. Sowa, M. H. Schraven, R. Streblow, D. Müller, and A. Monti, "Open source platform application for smart building and smart grid controls," *Autom. Constr.*, vol. 145, no. November 2021, 2023, doi: 10.1016/j.autcon.2022.104622.